MECHANISM OF DEATH RECEPTOR 5 (DR5) GENE EXPRESSION

APPLICATIONS TO CHRONIC LYMPHOCYTIC LEUKEMIA (CLL)

BY

BONNIE GRAHAM

A Thesis
Submitted to the Faculty of Graduate Studies
in Partial Fulfillment of the Requirements
for the Degree
of
Master of Science

Department of Biochemistry and Medical Genetics
University of Manitoba
Winnipeg, Manitoba
Canada

THE UNIVERSITY OF MANITOBA

FACULTY OF GRADUATE STUDIES

*****

COPYRIGHT PERMISSION

MECHANISM OF DEATH RECEPTOR 5 (DR5) GENE EXPRESSION APPLICATIONS TO CHRONIC LYMPOCYTIC LEUKEMIA (CLL)

by

Bonnie Anne Graham

A Thesis/Practicum submitted to the Faculty of Graduate Studies of The University of Manitoba in partial fulfillment of the requirement of the degree

Of

MASTER OF SCIENCE

ABSTRACT

Death receptor 5 (DR5) is a cell surface receptor that binds the ligand TRAIL and triggers apoptosis. Its expression is mediated by transcription factors nuclear factor κB (NFκB) and p53. Histone acetylation facilitates the interaction of transcription factors with nuclear DNA thereby affecting the transcription process. Histone acetyltransferases (HATs) allow the transcriptional machinery access to the DNA template for gene expression; whereas histone deacetylases (HDACs) prevent this access and lead to repression of gene expression. HDAC inhibitors bind HDACs and inhibit their activity by inducing histone acetylation. DR5 is upregulated by DNA damaging agents and radiation in a p53-dependent manner. Analysis of the DR5 gene found p53 and NFκB binding sites in the first intron. Using ChIPs on HEK293 cells we found that the p65 subunit of NFκB and p53 bind to the DR5 gene upon treatment with either etoposide, an apoptotic stimulus, or epidermal growth factor (EGF), a survival stimulus, and that p53 is required for the binding of p65 under etoposide treatment. Using luciferase assays on HEK293 cells we have determined that the basal level of promoter activity of DR5 dependent on NFκB activation, p65 expression, and the p53 and NFκB binding sites in the first intron. Using ChIPs on HEK293 cells, we have determined that there is acetylation of histone H3 occurring on the DR5 gene following etoposide treatment and that HDAC1 is recruited to the DR5 gene upon treatment with EGF and requires the binding of p65. Using ChIPs on HEK293 cells we have determined that treatment with HDAC inhibitor trichostatin A (TSA) enhanced the binding of p53 and NFκB to the DR5 gene but not HDAC1. Understanding the mechanism of DR5 gene expression could lead to its use as a target for chemotherapy in combination with other drugs, such as HDAC inhibitors. Chronic lymphocytic leukemia (CLL) is the most common form of leukemia in Manitoba, with approximately 100 new patients every year. Due to resistance to standard treatment, chlorambucil (CLB) and fludarabine (FLU), new therapies are required. DR5 is upregulated in many cancer cell lines, including primary CLL cells, however, upregulation of DR5 is not observed in normal lymphocytes. Using ChIP assays on primary CLL cells, we have found that the p65 subunit of NFκB and p53 are bound to the DR5 gene in CLL cells following either CLB or FLU treatment. In addition, acetylated histone H3 is found on the DR5 gene corresponding to p300 binding to the DR5 gene. HDAC1 is not found on the DR5 gene following FLU treatment and only at later time points following CLB treatment. Lysophosphatidic acid (LPA) was used as a survival stimulus, as CLL cells do not express EGF receptors. Using ChIP assays on primary CLL cells, we have found that the p65 subunit of NFκB and HDAC1 bind to the DR5 gene following LPA treatment, however there is no acetylated histone H3, p53 binding, or p300 binding to the DR5 gene. Using western blot, acid urea gels, and immunohistochemistry, we have determined that the overall level of histone acetylation is increased in CLL patient cells compared to normal cells. In addition, the level of acetylation is increased in CLL cells treated with FLU and decreased in CLL cells treated with LPA, compared to untreated cells, and that LPA protects against the FLU-induced acetylation. We have also determined that the overall level of histone phosphorylation is increased in CLL patient cells compared to normal cells. In contrast to acetylation, FLU did not induce an increase in histone phosphorylation but LPA did induce a decrease in histone phosphorylation. Histone methylation levels do not seem to be affected by either FLU or LPA treatment and there seems to be no difference between CLL and normal cells. These findings suggest that histone acetylation, p53, and NFκB are important in the regulation of DR5 gene expression and this could provide a mechanism to sensitize CLL cells to TRAIL-induced apoptosis.

ACKNOWLEDGEMENTS

First, I would like to thank my supervisor, Dr. Spencer Gibson, for the opportunity to work on this project and complete my master's degree in his lab. I could not have asked for a better supervisor. His willingness to offer his help, guidance, and knowledge whenever it was needed allowed me to always understand the purpose of each experiment and enabled me to complete my project with very few problems. He taught me to think critically, to set my goals high, and has made my time in the lab a great experience. I would like to thank my committee members, Dr. James Johnston and Dr. Jim Davie, for their guidance and advice throughout my time in the lab. They have both been a great source of knowledge in their respective fields. Thank you to CancerCare Manitoba and the Manitoba Institute of Child Health for the funding of my project.

I also need to thank Dr. Johnston for his help in the clinic, recruiting CLL patients for this study, as well as his guidance in CLL meetings every Friday. I would also like to thank all the nurses and technicians in the Department of Hematology for collecting the blood samples, with special thanks to Donna for consenting the CLL patients and Brenda for isolating the B cells from the blood samples.

I could not have completed my degree, nor had as much fun doing it, without the people in the Gibson/Johnston lab. I have made many great friends while working in the lab that have made this experience invaluable. To Meghan, thank you for all the great Hussieni stories and talks in our aisle, you are wise beyond your years. To Nicolle, thank you for being a great friend and bench partner and for all of the laughs. Your kindness and strength of character will make you a great doctor. To Liz, thank you for all your support and encouragement. You have been a great friend. To Brenda, thank you for all the chats in your office and the recipes. Thank you for all the walks, the advice, and the chocolate. And last but certainly not least, my lab mom, Eileen. You have been a constant support and source of encouragement. From the early morning chats to a hug anytime I needed one. Your friendship is one of the most precious things I will take with me.

Last, but no less important, I would like to thank my family. To my mom and dad, thank you for your encouragement and confidence in me. You have taught me the drive to succeed and to never sell myself short. To my brother, thank you for never caring about science, or how I did at school, and always being there to make me laugh. And to Andy, thank you for always being there to celebrate the goods times, to buy me ice cream in the bad times, and for always making me smile.

TABLE OF CONTENTS

LIST OF FIGURES

LIST OF TABLES

LIST OF ABBREVIATIONS

α	alpha
β	beta
Δ	delta
ε	epsilon
κ	kappa
λ	lambda
Ψ	psi
μ	micro
ΔΨm	mitochondrial transmembrane potential
μg	microgram
μL	microlitre
μm	micrometer
μM	micromolar
%	percent
Ab	antibody
AcH3	acetylated histone H3
ADP	adenosine di-phosphate
α-MEM	alpha – minimal essential media
amp	ampere
APS	ammonium persulfate
ATP	adenosine tri-phosphate
BCS	bovine calf serum
β-gal	beta-galactosidase
BH	Bcl-2 homology
BSA	bovine serum albumin
°C	degree Celsius
cAMP	cyclic-adenosine monophosphate
CARD	caspase activation and recruitment domain
CBP	CREB-binding protein
CD	cluster differentiation
cdk	cyclin-dependent kinase
cGMP	cyclic-guanine monophosphate
ChIP	chromatin immunoprecipitation
CLB	chlorambucil
CLL	chronic lymphocytic leukemia
CO_2	carbon dioxide
dH_20	distilled water
ddH_20	deionized distilled water

DAPI	4', 6-diamidino-2-phenylindole
DD	death domain
DcR1	decoy receptor 1
DcR2	decoy receptor 2
DED	death-effector domain
DISC	death-initiating signaling complex
DMEM	Dulbecco's Modified Eagle Media
DMSO	dimethylsulfoxide
DNA	deoxyribonucleic acid
DNMT	DNA methyltransferase
DR4	death receptor 4
DR5	death receptor 5
ECL	enhanced chemiluminescence reagent
EDG	endothelial differentiation gene
EDTA	ethylenediaminetetraacetic acid
EGF	epidermal growth factor
FADD	Fas-associated death domain
FasL	Fas ligand
FBS	fetal bovine serum
FCS	fetal calf serum
FLU	fludarabine
g	gram
H_20	water
HAT	histone acetyltransferase
HBSS	Hank's balanced salt solution
HCl	hydrochloric acid
HDAC	histone deacetylase
HEK	human embryonic kidney
HEPES	N-(2-Hydroxyethyl)piperazine-N'-(2-ethanesulfonic acid) hemisodium salt
HMT	histone methyl transferase
H_2SO_4	sulfuric acid
IAP1/2	inhibitor of apoptosis protein 1/2
Ig	immunoglobulin
IgV_H	immunoglobulin heavy chain
IκB	inhibitor-of-κB
IKK	IκB kinase
JNK	c-Jun N-terminal kinase
KCl	potassium chloride
$KHCO_3$	potassium hydrogen carbonate
KH_2PO_4	potassium dihydrogen phosphate
KOH	potassium hydroxide
L	litre
LB	Luria Bertani
LiCl	lithium chloride
LPA	lysophosphatidic acid

M	molar
MAPK	mitogen activated protein kinase
MBD	methyl-binding domain
MEF	mouse embryonic fibroblast
mg	milligram
$MgCl_2$	magnesium chloride
mL	millilitre
mm	millimeter
mM	millimolar
mRNA	messenger RNA
N	normality
Na	sodium
NaCl	sodium chloride
Na_2EDTA	sodium ethylenediaminetetraacetic acid
NaF	sodium fluoride
NFκB	nuclear factor kappaB
NH_4Cl	ammonium chloride
O.D.	optical density
PAGE	polyacrylamide gel electrophoresis
PAR	poly-ADP-ribosylation
PCAF	p300/CBP-associated factor
PBS	phosphate buffered saline
PCR	polymerase chain reaction
PKA	protein kinase A
pmol	pico mole
PMSF	phenylmethanesulfonyl fluoride
PP1	protein phosphatase 1
PVDF	polyvinylidene difluoride membrane
RNA	ribonucleic acid
RNase A	ribonuclease A
RNA pol	RNA polymerase
rpm	revolutions per minute
SAHA	suberoylanilide hydroxamic acid
SBHA	suberic bishydroxamate
SDS	sodium dodecyl sulfate
siRNA	small interfering RNA
Ser	serine
TBE	Tris-borate-EDTA buffer
TBP	TATA-Box Binding Protein
TBS	Tris buffered saline solution
TBST	Tris buffered saline-Tween 20 solution
TE	Tris-EDTA buffer
TEMED	N,N,N',N',-Tetramethylethylenediamine
Thr	threonine
TNF	Tumor necrosis f actor
TNFR	Tumor necrosis factor receptor

TRAIL	Tumor necrosis factor-related apoptosis inducing ligand
TRIS	Tris(hydroxymethyl)aminomethane
TSA	trichostatin A
UT	untreated
UV	ultraviolet
VEGF	vascular endothelial growth factor
VPA	valproic acid
v/v	volume / volume
x g	times gravity
ZAP-70	zeta-associated protein 70

1.1 APOPTOSIS

1.1.1 Introduction

Cell death is an integral part of the normal life of multicellular organisms. Along with cell division and migration, regulation of cell death allows for the tight control of cell number and tissue size, as well as protecting the organism from unwanted, damaged, or virally infected cells that would threaten its homeostasis (1, 2). The term apoptosis was suggested by Kerr et al. in 1972 to describe a form of cell death used to dispose of unwanted cells during embryonic development, normal cell turnover in proliferating tissues, and in pathological situations (3). Apoptosis can be observed with an electron microscope by identifying morphological changes (See Figure 1). Within the nucleus, chromatin are condensed and in the later stages of apoptosis the nucleus is fragmented into several particles. Upon disintegration of the cell, these particles are packaged into apoptotic bodies and are taken up by phagocytes and neighboring cells (1, 3). In terms of the cell's shape, the cells round up and sever contacts with neighboring cells. In addition, protrusions, or "blebs", from the cell surface become visible and later condensation/shrinkage of the cell occurs leading to its disintegration into apoptotic bodies (1, 3, 4). Molecular changes also occur during apoptosis, such as internucleosomal DNA cleavage and the random distribution of phosphatidyl serine between the inner and outer leaflets of the plasma membrane (4, 5). Due to the extensive impact that apoptosis has on the organism, abnormalities in this process can lead to diseases such as cancer, autoimmune diseases, and degenerative disorders (5). There are two main apoptotic pathways; the intrinsic pathway, operated through the mitochondria, and the extrinsic pathway, operated through TNF ligands and the TNFR

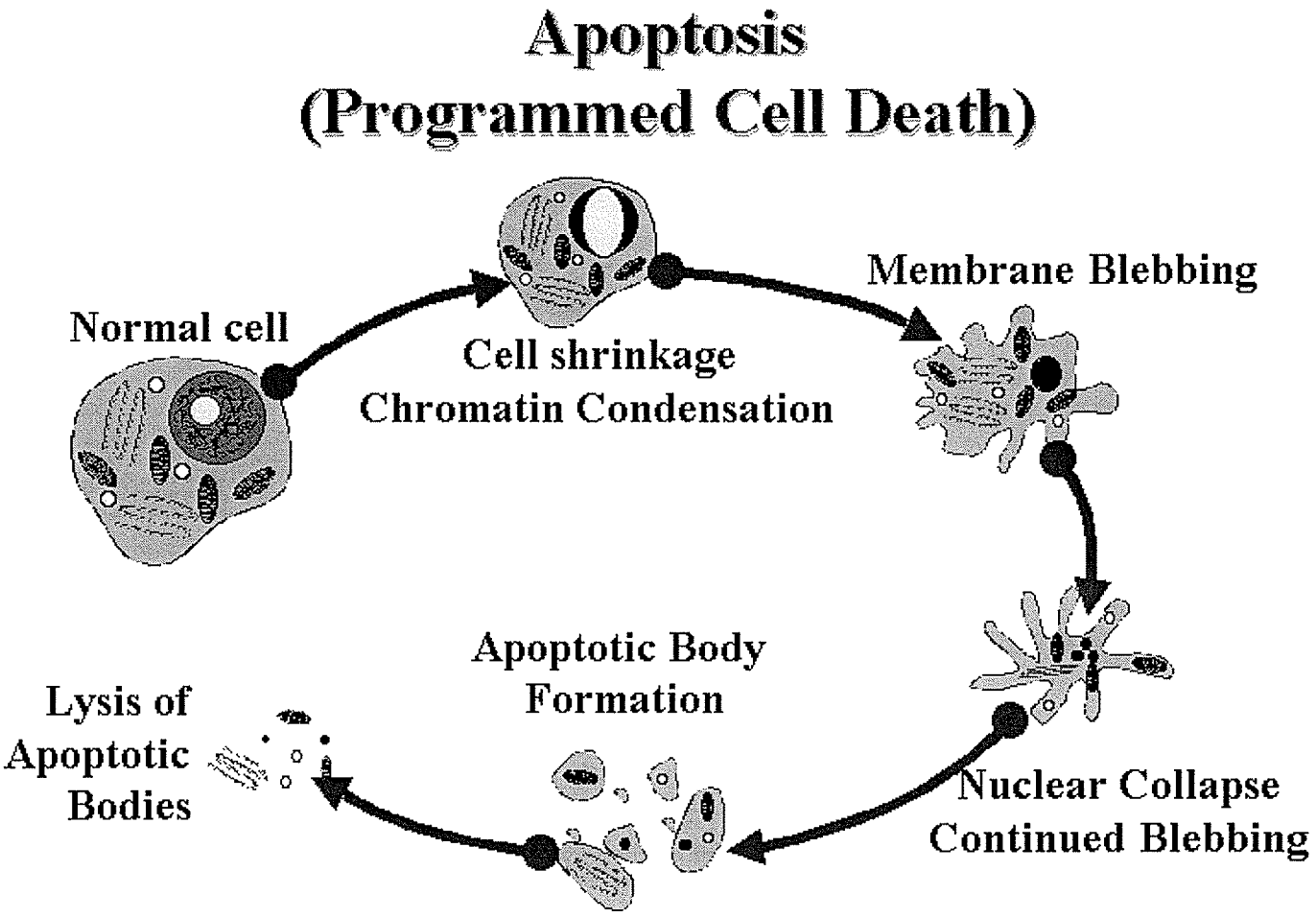

Figure 1

Diagram illustrating the morphological changes that occur to the cell when it undergoes apoptosis.
(http://www.micro.msb.le.ac.uk/3035/kalmakoff/baculo/pics/Apoptosis.gif)

family. There are thought to be four major groups involved in the regulation of these apoptotic pathways. They are caspases, adaptor proteins, members of the tumor necrosis factor receptor (TNFR) superfamily, and the Bcl-2 family of proteins.

1.1.2 Caspases

Caspases were first implicated in the process of apoptosis with the discovery of CED-3 and its involvement in cell death in the nematode *Caenorhabditis elegans* (6). Its discovery lead to the identification of the first caspase (caspase-1 or interleukin-1β-converting enzyme (ICE)) in mammals due to its similarities to CED-3 (6). At least 14 caspases have been identified in mammals (1, 5). Caspases are cysteine proteases that are highly conserved through evolution, having been found in humans down through hydra (2, 5). They recognize a tetrapeptide motif, four residues amino-terminal to the cleavage site, that gives them distinct substrate specificities (2, 5). They cleave their substrates on the carboxyl side of an aspartate residue. Caspases are synthesized as zymogens, with very low intrinsic enzyme activity. The zymogens are composed of three domains: an N-terminal prodomain, and the p20 and p10 domains, found in the mature enzyme (2). The functional enzyme is a heterotetramer composed of two p20 subunits and two p10 subunits (2, 5). The functional enzyme is produced by cleavage from another caspase or it is also thought possible that an aggregation of caspase zymogens can self-initiate cleavage and activation (1, 5). The cascades of caspases found in the apoptotic pathways are thought to be initiated by the activation of an initiator caspase, such as caspase 8 or 9, through protein-protein interaction, involving their death effector domain, and leading to the activation of downstream effector caspases, such as caspase 3 or 7 (5, 7, 8). Caspase 8

is the initiator caspase in the extrinsic apoptotic pathway and caspase 9 is the initiator caspase in the intrinsic apoptotic pathway (2). The pathway that each caspase affects is likely based on its protein-protein interaction module within its prodomain (2). This module allows each caspase to bind to and associate with upstream regulators. Caspase-8 and –10 contain a death-effector domain (DED), whereas caspase-2 and –9 contain a caspase activation and recruitment domain (CARD) (2).

1.1.3 Adaptor Proteins

Adaptor proteins link the cell death effectors, caspases, with the cell death regulators, death receptors, and Bcl-2 family members. The adaptor proteins form a bridge between the caspases and the upstream regulators of apoptosis (5). These bridges are made through domains such as the death domain (DD), the death effector domain (DED), and the caspase recruitment domain (CARD) (5). The adaptor proteins such as Apaf-1 in the intrinsic apoptosis pathway and death receptors in the extrinsic apoptosis pathway were discovered through their homology to CED-4 in *C. elegans* (9). Other examples of adaptor proteins include FADD, TRADD, etc.

1.1.4 The Tumor Necrosis Factor Receptor (TNFR) Family

Members of the TNFR family are pleiotropic. They can trigger proliferation, survival, differentiation, or death, depending on the cell type and the other signals received by the cell (5). Examples of members of the TNFR family include TNF-R1, CD95, death receptor 4 (TRAIL-R1, DR4), death receptor 5 (DR5), and decoy receptor 1 (DcR1). These receptors are activated by ligands belonging to the TNF ligand family, such as

TRAIL, most of which are synthesized as membrane-anchored trimers (5). Members of the TNFR receptor family contain cytoplasmic regions that are essential for inducing apoptosis. CD95 and TNF-R1, as well as others, contain a death domain (DD) within their cytoplasmic regions, allowing them to interact with adaptor proteins.

1.1.4.1 Death Receptor 5 (DR5)

DR5, also known as TRAIL-R2, Apo2, TRICK2, and KILLER, is a member of the tumor necrosis factor receptor (TNFR) superfamily. It possesses a death domain sequence within its C-terminus that is required to induce cell death. DR5 is a receptor for the ligand TRAIL and their association leads to the induction of the extrinsic pathway of apoptosis. Death receptor 5 (DR5) is upregulated by DNA damaging agents and radiation in a p53-dependent manner (10). It has been shown that up-regulation of DR5 in lung cancer cell lines is p53 dependent (10), as well, primary chronic lymphocytic leukemia (CLL) cells lacking functional p53 fail to up-regulate DR5 following genotoxin treatment (11). The p53 responsive element responsible for DR5 expression has been identified in the first intronic region of the DR5 gene (10). Another factor involved in the up-regulation of DR5 is the transcription factor NFκB. Blockage of NFκB effectively inhibits etoposide and TRAIL induced DR5 expression and any synergistic apoptotic response (12, 13). The binding of TRAIL to DR5 also leads to the activation of NFκB. A putative NFκB binding site has been identified in the first intronic region of the DR5 gene near the p53 responsive element (14). Although we know some of the factors involved in the regulation of DR5 gene expression we do not know the mechanism for the regulation of the DR5 gene at the transcriptional level.

1.1.5 The Bcl-2 family of proteins

In mammals, the Bcl-2 family of proteins is made of 20 relatives of the Bcl-2 protein, all sharing at least one conserved Bcl-2 homology (BH) domain (See Figure 2) (15). The Bcl-2 family of proteins includes differentially regulated mammalian homologs of CED-9 (1). This family of proteins is divided into two groups, those that inhibit apoptosis and those that promote apoptosis. Some members of this family can homodimerize however the pro-apoptotic members and the anti-apoptotic members can heterodimerize thereby neutralizing the other's effect (2). Therefore whether a cell survives following an apoptotic stimulus could be determined by the ratio of pro-apoptotic versus anti-apoptotic members, as well as the level of caspase activation (1). Bcl-2, Bcl-x_L, Bcl-w, A1/Bfl-1, and Mcl-1 promote cell survival whereas Bax, Bak, Bid, Bik/Nbk, and Bim/Bod induce apoptosis (5). The anti-apoptotic members associate with the mitochondrial outer membrane, endoplasmic reticulum, and the nuclear envelope through their hydrophobic carboxy-terminal domain. They can prevent cytochrome c release from the mitochondria and therefore prevent caspase 9, and probably others, from activation (15). The presence of the pro-apoptotic members is essential for apoptosis, specifically Bax and Bak (15).

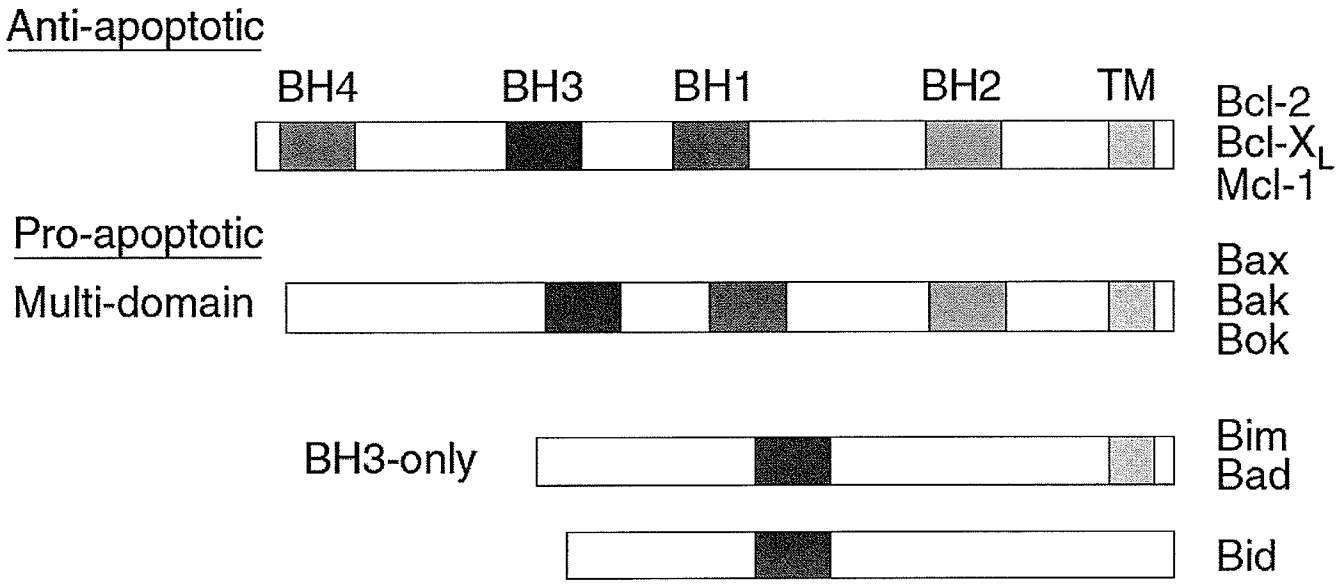

Figure 2

Schematic diagram of representative Bcl-2 family proteins. Examples of anti-apoptotic (Bcl-2, Bcl-X_L, and Mcl-1), pro-apoptotic multidomain (Bax, Bak, and Bok), and pro-apoptotic BH3-only (Bid, Bim, and Bad) proteins are shown. Bcl-2 homology (BH) and transmembrane (TM) domains are indicated (137).

1.1.6 Two Main Pathways for Induced Apoptosis

1.1.6.1 The Mitochondrial Pathway (Intrinsic Pathway)

The intrinsic pathway is induced by stress such as DNA damage or withdrawal of growth factors and survival stimuli (8). This pathway involves the release of molecules, normally contained within the intermembrane space of the mitochondria, into the cytosol under the influence of the Bcl-2 family of proteins (see Figure 3) (16). The events leading to the release of molecules include pore formation in the external mitochondrial membrane by proteins such as Bax, rapid loss of mitochondrial transmembrane potential $\Delta\Psi m$ following permeability transition and disruption of the outer membrane as a result of mitochondrial swelling(16). Cytochrome c is one of the molecules released into the cytosol. It recruits the caspase adaptor molecule Apaf-1, which in turn binds to the initiator caspase, procaspase-9, forming an apoptosome complex (8, 16). This leads to the activation of caspase 9, activating a downstream caspase cascade, and ends in the induction of apoptosis (8, 16).

1.1.6.2 The Death Receptor Pathway (Extrinsic Pathway)

Binding of a ligand trimer from the TNF ligand family, such as TRAIL, to a receptor from the TNFR receptor family, such as DR5, induces trimerization of the receptor. This leads to the formation of a DISC (death-initiating signaling complex) complex consisting of the ligand –receptor trimer and an adaptor protein called FADD (Fas-associated death domain), which is constitutively bound to procaspase-8 (see Figure 3). FADD binds to the cytoplasmic region of the receptor through their respective death domains and binds to procaspase-8 through a death effector domain (8, 16, 17). The formation of the

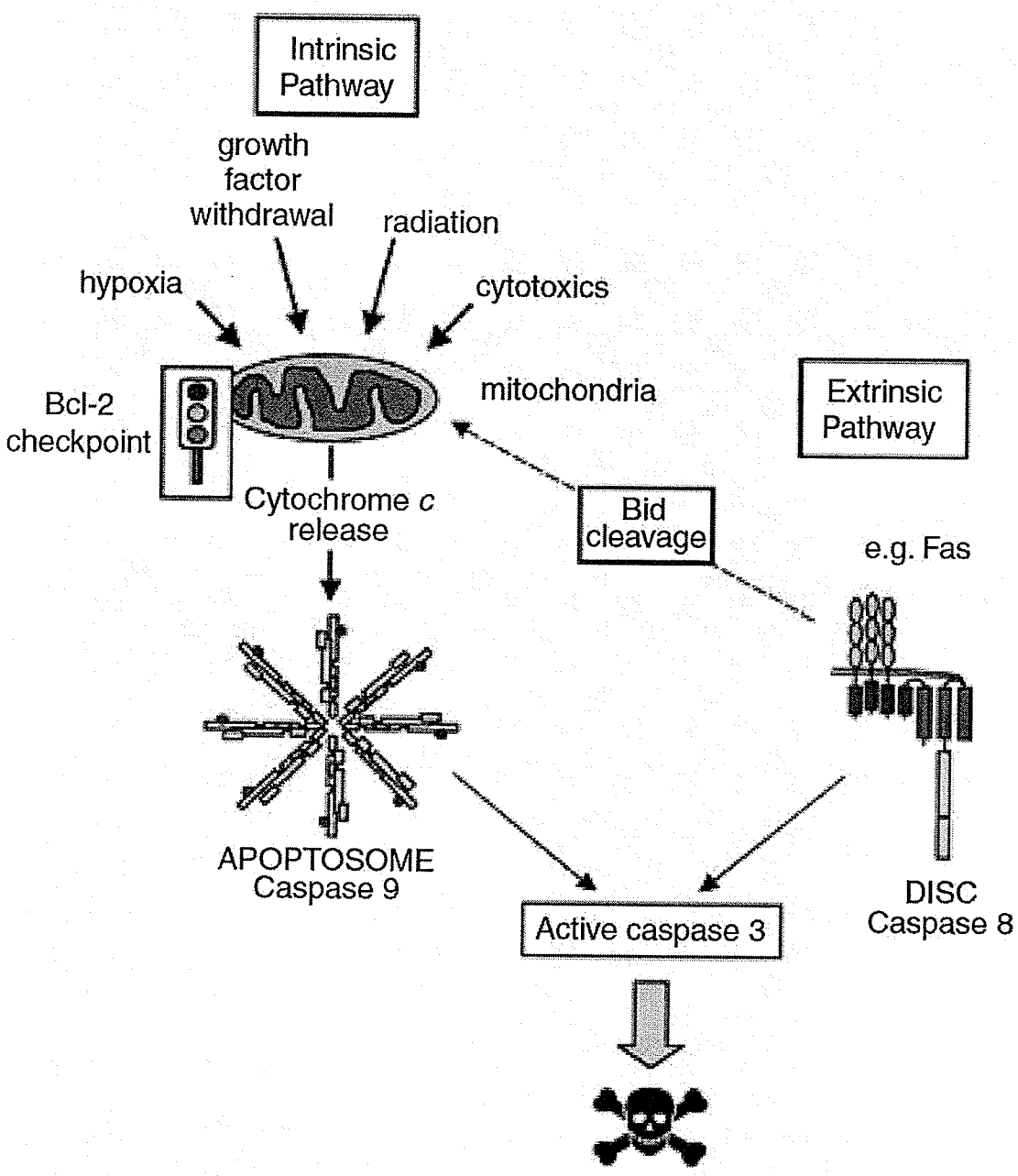

Figure 3

Schematic diagram of the two main pathways of apoptosis. The "intrinsic" and "extrinsic" apoptosis pathways converge on the effector caspase, caspase 3, and promote apoptosis. The "extrinsic" pathway is activated by cell-surface death receptors, such as Fas and DR5, and is mediated by the activation of caspase 8, within a death-inducing signalling complex (DISC). The "intrinsic" pathway is activated by a wide range of stimuli which trigger the release of cytochrome c from the mitochondria. This leads to the activation of caspase9, within the apoptosome. In some situations the two pathway are combined (137).

DISC complex leads to the activation of caspase 8 which either directly activates a caspase cascade leading to apoptosis or it cleaves the pro-apoptotic member of the Bcl-2 family, Bid, leading to the translocation of tBid to the mitochondria activating the mitochondrial pathway of apoptosis (16, 17). Two specific examples of this pathway include the FasL-Fas pathway and the TRAIL-DR4/DR5 pathway (8).

1.2 REGULATION OF TRANSCRIPTIONAL ACTIVATION OF A GENE

Controlling the selective expression of genes involves limiting the access of transcription factors to the genomes. This is achieved by packaging the genes into chromatin, thereby preventing the binding of transcription factors to their target DNA (18). A diverse group of enzymatic complexes are involved in the regulation of accessibility to the DNA by modulating the nucleosome structure through histone modifications or ATP-dependent remodeling (18). It has been shown that these complexes function in a promoter-specific manner determined by their association with particular classes of DNA binding proteins (19, 20). The order in which these proteins associate with their target promoters is perhaps gene specific however one popular view is that the activators must first bind to the promoters in conjunction with chromatin-remodeling or –modifying complexes. The core promoter recognition factors (TFIIA, B, D, E, F, and H) and RNA pol II are then recruited, forming an active initiation complex (18). In addition to these factors, the process of transcription also requires proteins called "mediators". These proteins interact with either repressors or activators and RNA pol II and either facilitate or repress

transcription by relaying signals between the regulatory factors and the basal initiation machinery (18).

1.2.1 NF kappa B (NFκB)

NFκB is an ubiquitously expressed family of proteins consisting of five members; p65 (RelA), p50, c-Rel, p52, and RelB (21, 22). These proteins share sequence similarity through an approximately 300 amino acid Rel homology domain (RHD). The N-terminal portion of the RHD mediates both backbone and sequence-specific contacts with the major groove of DNA whereas although the C-terminal portion also contributes to backbone contacts, it also controls dimerization with other Rel family members (23). All NFκB members bind DNA, however only p65, c-Rel, and RelB have extended carboxy termini harboring transactivation function (24). NFκB subunits are able to form heterodimers or homodimers with the predominant form of NFκB in cells being a p65/p50 heterodimer. NFκB is an inducible transcription factor that plays a role in both survival and apoptotic signaling pathways, as well as immune and inflammatory responses (21, 22, 24-29). In unstimulated cells, NFκB complexes are normally sequestered in the cytoplasm as a result of their interaction with members of the inhibitor-of-κB (IκB) family (21). In response to external stimuli, IκB kinase (IKK), a multimeric kinase complex, phosphorylates IκB (30). Phosphorylated IκB is then targeted for ubiquitination and proteosomal degradation, allowing the nuclear translocation of NFκB complexes (see Figure 4). Once in the nucleus, NFκB can bind to cognate sequences of DNA present in a wide array of gene promoters leading to

Activation of NFκB

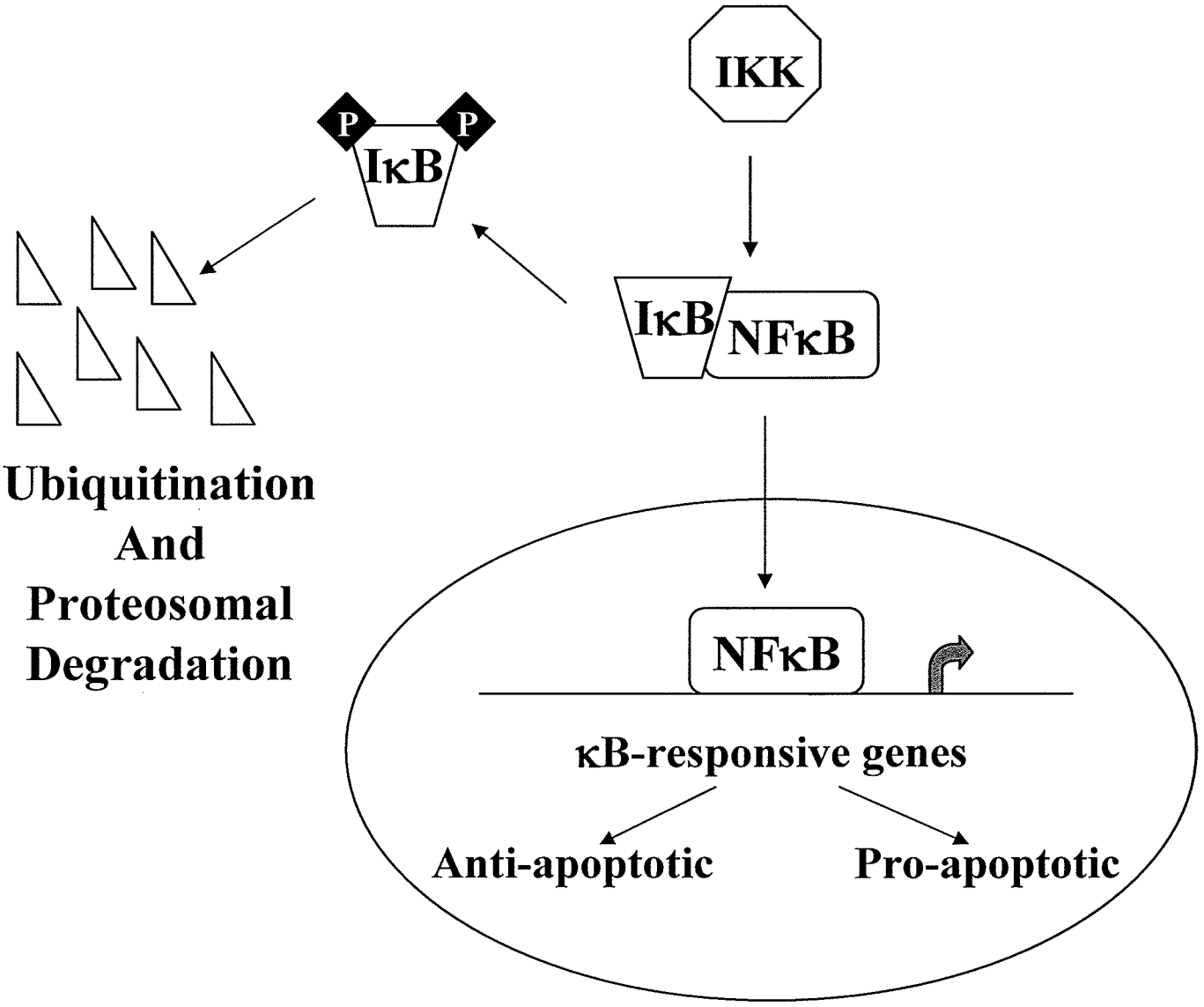

Figure 4

Schematic diagram of NFκB activation. NFκB is complexed with inhibitor-of-κB (IκB) and sequestered in the cytoplasm. In response to an external stimuli, IκB kinase (IKK) phosphorylates IκB. Phosphorylated IκB is then targeted for ubiquitination and proteosomal degradation allowing the translocation of NFκB into the nucleus, enabling it to bind to sequences of DNA in a wide array of promoters leading to transcriptional activation.

transcriptional activation. In particular, NFκB is involved in the up-regulation of anti-apoptotic genes such as Bcl-2, Bcl-x_L, Mcl-1, and Inhibitor of apoptosis protein 1/2 (IAP1/2) that effectively promote cell survival (31-35). Our lab has previously shown that epidermal growth factor (EGF), an inducer of survival, induces NFκB upregulation of Mcl-1 expression by blocking TRAIL induced cell death (32). In contrast, NFκB has been implicated in the upregulation of the pro-apoptotic genes DR5, Fas, and FasL (32). It has been shown that blocking NFκB activation leads to the inhibition of DR5 expression in epithelial derived cell lines (13). Our lab has shown that if NFκB activation is inhibited, the pro-apoptotic DR5 gene is not up-regulated (36). NFκB activation also cooperates with p53 to induce apoptosis (37).

1.2.2 p53

The p53 gene was first discovered in 1979 (38). It is a polyfunctional protein that functions in the nucleus (39). It forms a tetrameric complex that recognizes specific DNA sequences, stimulating transcription of genes having an appropriate DNA element adjacent to their promoter (39). The p53 protein consists of 392 amino acids and contains two N-terminal activation domains, a sequence-specific DNA binding domain, and a C-terminal oligomerization domain (39-41). The N-terminal sequence (amino acids 1-50) contains a domain involved in the activation of transcription of target genes and also plays a role in the regulation of p53 activity (39). The central domain (amino acids 100-300) participates directly in the recognition and binding of specific DNA sequences and is the site of most missense mutations (39). A linker sequence (amino acids 305-323) is responsible for the nuclear localization of p53 and a locus between amino acids 323 and

356 is responsible for its tetramerization (39). The DNA binding activity of p53 is thought to be negatively regulated through two regions within its C-terminal domain (amino acids 363-393) and this inhibition can be relieved by acetylation, phosphorylation, or protease cleavage (39, 40, 42). p53 is a short-lived protein that is maintained at low, often undetectable levels in normal cells (43). The p53 gene is continuously transcribed and translated, however the protein is rapidly subjected to ubiquitin-dependent proteosomal degradation (39). It is only activated/stabilized when cells are under stress or damaged (38). Damage as small as a single break in double-stranded DNA is all that is needed to trigger an increase in p53 levels and produce a response (38, 41). There are thought to be three independent pathways by which p53 is activated. The first pathway is induced by DNA damage, such as that caused by ionizing radiation. The second pathway is induced by aberrant growth signals, such as those from the expression of oncogenes Ras or Myc. The third pathway is induced by chemotherapeutic drugs, ultraviolet light, and protein-kinase inhibitors (38). All three of the pathways stabilize p53 at high concentrations by inhibiting its degradation, allowing it to bind to specific DNA sequences and activate the expression of adjacent genes leading to apoptosis or the inhibition of cell division (38). p53 is a sequence-specific DNA binding protein that activates the transcription of many target genes such as p21, Mdm2, GADD45, and Bax (40). The p21-WAF1 protein is a powerful inhibitor of cyclin-dependent kinases (cdk) and is responsible for the arrest at the G_1 phase of the cycle. This arrest occurs as a result of the over-expression of p53 following DNA damage (7, 39). The BAX gene contains a p53-responsive element and can be activated by p53 (39). Its expression promotes apoptosis by increasing the release of cytochrome c from the

mitochondria (39). The Fas-receptor gene (APO1), as well as the DR5 gene, are activated by p53 (39). Expression of either of these genes leads to a caspase cascade and eventually apoptosis. p53 has also been shown to interact with NFκB. Expression of p53 leads to an increase in NFκB DNA-binding activity, with NFκB consisting mainly of the p50 and p65 subunits, in turn, loss of NFκB activity diminishes the p53-mediated apoptotic response (37, 44). In order for p53 to activate transcription of these and other genes it must interact with a specific DNA element and other molecules to form a complex. It requires the interaction of its N-terminal transcription-activator region with components of the transcription apparatus, such as proteins of the TFIID complex including TBP (TATA-Box Binding Protein) and TBP-associated factor TAFII (39). In addition to the components of the transcription apparatus the presence of coactivators, CREB-binding protein (CBP) and p300, is required (39). These coactivators display histone acetylase activity, facilitating the access of the chromatin to the transcription machinery. The p53 gene was the first gene identified as a tumor suppressor gene and is the most frequently mutated gene in cancers, with it occurring in approximately 50% of all human cancers (38, 41, 43). The p53 protein prevents the multiplication of stressed cells by temporarily inhibiting progress through the cell cycle for repair or can cause apoptosis of the cells in an attempt to contain the damage and protect the organism (38, 39). Mutations of p53 commonly result in cancer because it regulates such important processes as cell cycle progression and apoptosis. Mice in which p53 is knocked out, produce normal offspring; however, they rarely live more than six months because they are extremely sensitive to tumor development and progression (39).

1.3 HISTONES

1.3.1 Background

The basic structural repeating unit of chromatin is the nucleosome, around which 146 bp of DNA are wrapped. The nucleosome is made of an octamer of histones consisting of two histone H2A-H2B dimers bound to a histone H3 and H4 tetramer (45). The four core histones, H2A, H2B, H3, and H4, have a basic N terminal tail and a central globular domain, organized into a histone fold and a C terminal tail. The central histone fold domain is involved in histone-histone and histone-DNA interactions and therefore is important in histone octamer and nucleosome formation (46). The histone N terminal tails protrude from the core particle in all directions and vary in length (46). These N terminal tails can undergo a series of post-translational modifications, such as acetylation, phosphorylation, methylation, ubiquitination, and sumoylation, at specific amino acids.

1.3.2 Histone Modifications

Histones can undergo a series of post-translational modifications including lysine acetylation, lysine and arginine methylation, serine and threonine phosphorylation, ADP-ribosylation, ubiquitination, and sumoylation (See Figure 5) (47). Most of these modifications occur on the N-terminal tail domain, with the exception of ubiquitination which occurs on the C-terminal tail domain (48). These modifications lead to the remodeling of chromatin and therefore have an effect on the transcription process. The "histone code hypothesis" was put forward to try to explain the complex nature in which these modifications interact with each other. It states that one modification, or a specific combination of histone modifications, can affect distinct downstream events by altering the structure of the chromatin and/or generating a binding platform for protein effectors that can specifically recognize the modification(s) and initiate gene transcription or repression (47).

1.3.3 Histone Acetylation

1.3.3.1 Characteristics

Histone acetylation is the best-studied histone modification to date. It occurs at the ε amino groups of the lysine residues located on the N-terminal tails of histones. Each core histone, with the exception of H2A, can be acetylated at 4 to 5 sites giving the nucleosome 26 sites of acetylation (48). It is known to regulate transcription by remodeling chromatin structure. Acetylation of the core histones disrupts the nucleosome structure resulting in the unfolding of chromatin. This allows transcription factors access to bind their target promoters. The N-terminal domain of histones can be acetylated at various lysine residues (5 in H3; 4 in H4; 4 in H2B; and 1 or 2 in H2A) and therefore can

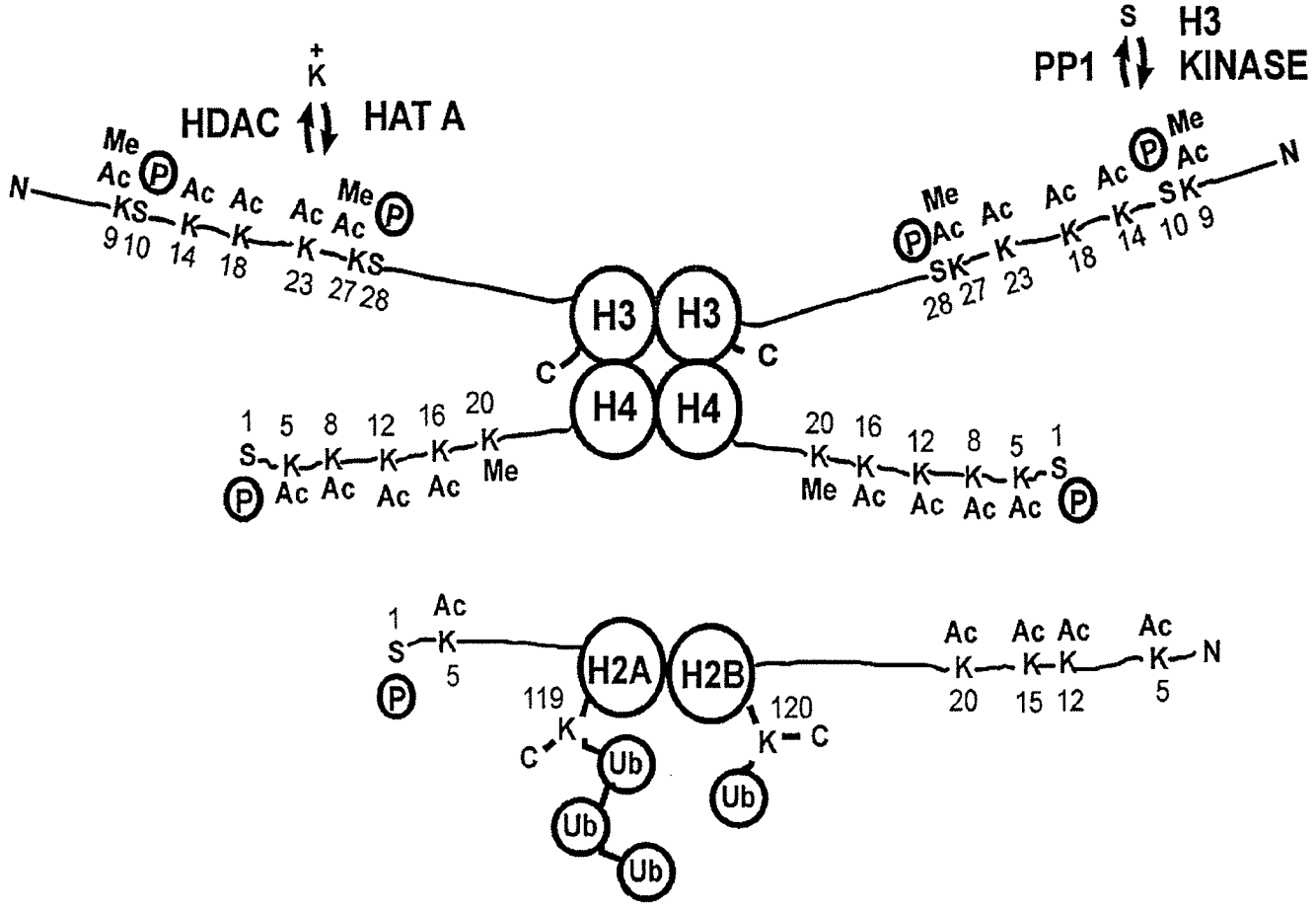

Figure 5

Schematic diagram depicting the sites of post-synthetic modifications on the histones. The structures of the H2A-H2B dimers, $(H3\text{-}H4)_2$ tetramers, and the sites of modification are shown. The modifications shown are acetylation (Ac), methylation (Me), phosphorylation (P), and ubiquitination (Ub). The enzymes catalyzing reversible acetylation and phosphorylation are shown (HAT, histone acetyltransferase, HDAC, histone deacetylase, PP1, protein phosphatase 1) (45).

be mono-, di-, tri-, and tetra-acetylated (49). Acetylation of histones is regulated by the opposing activities of histone acetyltransferases (HATs) and histone deacetylases (HDACs) (see Figure 6).

1.3.3.2 Histone Acetyltransferases (HATs)

HATs transfer the acetyl moiety from acetyl coenzyme A to the N-terminal lysine of the histone protein and neutralize its positive charge. This leads to the relaxation of the chromatin structure and allows for active transcription (23). Examples of potent HATs are CBP (CREB-binding protein), p300, PCAF (p300/CBP-associated factor), and Tip60. They also exist in multiprotein complexes that recruit general transcription factors and RNA polymerase II (49). Each HAT has a different target substrate and the specificity for this substrate depends on the proteins associated with the HAT (46).

1.3.3.3 Histone Deacetylases (HDACs)

HDACs are responsible for the deacetylation of histones by removing the acetyl groups from the N-terminal lysine of histone proteins and restoring the positive charge. Deacetylation leads to the folding of chromatin, limiting the access of activation factors, as well as allowing the binding of repressor complexes to the DNA, and thereby silencing transcription (23). There are three classes of HDACs, divided based on their size and sequence homologies to yeast deacetylases, but they are all a part of multisubunit complexes within the cell. Class I includes HDAC 1,2,3, and 8. They have a single deacetylase domain at the N-termini, diversified C-termini, and are constitutively nuclear, playing important roles in dynamic gene regulation (50). They are approximately 400-

Histone Acetylation

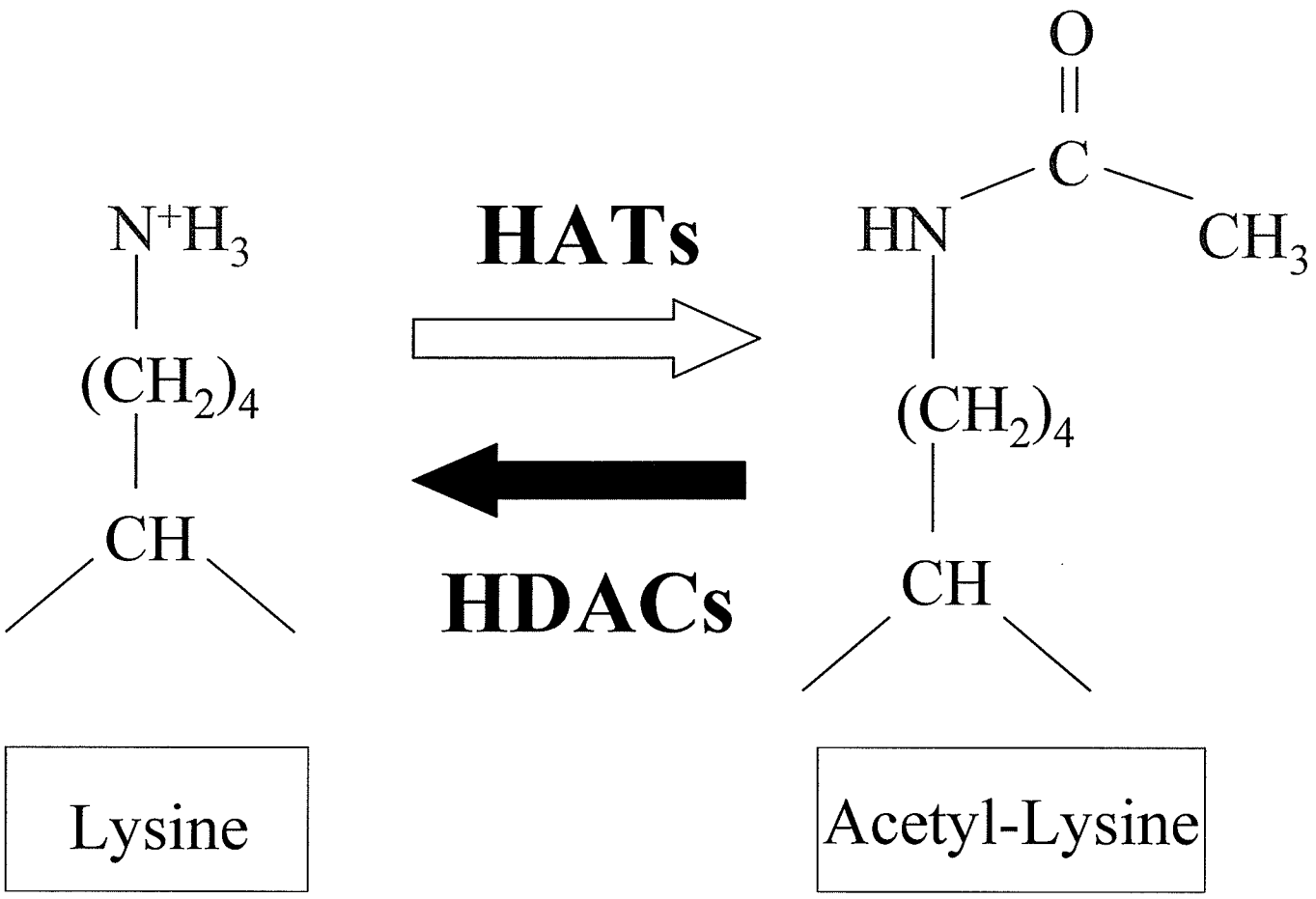

Figure 6 : Schematic representation of histone acetylation

Histones are acetylated on the lysine residues on their N-terminal tails. Acetylation is controlled by the balance between two enzymes; histone acetyltransferases (HATs) and histone deacetylases (HDACs). HATs add an acetyl group to the N-terminus, neutralizing the positive charge, and leading to the opening of the DNA helix. HDACs remove the acetyl group, restoring the positive charge, and leading to a closed DNA conformation.

500 amino acids in length and share homology with the yeast Rpd3 deacetylase (46). Class II includes HDAC 4,5,6,7,9, and 10. They have a deacetylase domain at a more C-terminal position and are capable of translocating from the cytoplasm to the nucleus in response to external stimuli (50). They are approximately 1000 amino acids and share structural homology with yeast Hda1 deacetylase (46). Class III includes deacetylases that share homology to the yeast silent information regulator (Sir 2) gene and are dependent on NAD+ and ADP-ribosylase activity (46). Sir2 functions in numerous cellular processes, including gene silencing and DNA damage repair (51). In addition to deacetylating histones it also deacetylates proteins such as p53 (51).

1.3.3.4 Protein Acetylation

Originally substrates for acetylation were thought to be mainly histones, however they now include DNA-binding proteins, non-nuclear proteins, and proteins that shuttle from the nucleus to the cytoplasm (52, 53). As well, histone acetylation has commonly been viewed as being an inducer of transcription , however, as there are acetylation targets within transcription factors this has not held true (52). Acetylation is now shown to affect not only transcription but DNA binding, protein stability, and protein-protein interactions as well. Both HATs and HDACs are recruited to specific regions of the genome by transcription factors. Transcription factors existing as multimers, such as Sp1 and p53, are capable of simultaneously recruiting HATs and HDACs, whereas recruitment by other factors, like ligand-activated transcription factors and modified factors (NFκB), is governed by the ligand or modifying enzyme (49).

1.3.3.4.1 NFκB and p53

The transcription factors p53 and NFκB associate with HATs. CBP, p300, and PCAF coactivators interact with the p65 subunit of NFκB to enhance its ability to activate transcription (24, 54). Studies have revealed that both the N-terminal RHD and the C-terminal transcriptional activation domain of p65 interact with the amino-terminal CH1 domain of p300 (55). This interaction is suggested to be regulated by the phosphorylation status of NFκB, where phosphorylation of p65 enhances the interaction between p65 and CBP (24, 54, 56). The interaction between these co-activators and NFκB also leads to the acetylation of NFκB. Acetylation of NFκB enhances its DNA binding effects, its transactivation, as well as regulating its nuclear export (54, 56).

CBP/p300 has also been shown to acetylate p53, at multiple lysine residues within its C-terminal regulatory domain (45, 57, 58). The level of p53 acetylation is increased by DNA damage and it is thought that phosphorylation in response to the DNA damage enhances the interaction of p53 with p300 and PCAF and therefore p53 acetylation (59, 60). Acetylation of p53 has been shown to not only increase p53 DNA binding activity but to also increase its stability and protein-protein interactions (58). In contrast to NFκB, p53 associates with its nucleosomal target sites in the absence of chromatin remodeling or modifying complexes and once bound it recruits p300 to the promoter (40). The N-terminal activation domain of p53 physically interacts with the carboxy-terminal portion of the CBP protein both in vitro and in vivo (43). The possibility exists that CBP and PCAF acetylation of p53 enhances its binding affinity for promoters of target genes and once bound p53 recruits a CBP-PCAF coactivator complex which then acetylates nucleosomal histones promoting access of RNA polymerase II and other basal

transcription factors to DNA (59). The acetylation of p53 seems to be tightly regulated by the action of deacetylases. This regulation is thought to be due to an indirect interaction between p53 and HDAC1 (61).

1.3.4 Histone Phosphorylation

Phosphorylation is another important histone modification, although it is less studied than acetylation. It has been associated with chromosome/chromatin condensation, including apoptosis and DNA damage, chromosome decondensation events, and events regulated by different histone kinases (47). The core histones, as well as histone H1, can undergo phosphorylation on specific serine (Ser) and threonine (Thr) residues. Histone H1 can be phosphorylated on Ser/Thr residues on both its C-terminal and N-terminal tail domains whereas histone H3 is mainly phosphorylated on Ser/Thr residues on its N-terminal tail domain (48). Phosphorylation of histones has been shown to play a role in gene transcription. Phosphorylation of histone H1 is associated with the activation of the MMTV promoter whereas dephosphorylation of histone H1 is associated with deactivation of the promoter (45). The cyclin-dependent kinases (CDKs), as well as the cAMP and cGMP dependent kinases, are involved in the phosphorylation of histone H1 (45). Phosphorylation of histone H3 occurs in the cell-cycle on both serine 10 and 28 of histone H3 and is required for the initiation of chromosome condensation in mammalian cells (62). The kinase responsible for this phosphorylation is the aurora B kinase, which works together with type 1 phosphatase (PP1) (62). It has been suggested that aurora kinase B-mediated histone H3 phosphorylation is required for the recruitment of condensin, a five-subunit protein complex required for assembly and maintenance of mitotic chromatin structure, to the chromosome (63). Histone H3 phosphorylation, on

serine 10 and 28, is also associated with the activation of the Ras-mitogen activated protein kinase (MAPK) pathway of serum starved cells, following stimulation with growth factors and phorbol esters, and is also associated with the transcriptional activation of the early response genes c-fos and c-jun (45). The state of phosphorylation is dependent upon phosphatases, kinases, as well as the acetylation state of the histone. Phosphorylation of histone H3, leading to the activation of c-fos and c-jun, is restricted to H3 histones that are highly acetylated. However it has not been shown in yeast that one modification predisposes H3 to the other (45, 64). The kinases responsible for this phosphorylation include MSK1 and MSK2, nuclear proteins which are widely expressed in tissues and belong to the AGC kinase family (64). Phosphorylation of histone H3 can also involve cAMP-dependent protein kinase A (PKA) activity as well as Rsk2, a member of the $pp90^{rsk}$ kinases (45).

1.3.5 Histone Methylation

Histone methylation can occur on both lysine and arginine residues on core histones H2B, H3, and H4. The lysine residues can be mono-, di-, or tri-methylated whereas the arginine can only be mono- or di-methylated (47). Methylation of histones can lead to both activation and inactivation of transcription depending on which residue is methylated. Methylation on the arginine residues seems to be more dynamic and correlate well with gene activation and demethylation of these residues correlates with gene inactivation (47). Conversely, methylation of lysine residues are more stable but not as straightforward. For example, methylation of lysine 4 on histone H3 correlates with gene activation whereas methylation of lysines 9 and 27 on histone H3 correlates with gene

inactivation (47). DNA methylation occurs through the activity of histone lysine (K) methyltransferases (HKMTs) and protein arginine (R) methyltransferases (PRMTs). The first HKMT was first discovered as a homologue to Su(var)3-9 in *Drosophila* but there are now many members of this family, including SUV, SET1, SET2, and RIZ (65). The HKMTs differ in their substrate specificity as well as the number of methyl groups they are able to transfer (65). PRMTs consist of two major types, where type I can catalyze the formation of monomethylarginine and asymmetric dimethylarginine and type II can catalyze the formation of monomethylarginine and symmetric dimethylarginine (65). PRMT5 has been shown to dimethylate histone H3 and H4 and PRMT1, as well as PRMT4, has been shown to methylate histones H3, H4, and H2B (65). The effect of histone methylation on transcription does not involve the disruption of the nucleosome structure, as seen with acetylation, but could involve the recruitment of effector proteins as it has been shown that pre-incubation of a chromatin template with p53 and PRTM1 significantly stimulated the HAT activity of p300 (65). Less is known about histone demethylation as the first histone lysine demethylase, LSD1, was only discovered in 2004 (66, 67). The enzyme was previously identified as a component of HDAC complexes but can demethylate mono- and di-methylated histone H3 lysine 4 in an amine oxidase reaction (68). It has been shown to play a role in both gene activation and transcriptional repression.

1.3.6 Histone Ubiquitination

Histones H2A, H2B, and H3 can be reversibly ubiquitinated. Ubiquitin is a highly conserved 76 amino acid protein that can bind to other proteins or to itself by isopeptide

bonds to form a chain of ubiquitin molecules. The carboxyl end of ubiquitin is attached to the ε amino group of lysine and both H2A and H2B can be polyubiquitinated (45). H2A is typically more highly ubiquitinated than H2B, both singly and polyubiquitinated, and ubiquitination of both core histones is associated with transcriptionally active DNA (45). The ubiquitination of histone H2B seems to be associated with transcription to a greater extent then H2A. This could be due to the location of the ubiqutination site. The C-terminal sequence of H2B is buried in the nucleosome and during transcription the nucleosome structure is disrupted, exposing this sequence to enzymes capable of catalyzing the addition of ubiquitin molecules (45).

1.3.7 Histone Sumoylation

The process of sumoylation is similar to ubiquitination however its effect in the cell is quite different. Small ubiquitin-related modifier (SUMO) is a member of a growing family of ubiquitin-like proteins (69). In mammals there are three members of the SUMO protein family; SUMO-1, SUMO-2, and SUMO-3. The process of sumoylation consists of the covalent attachment of SUMO from the E2 enzyme to the substrate protein through an enzyme cascade (E1-E2-E3), similar to ubiquitination (70). To date only one activating enzyme, one conjugating enzyme, and several ligases are known. The process of sumoylation can also be reversed through the action of SUMO-specific isopeptidases (70). Unlike ubiquitination, the outcome of sumoylation is not protein degradation. Sumoylation is involved in the regulation of protein-protein and protein-DNA interactions, cellular localization, inhibition of ubiquitin-mediated degradation, and enhancement of transcriptional activity (69, 70). It has been shown that histone H4 is

modified by sumoylation and to a lesser extent H2A, H2B, and H3 (69). Histone sumoylation has been shown to be associated with transcriptional repression through the recruitment of HDACs and heterochromatin protein 1 (69).

1.3.8 Histone ADP-ribosylation

Poly-ADP-ribosylation (PAR) modifies histone proteins. The PAR modification results in an increase in net negative charge by the addition of two ADP-ribose units, each containing a negatively charged phosphate group (71). This results in a change in electrostatic interaction between histones and DNA leading to alterations in conformation and functional state. PAR is also thought to be a potential biomarker of carcinogensis as it is known that during the initiation stage of carcinogenesis the level of PAR in cellular proteins, especially histones, is reduced (71).

1.4 CANCER TREATMENT

1.4.1 TNF-Related Apoptosis Inducing Ligand (TRAIL)

Tumor necrosis factor (TNF)-related apoptosis inducing ligand (TRAIL) is a member of the TNF ligand family. It has been shown to induce apoptosis in a wide variety of transformed cell lines but seems to have little or no cytotoxic effect on normal cells *in vitro* or *in vivo* (72-75). TRAIL binds to four known receptors; death receptor 4 (DR4), death receptor 5 (DR5), decoy receptor 1 (DcR1), and decoy receptor 2 (DcR2) (76-80). The binding of TRAIL to DR4 or DR5 leads to the induction of apoptosis through the extrinsic pathway, as described in section 1.1.6.2. Decoy receptors (DcR's) compete for TRAIL but do not produce an apoptotic response due to the fact that decoy receptor 1

lacks a death domain and decoy receptor 2 lacks a functional death intracellular death domain (50). Decoy receptors are expressed preferentially in many normal tissues but only in a few transformed cells and it is therefore suggested that the expression of decoy receptors in normal tissues might protect them from the induction of apoptosis by TRAIL (81). Other studies have reported that DR5, a cell surface receptor that binds the ligand TRAIL, is expressed more strongly in cancer cells compared to normal cells and this expression may contribute to the tumor-selective induction of apoptosis by TRAIL (81). It is for this reason that DR5 is considered an attractive target for cancer therapies and has lead to the development of monoclonal antibodies against DR5 and DR4. HGS-ETR1 and HGS-ETR2 are high affinity, recombinant, fully human, $IgG_1\lambda$ monoclonal antibodies that are agonisitic and specific to cell death receptors DR4 and DR5, respectively (82). Treatment of colorectal tumor cell lines with TRAIL receptor antibodies, HGS-ETR1 and HGS-ETR-2, and irradiation leads to an increased induction of apoptosis and growth delay (82). Both HGS-ETR1 and HGS-ETR2 were shown to induce killing in primary melanoma cells, using both the intrinsic and extrinsic apoptotic pathways, and HGS-ETR2 was shown to induce cell death in primary human renal carcinoma cells, through the activity of caspases 9, 8, 6, and 3 (83, 84). These antibodies have also been tested in CLL cells and were shown to demonstrate a synergistic or additive effect when used in combination with doxorubicin or bortezomib (85). Antibodies against TRAIL death receptors are in clinical trials for a variety of cancers (86).

In breast cancer, it has been shown that it is unlikely that sensitivity to TRAIL-induced apoptosis is completely controlled by the levels of DR4, DR5, and DcR1, but could also be due to DcR2, osteoprotegrin, or other mechanisms such as activation of NFκB (87).

Sensitization of breast cancer cell lines to TRAIL-induced apoptosis appears to be mediated through caspases, as chemotherapy agents that activate caspases augment TRAIL-induced apoptosis, whereas chemotherapy agents that do not activate caspases do not show induction (87).

1.4.2 HDAC Inhibitors

Histone modifications play an important role in diseases as well. In cancer, dysregulation of HAT and HDAC activity often occurs (35, 88, 89). This altered HAT or HDAC activity is associated with the formation and development of certain human cancers by changing the expression pattern of various genes (50). In leukemia, chimeric fusion proteins produced by chromosomal translocations alter normal gene regulation through modification of chromatin (90). HDAC inhibitors are a class of chemotherapeutic agents that alter the expression of genes by inhibiting the HDAC activity and thereby increasing histone acetylation. There are several chemical structural classes of HDAC inhibitors including hydroxamic acids (eg. TSA, SAHA), short-chain fatty acids (eg. butyric acid, valproic acid), cyclic tetrapeptides containing a AOE moiety (eg. trapoxin), cyclic peptides not containing the AOE moiety (eg. depsipeptide), and benzamides (eg. MS-27-275) (see Table 1) (91). HDAC inhibitors are now being evaluated in clinical trials as they appear to be non-toxic to normal cells but induce apoptosis in cancer cells (11, 12, 92-96).

Table 1

Examples of some HDIs

HDIs	Range	Ref.
Short-chain fatty acids		
Butyrate and phenylbutyrate	mM	Kruh (1982)
Valproic acid	mM	Phiel et al. (2001) and Gottlicher et al. (2001)
Hydroxamic acids		
Trichostatins	nM	Yoshida et al. (1990)
SAHA and its derivates	μM	Richon et al. (1998)
Oxamflatin	μM	Kim et al. (1999)
CBHA (*m*-carboxy cinnamic bishydroxamidic acid)	μM	Richon et al. (1998)
Scriptaid	μM	Su et al. (2000)
Pyroxamide	μM	Butler et al. (2001)
Propenamides	μM	Massa et al. (2001)
Epoxyketone-containing cyclic tetrapeptides		
Trapoxins	nM	Kijima et al. (1993)
HC-toxin	mM	Brosch et al. (1995)
Chlamydocin	nM	Brosch et al. (1995)
Diheteropeptin	μM	Masuoka et al. (2000)
Non-epoxyketone-containing cyclic tetrapeptides		
FR901228 (depsipeptide or FK228)	μM	Nakajima et al. (1998)
Apicidin	nM	Darkin-Rattray et al. (1996)
CHAPs (CT-hydroxamic hybrid)	nM	Furumai et al. (2001)
Benzamides		
MS-275 (MS-27-275)	μM	Saito et al. (1999)
CI-994 (*N*-acetyl dinaline)	μM	Kraker et al. (2003)
Epoxides		
Depudicin	μM	Johnstone (2002)

1.4.2.1 Hydroxamic Acids

Suberoylanilide hydroxamic acid (SAHA) is a hydroxamate-containing small molecule HDAC inhibitor that directly interacts with the hydrophobic catalytic site of HDACs (97). SAHA's aliphatic group fits into the pocket that co-ordinates the Zn^{2+} ion that is necessary for catalytic activity (97). SAHA is currently in clinical trials for the treatment of solid tumours and haematological malignancies. In breast cancer cells, SAHA has been shown to induce growth inhibition, cell cycle arrest, and apoptosis by regulating genes such as p21, p27, Rb, and gelsolin (97). SAHA, as well as trichostatin A (TSA), have been shown to produce a synergistic induction of apoptosis when combined with TRAIL in both TRAIL-sensitive and –resistant breast cancer cells. This appears to be due to the upregulation of DR4 and/or DR5, the activation of caspase-3, -9, and –8, the induction of pro-apoptotic Bcl-2 family members, and the inhibition of Bcl-2 and/or Bcl-x_L (50, 81). The same group, Nakata S et al., showed that TSA, SAHA, and sodium butyrate upregulated DR5 mRNA and protein in a dose- and time-dependent manner, as well as activating the transcription of DR5 gene in a p53-independent manner (81). In prostate cancer, SAHA produces an additive effect in combination with radiotherapy (97).

1.4.2.2 Depsipeptide (FR-901228)

The HDAC inhibitor depsipeptide is a natural product purified from *chromobacterium violceum*, which undergoes intracellular reduction to generate an active HDAC inhibitor (97). It is a cyclic peptide that is pro-apoptotic, anti-proliferative, and anti-angiogenic (97). It is currently in clinical trials for the treatment of several cancers including chronic

lymphocytic leukemia, acute myeloid leukemia, cutaneous T cell lymphoma, and small cell or non-small cell lung cancer (98).

1.4.2.3 Suberic bishydroxamate (SBHA)

SBHA is a relatively new HDAC inhibitor. It has been shown to induce apoptosis in the majority of melanoma cell lines through mitochondrial and caspase-dependent pathways (99). Along with inducing apoptosis by itself it has also been shown to induce synergistic apoptosis when treated with TRAIL (99). SBHA is thought to exert its effects through the down-regulation of anti-apoptotic proteins such as X-linked IAP (XIAP), Mcl-1, and Bcl-x_L, and the up-regulation of pro-apoptotic proteins Bid, Bim, Bax, and Bak (99).

1.4.3 Proteosome Inhibitors

Much like apoptosis the process of protein degradation is essential for cell homeostasis. It is mediated primarily through the ubiquitin-proteosome pathway and the proteosome itself. The proteosome inhibitors are a relatively new class of drugs shown to inhibit the proteosome. They are peptide aldehydes and reversible serine and cysteine protease inhibitors (86).The best characterized inhibitor to date is bortezomib (VELCADE, PS-341). It is a dipeptidyl boronic acid that reversibly inhibits the chymotrypsin-like activity of the proteosome and shows selectivity towards the proteosome as opposed to the serine and cysteine proteases (86). It has been shown to possess antitumor properties, as well as the ability to sensitize cells to the apoptotic effects of other agents, and is the first inhibitor to undergo clinical trials. It has been shown to be effective in the treatment of many cancers including multiple myeloma, non-Hodgkin lymphoma (NHL), and chronic

lymphocytic leukemia (CLL) (86). The inhibition of the proteosome seems to be selective for transformed cells. This is thought to be due to the fact that actively proliferating cells are more susceptible than quiescent cells, although this does not explain the susceptibility of CLL cells to the inhibitors, as they are predominantly in the G_0 phase of the cell cycle (86).

1.5 Chronic Lymphocytic Leukemia (CLL)

1.5.1 Clinical Features

Chronic lymphocytic leukemia (CLL) is the most common form of leukemia in North America and Europe, accounting for one third of all cases, and is far less common in the Orient (96, 100). Older patients, with an average age of 72 years, are most affected by this disease and men are affected twice as often as women (96). CLL is typically a B-cell malignancy. It is characterized by an accumulation of non-proliferating, mature-appearing CD5+ B lymphocytes (frequently CD19+, CD20+) in the blood, marrow, lymph nodes, and spleen (96). The disease is detected with a complete blood cell (CBC) count and is diagnosed when the patient exhibits a persistent peripheral lymphocyte count of $>5x10^9$ / L with a typical CD5+, CD19+ cell morphology. A scoring system described by Matutes et al. is often used as an aid in the diagnosis of CLL (see Table 2) (100). One third of CLL patients will never require treatment, however the disease in the other patients progresses at variable rates and therapy will be required at some point (11).

Table 2

Scoring system for the diagnosis of CLL[a]

Marker	Score points[b]	
	1	0
SmIg	Weak	Strong
CD5	Positive	Negative
CD23	Positive	Negative
FMC7	Negative	Positive
CD22 or CD79b	Weak	Strong

[b] Scores in CLL are usually >3, in other B-cell malignancies the scores are usually <3.

1.5.2 Immunophenotyping

CLL begins with the malignant transformation of a single B lymphocyte and its clonal expansion (101). CLL cells have a number of distinct markers that aid in its diagnosis. These include expression of either κ or λ light chains on the cell surface membrane, the presence of unique idiotypic specificities on the immunoglobulins produced by CLL cells, and by immunoglobulin gene rearrangements (101). CLL cells have low to undetectable amounts of monoclonal polyreactive IgM autoantibodies on the cell surface and often present with IgV_H mutations (101, 102). The cells usually B cell markers CD5, CD19, CD20, CD21, CD23, and CD24 and most are positive for Ia (DR and DC), Fc receptors, and have receptors for mouse erythrocytes (see Table 3) (101, 102). Some variable immunophenotypes include CD38 expression and intracellular expression of ZAP70, and both are thought to have some prognostic importance (102). Bone marrow can also be checked for common chromosomal abnormalitites (del(17p), del(11q22-23), del(13q14), and trisomy 12) to improve the prognostic information (102).

1.5.3 Staging

The most commonly used staging systems were reported by Rai et al. (see Table 4) and Binet et al. (see Table 5). Rai's staging system uses lymphadenopathy, splenomegaly, anemia, and thrombocytopenia as markers of progressive disease bulk. The stages range from 0 to IV (100, 102). Binet's staging system is a more simplified staging system and uses the number of enlarged lymph nodes and the presence of anemia or thrombocytopenia. The stages range from A-C (102). Regardless of the staging system, patients with the most advanced stage have a predicted survival of 4 to 5 years, whereas

Table 3

Differential diagnosis of CLL and other B-lymphoproliferative disorders according to selected immunophentypic features[a]

Disease	SmIg	CD5	CD20	CD23	FMC7	CD22	CD10	CD25	CD103	CD11C
CLL	dim	++	dim	++	–/+	–/+	–	–/+	–	–/+
Prolymphocytic leukemia	+++	–/+	+++	–/+	++	++	–/+	+/–	–	–/+
Hairy-cell leukemia	+++	–	+++	–	++	+++	–	+++	+++	++
Mantle-cell lymphoma	++	++	++	–	+	++	–	–	–	–
Splenic lymphoma with villous lymphocytes	++	–/+	++	+/–	++	++	–/+	+/–	+/–	+/–
Follicular lymphoma	++	–	++	–	++	++	+/++	–	–	–

Table 4

Rai clinical staging

Stage	Clinical feature
0	Lymphocytosis alone
I	Lymphocytosis, lymphadenopathy
II	Lymphocytosis, splenomegaly and/or hepatomegaly
III	Lymphocytosis, anemia (*Hb* < 11.0 g/dl)
IV	Lymphocytosis, thrombocytopenia (platelets < 100×10^9/l)

(100)

Table 5

Binet clinical staging

Stage	Clinical features[a]
A	No anemia, no thrombocytopenia, less than three lymphoid areas involved
B	No anemia, no thrombocytopenia, more than three lymphoid areas involved
C	Anemia (*Hb* < 10.0 g/dl) and/or thrombocytopenia (platelets < 100×10^9/l)

[a] The Binet staging system evaluates enlargement of the following: lymph nodes (whether unilateral or bilateral) in the head and neck, axillae, and groin; spleen; and liver.

(100)

patients with the lowest stage of disease have a predicted survival of over 10 years (102). Due to the variable clinical course of the disease however, the staging system cannot be used solely to predict the rate at which the disease will progress and prognostic factors are used to aid in the identification of high risk patients.

1.5.4 Prognostic Factors

Due to the indolent clinical course of many CLL patients the ability to identify patients who are at risk of early disease progression is an important step in formulating treatment regimens. Some of the factors used to predict the prognosis of a patient include: (1) patient characteristics, such as age and gender; (2) laboratory parameters, such as lymphocyte count, lymphocyte doubling time, lactate dehydrogenase elevation; (3) serum markers, such as serum beta-2 microglobulin, soluble CD23, or thymidine kinase, and (4) genetic markers of tumour cells, such as genomic aberrations (such as p53 deletion), mutational status of immunoglobulin heavy chain gene, or surrogate markers for these factors such as CD38 expression and ZAP70 (zeta-associated protein) expression (see Table 6) (100, 102, 103). A rapid doubling time is where the peripheral blood lymphocyte count doubles in less than 12 months and patients with low doubling time have a median survival of over 118 months whereas those with a rapid doubling time have a median survival of 61 months (102). CD38 is a cell surface molecule. It is expressed on leukemic cells in patients who develop early CLL progression and is also associated with a poor response to fludarabine (102). A level of CD38 expression in more than 30% of CLL cells indicates a poor prognosis and correlates with an absence of IgV_H mutation (102). The absence of a mutation in the immunoglobulin heavy chain (IgV_H) has long been associated with a high

Table 6

Prognostic factors in Cl _30]

Prognostic factor	Clinical risk	
	Low	High
Major		
Patient gender	Female	Male
Clinical stage	Binet A	Binet B or C
	Rai O, I	Rai II, III, IV
Pattern of bone marrow biopsy infiltration	Non-diffuse	Diffuse
Lymphocyte morphology	Typical	Atypical
Lymphocyte doubling time	>12 months	<12 months
CD38 expression	<20–30%	>20–30%
Genetic abnormalities	None	del 11q23
	del 13q (sole)	Loss/mutation of p53
Serum thymidine kinase levels	Low	High
IgVH gene status	Mutated	Unmutated
ZAP-70 expression	Low	High
Others		
Beta-2-microglobulin	Low	High
Soluble CD23 levels	Low	High

(100)

risk for early disease progression but there is not a readily available test. However, associated with this mutation is the high expression of ZAP70, an intracellular signaling molecule (100, 102, 103). There is a commercial kit available to test for ZAP70, which serves as a surrogate marker for a lack of IgV_H mutation, but so far has not been proven to work. Several cytogenetic changes have been associated with a decrease in survival for CLL patients whereas others were associated with a more favourable survival rate. The most unfavourable deletion is 17p (loss of p53 gene), with a median survival of 32 months, possibly due to the patients being refractory to treatment (102, 104). Deletion of 11q22-23 is also unfavourable, with a median survival of 79 months, and is commonly seen in younger patients (102, 104). The more favourable changes include deletion of 13q14, usually associated with benign disease, CD38- cells, and with a median survival of 133 months. The median survival of patients with trisomy 12 is 114 months, although it is still associated with a higher rate of cell proliferation and CD38 positivity (102, 105). The unfavourable changes occur more frequently in unmutated V_H tumor cells whereas the more favourable changes seem to occur more frequently in the V_H mutated cells (103).

1.5.5 Treatment

Even with the development of new therapies for the treatment of CLL, it remains an incurable disease with varying prognosis. Due to the fact that CLL is generally a slowly progressing disease, most patients are monitored for years before requiring treatment or never require treatment at all. However for those that require treatment, standard therapies include the nucleoside analog fludarabine (FLU) and the alkylating agent chlorambucil (CLB). Chlorambucil alkylates DNA, RNA and cellular proteins resulting

in the activation of caspases and the induction of apoptosis (106). Fludarabine is dephosphorylated in the plasma from F-ara-AMP to F-ara-A. Following cellular uptake it is phosphorylated to F-ara-ATP, which produces DNA breaks resulting in the activation of caspase 9 and the subsequent induction of apoptosis (107-109). Although patients initially respond to this therapy, most eventually develop drug resistance (11). Therefore understanding the mechanism of CLB and FLU-induced apoptosis will aid in developing more targeted therapies for CLL patients.

TRAIL is expressed on the surface of many cancer cells, including leukemia cells, and has been suggested as a new therapy for treatment of cancers, although it is ineffective at inducing apoptosis in CLL cells (11, 110). However, a synergistic apoptotic response does result when CLL cells are treated with both TRAIL and either CLB or FLU (11). The resulting apoptotic response could be due to the increase in DR4 and DR5 mRNA, protein, and cell surface expression levels that occur when CLL cells are treated with CLB or FLU (11). Of note is the fact that CLB and FLU do not affect the expression of DR4 or DR5 in normal lymphocytes (11). Inhibiting TRAIL from interacting with DR4 and DR5 leads to a decrease in the CLB- and FLU-induced apoptosis in CLL cells, showing the involvement of TRAIL in the mechanism of action of chemotherapy (11). New therapeutic approaches are desperately needed for CLL patients, as the overall survival has not improved significantly despite new therapeutic agents, especially for those patients with clinical resistance to fludarabine or mutations of p53 (110). Studies have shown that TRAIL-induced apoptosis in cancer cells is achieved by signaling through DR5 as opposed to DR4 (110). The reason for studying the regulation of DR5

expression in CLL cells is that understanding this regulation will aid in sensitizing CLL cells to TRAIL-induced apoptosis.

1.5.6 Defect(s) of Apoptosis in CLL

One of the hallmarks of B-cell CLL is the accumulation of mature B-cells, due to their ability to escape programmed cell death and undergo cell cycle arrest in the G_0 phase (101). There are several molecular defects, such as over-expression of Bcl-2 family members and mutations of p53 gene, and chromosomal abnormalities, such as trisomy 12, 13q14 deletion, 11q deletion, and 17p deletions, that could be responsible for the defects in apoptosis and therefore a poor prognosis (101). Bcl-2 may exert its anti-apoptotic effect by inhibiting pro-apoptotic proteins such as Bax. Mcl-1 protein, another member of the Bcl-2 family, has also been shown to affect apoptosis. Expression of Mcl-1 was shown to be associated with resistance to fludarabine and chlorambucil therapy and a low complete response rate (101). p53 is the most commonly mutated gene in human cancers. Since p53 is important in the regulation of cell cycle arrest and apoptosis, a mutation of the p53 gene is a good predictive marker for drug resistance and survival in CLL. Mutations of the p53 gene occur in approximately 10-20% of CLL patients (101).

1.5.7 Lysophosphatidic acid (LPA)

LPA is a naturally occurring phospholipid present in serum at concentrations of 2-20 μM, but the serum level becomes increased in tumor-bearing patients (111, 112). It was initially identified as an intermediate in a de novo lipid biosynthesis pathway (113). It exhibits pleiotrophic biological activities by interacting with 4 specific cell-surface G protein-coupled receptors of the endothelial differentiation gene (EDG) subfamily; LPA1/Edg-2, LPA2/Edg-4, and LPA3/Edg-7, and LPA4 (112-114). LPA1 receptor is the

most widely expressed of the four receptors, due to the other three receptors having restricted patterns of expression (113, 114). LPA can stimulate cellular proliferation, platelet aggregation, smooth muscle cell contraction, and tumor cell invasion (113). LPA is found in high concentrations in the ascitic fluid and plasma of ovarian cancer patients (112). LPA signaling has been shown to be involved in the initiation, progression, and metastasis of ovarian cancer (114). Poor prognosis in ovarian cancer patients with high levels of LPA may be due to its ability to increase ovarian cancer cell proliferation by directly increasing the level of cyclin D1 and thereby inducing proliferation and protecting the cells from apoptosis (112, 114). LPA has also been shown to facilitate tumor angiogenesis by increasing the production of potent growth factors, such as VEGF and IL-8 (114). Tumor angiogenesis is essential for tumor growth and is induced by the binding of vascular endothelial growth factor (VEGF) to one of its two receptors, Flt or KDR (112). Cancer patients have increased levels of serum VEGF and elevated levels of VEGF mRNA have been observed in the majority of human cancer cells (112). LPA has also been shown to induce survival effects in a prostate cancer cell line through the activation of both Akt and NFκB (115). LPA can also effectively block TRAIL/death receptor-induced apoptosis through the suppression of caspase-8 activation and mitochondrial cytochrome c release by increasing cFLIP expression and Bad phosphorylation (111, 113). All of these data indicate that LPA acts as a general survival factor. The importance of LPA to this study is the fact that it has been shown to protect cells against TRAIL-induced apoptosis and, more specifically, that LPA protects primary CLL cells from spontaneous, fludarabine-, chlorambucil-, and etoposide- induced apoptosis (111, 113). This effect could be due to the increased expression of LPA1

receptors in primary CLL cells compared to normal B-cells. Thus, LPA is a survival factor for primary CLL cells and may be responsible for the decreased apoptosis in these cells. This provides us with a means of looking at the effect of LPA/survival using primary CLL cells.

2. MATERIALS AND METHODS

2.1 REAGENTS

All laboratory chemicals were ordered from Sigma-Aldrich Chemicals (Sigma-Aldrich Ltd., Oakville, Ontario, Canada) unless otherwise noted. All solutions, buffers, and bacterial media were prepared using distilled deionized water (ddH_2O) and sterilized by autoclaving prior to use.

2.1.1 Antibodies

Rabbit polyclonal antibody against acetyl-histone H3 (Upstate Cell Signaling Solutions, New York, USA) was used for western blot (1:3000), immunohistochemistry (1:500), and ChIPs (3μg). Rabbit polyclonal against histone H3 (Cell Signaling Technology, Danvers, Massachusetts, USA) was used for western blots (1:3000). Rabbit polyclonal antibody against phosphorylated NFκB p65 (RelA) (serine 529) (Rockland Inc., Gilbertsville, Pennsylvannia, USA) was used for western blots (1:1000). Rabbit polyclonal antibody against DR5 (Medicorp, Montreal, Quebec, Canada) was used for western blots (50μL in 5mL). Rabbit polyclonal antibody against dimethyl-histone H3 (lysine 79) (Upstate Cell Signaling Solutions, New York, USA) was used for western blots (1:1000) and immunohistochemistry (1:500). Rabbit polyclonal antibody against phospho-histone H3 (serine 10) was used for western blots (1:200) and immunohistochemistry (1:500). Rabbit polyclonal antibody against NFκB p65 (Rel A) (Santa Cruz Biotechnology Inc., California, USA) was used for western blot (1:200) and ChIPs (3μg). Rabbit polyclonal antibody against p53 (Sigma-Aldrich Ltd, Ontario, Canada) was used for ChIPs (3μg). Rabbit polyclonal antibody against HDAC1 (Cedarlane Laboratories Limited, Ontario, Canada) was used for ChIPs (3μg) and

western blot (0.5μg/mL). Rabbit polyclonal antibody against p300 (Santa Cruz Biotechnology Inc., California, USA) was used for ChIPs (3μg). Goat anti-rabbit horseradish peroxidase (1:3000) and enhanced chemiluminescence developing reagents were used to detect the immunoreactive bands.

2.1.2 Drug Preparation

2.1.2.1 Epidermal Growth Factor (EGF) – 1mg/mL

First we made a BSA/Acetic acid buffer by combining 5mL of 10M acetic acid with 0.05g of BSA. We filter sterilized this buffer in the fumehood by passing the solution through a 0.2μM syringe filter (Corning Inc., Corning, New Jersey, USA) into a 15mL centrifuge tube (BD Biosciences, Mississauga, Ontario, Canada). Still in the fumehood and on ice we add 200μL of sterilized BSA/Acetic acid solution to the vial of rhEGF (0.2mg) and mixed until the powder dissolved. We then aliquoted the drug into sterilized eppendorf tubes and stored at -20°C.

2.1.2.2 Etoposide (100mM) and Fludarabine (100mM)

We resuspended both fludarabine and etoposide in the appropriate amount of DMSO. Etoposide was stored at 4°C and fludarabine was aliquoted into sterilized eppendorf tubes and stored at -20°C.

2.1.2.3 Chlorambucil (5mM)

First we made acidified ethanol by making up 0.1N HCl using ethanol, this solution can be stored at room temperature. We then dissolved 1.52mg of chlorambucil in 1mL of acidified ethanol. This solution can stored at 4°C but is only good for one day.

2.1.2.4 Lysophosphatidic Acid (300μM)

We resuspended a 5mg vial of lysophosphatidic acid in 35mL of 1xPBS and 0.035g of BSA. We aliquoted this solution into sterilized eppendorf tubes and stored at -20°C.

2.1.2.5 SAHA (5mM)

We dissolve 1mg of SAHA (Cedarlane Laboratories, Limited, Ontario, Canada) in 740μL DMSO. We aliquoted it into sterilized eppendorf tubes and stored at 4°C.

2.1.3 Plasmids

The DR5 promoter-intron DNA in PGL3 plasmid was provided by T. Sakai (Kyoto Prefectural University of Medicine, Japan). The following primers were used to generate the vectors for:

DR5 promoter intron and to introduce mutations in the NFκB and p53 binding sites (14)

5' GGGAGATCTCCTGAGGTGGGAGTATCGCTTG 3'

5' GGGAAGCTTACGCAGCTTACTCGGGAATTC 3'

NFκB binding site point mutations

5' GGGAGATCTCCTGAGGTGGGAGTATCGCTTG 3'

5' GGAAGCTTACGCAGCTTACTCGGTAATTACT 3'

p53 binding site point mutations

5' GCGGGAATATCCGGGCAAGA 3'

5' CGTCTTGCCCGGATATTCCC 3'

2.2 GROWTH MEDIA

2.2.1 Bacterial Media

All bacterial cultures were grown in standard Luria Bertani broth. Commercially available pre-mixed powder for Luria Bertani (LB) broth from Difco Laboratories (Detroit, MI, USA) was dissolved in the required amount of distilled deionized water (ddH_20) and autoclaved at 120°C for 20 minutes. The LB broth was stored at 4°C until required and was supplemented with ampicillin at a final concentration of 50μg/mL prior to use.

2.2.2 Tissue Culture Media

Dulbecco's Modified Eagle Media (DMEM, GIBCO BRL Life Technologies) and α-minimal essential medium (α-MEM, GIBSO BRL Life Technologies) were made according to manufacturers' instructions. The pH was adjusted to read between 7.0 to 7.2 using concentrated HCl. Both media were filter sterilized in the culture hood, using a 75mm Nalgene bottle-top filter, into autoclaved sterile glass bottles. Media was stored in the dark at 4°C. Serum Free Hybridoma media was ordered from Invitrogen (Burlington, Ontario, Canada) and used for primary CLL cells.

2.3 TISSUE CULTURE CELL LINES

Human Embryonic Kidney cell line (HEK) 293, HEK293 Vector alone, and HEK293 ΔIκB cell lines were maintained in DMEM supplemented with 10% volume/volume (v/v) Bovine Calf Serum (BCS) (Gibco BRL Life Technologies, Burlington, Ontario, Canada), 100 units/ml penicillin, 100 μg/ml streptomycin (Gibco BRL Life Technologies,

Burlington, Ontario, Canada). Cells stably expressing vector alone (pcDNA3), ΔIκB were under selection with 1.5 mg/ml G418 (Gibco BRL Life Technologies, Burlington, Ontario, Canada) at 37°C and 5% CO_2. The MCF-7 breast cancer cell line was maintained in α-MEM supplemented with 10% Fetal Calf Serum v/v (FCS), 100 units/ml penicillin, 100 μg/ml streptomycin, 100mM sodium pyruvate, and 50mM HEPES (all from Gibco BRL Life Technologies, Burlington, Ontario, Canada). The 3T3-Murine Embryonic Fibroblast (MEF) cell line was maintained in DMEM media supplemented with 10% v/v BCS, 100 units/ml penicillin, and 100 μg/ml streptomycin. All cell lines were grown in humidified incubators in the presence of 5% CO_2 at 37°C.

2.4 PERIPHERAL BLOOD COLLECTION AND SEPARATION

2.4.1 Patient Recruitment and Collection of Peripheral Blood Samples

CLL patients were consented to donate blood for research by Donna Hewitt, a research nurse working for the Manitoba CLL Tissue Bank. Blood was collected by venipuncture into 16x100nm vacutainers containing 143 USP of sodium heparin (BD Biosciences, Mississauga, Ontario, Canada) by the staff in The Department of Hematology, on the first floor CancerCare Manitoba (Winnipeg, Manitoba, Canada). If possible 60 cc of blood was collected per patient but the volume collected was dependent on the patient's lymphocyte count.

2.4.2 Collection of Normal Control Peripheral Blood Samples

Normal donor blood samples were collected from healthy normal volunteers. These volunteers were consented to donate blood for research by Donna Hewitt, a research nurse working for the Manitoba CLL Tissue Bank. Blood was collected by venipuncture

into 16 x 100nm Vacutainers containing 143 USP of sodium heparin (Becton Dickenson and Company) and mixed gently by inversion to dispense the heparin and prevent the blood from clotting. Donors ranged from the age of 26 to 49 years of age and included males and females. All normal donors were healthy at the time of donation and had lymphocyte counts $<5.0 \times 10^9$ cell/L.

2.4.3 Peripheral Blood Separation

The vacutainers were centrifuged at 1500rpm for 10 minutes at room temperature in a bench-top Damon/IEC, model# HN-SII centrifuge (Needham Heights, Massachusetts, USA) to separate the plasma from the cells. The buffy coat, containing lymphocytes, monocytes, neutrophils, and contaminating red blood cells, was transferred to a sterile 50ml Corning tube (Sigma-Aldrich Ltd., Ontario, Canada) using a sterile pasteur pipette. For patients whose white blood cell count was between 10-40 x 10^9 cells/L, the T cells and monocytes were removed by adding 40µl of Rosette Sep B cell enrichment cocktail (Stem Cell Technologies, Vancouver, BC, Canada). The mixture was then incubated for 30 minutes with gentle agitation after every 10 minutes. An equal volume of sterile Hank's Buffered Saline Solution (HBSS) (GIBCO BRL Life Technologies, Burlington, Ontario, Canada) was added to the mixture. Into a sterile 15mL tube, 5ml of Ficoll-Paque (GE HealthCare BioSciences Inc., Baie d'Urfe, Quebec, Canada) was added to the bottom of the tube and 7-8ml of the buffy coat mixture was carefully layered overtop of the ficoll. The Ficoll-Paque density gradient was then centrifuged at 1500rpm for 30 minutes at room temperature in a bench-top Damon/IEC, model# HN-SII centrifuge (Needham Heights, Massachusetts, USA) to separate the lymphocytes and monocytes, which remain in the interphase, from the neutrophils and contaminating red blood cells

that pass through the Ficoll-Paque. The lymphocytes and monocytes were then collected from the interphase using a sterile pasteur pipette and placed in a sterile 50mL Corning tube. The B cells were then washed with an equal volume of HBSS and centrifuged again at 1500 rpm for 10 minutes at room temperature. To lyse any remaining red blood cells, 5ml of ACK lysis buffer (0.15M ammonium chloride (NH_4Cl), 7.2mM potassium carbonate ($KHCO_3$), 0.11mM sodium ethylenediaminetetraacetic acid (Na_2EDTA), pH7.4) was added and the cells incubated for 10 minutes at room temperature followed by centrifugation at 1500 rpm for 10 minutes at room temperature. This was repeated until the pellet no longer had a red tinge. The cells were again washed by resuspending the pellet with 5-10ml of HBSS and centrifuging at 1500 rpm, 10 minutes, room temperature. The pellet was then resuspended in 5-7ml of HBSS and the cell amount determined via coulter counter (Beckman Coulter Z2). The appropriate number of cells was then plated with hydridoma serum free media.

2.5 TREATMENT OF CELL LINES AND PRIMARY CELLS

2.5.1 Treatment of Cell Lines

HEK 293 cells were grown to 80% confluency before treatment. Cells were split 24 hours before treatment. Cells were treated with Etoposide (100mM), EGF (1mg/mL), or TSA (45nM) directly into the culture media and then returned to the incubator, 37°C and 5%CO_2, for the indicated amount of time.

2.5.2 Treatment of primary CLL cells

Isolated B lymphocytes from patient samples were plated in hydridoma, serum-free, media at a concentration of $1x10^8$ cells per plate. The cells were left overnight at 37°C,

5%CO_2. Cells were then treated with 10μM chlorambucil, 10μM fludarabine, 10μM LPA, or 5μM SAHA. In combination studies, cells were first treated with LPA and one hour later treated with either SAHA or fludarabine.

2.6 PLASMID PREPARATION (QIAGEN KIT)

We use the Q1Aprep Spin Miniprep Kit (Cat# 27106). Firstly, starter cultures are made by adding, using sterile methods, a loopful of glycerol stock, stored at -80°C, to 5mL of LB broth and 5μL of ampicillin (50mg/mL) and growing the culture for 4 hours at 37°C on a shaker. After the 4 hours we inoculated 500mL of LB broth with 500μL of ampicillin and the starter culture and grew this overnight at 37°C on a shaker. The next day we divided the culture into large 300mL centrifuge tubes and centrifuged them for 30 minutes at 6000 x g, 4°C on a Sorvall RC5C centrifuge with a GS-3 rotor. We then remove the supernatant and resuspend the pellet in 10mL of Buffer P1. We transfer the suspension to smaller centrifuge tubes and add 10mL of Buffer P2. We mix the suspension by inverting 4-6x and incubate the tubes for 5 minutes at room temperature. We then added 10mL of chilled Buffer P3 and mixed by inverting 4-6x. We incubated this mixture on ice for 20 minutes and then centrifuged for 30 minutes at 20 000xg, 4°C on a Sorvall RC5C centrifuge in a SS34 rotor. We transferred the supernatant to a new tube and centrifuged again for 15 minutes at 20 000xg, 4°C in the same centrifuge and rotor. We used the provided column and applied 10mL of Buffer QBT followed by the supernatant from the last spin. We then washed the column twice with 30mL Buffer QC for each wash and eluted the DNA with 15mL of Buffer QF, collecting the flow through in glass centrifuge tubes. We precipitated the DNA by adding 10.5 mL of room

temperature isopropanol and centrifuging for 30 minutes at 15000xg, 4°C in a Sorvall RC5C centrifuge in an SS34 rotor. We carefully decanted the supernatant and washed the pellet with 5mL of room temperature 70% ethanol and centrifuged for 10 minutes at 15000xg, 4°C in the same centrifuge and rotor. We decanted the supernatant and dried the pellet upside down for 5-10 minutes. We re-dissolved the pellet in 100-300μL TE buffer pH8 and stored at -20°C.

2.7 TRANSFECTION

2.7.1 Transient Transfection: Lipofectamine method

In preparation for transient transfection, HEK 293 cells were plated in 100mm plates until they reached 50-80% confluency. Cells were transfected using the polycationic lipid LipofectAMINE reagent (Invitrogen, Burlington, Ontario, Canada). For each transfection 2μg of the desired plasmid and 0.2μg of the plasmid monitoring for transfection efficiency (β-galactosidase in pcDNA3) were diluted in 800μl of plain DMEM in an eppendorf tube. In another tube, 24μl of lipofectamine reagent was diluted in 800μl of plain DMEM. The diluted DNA was added to the lipofectamine reagent, dropwise. The DNA-liposome complexes were allowed to form for 30 minutes at room temperature. An additional 3.4ml of plain DMEM was added to the lipofectamine/DNA mixture. Cells were washed twice with plain DMEM and then the now 5ml transfection mixture was laid on cells. After incubating the cells for 5 hours at 37°C, 5ml DMEM / 20% BCS was added to the plate and then incubated a further 19 hours at 37°C, 5% CO_2.

The cells were then cultured and treated as required for luciferase activity.

2.7.2 Transient Transfection: Geneporter 2 method

In preparation for transient transfection, MCF-7 cells were plated in 100mm plates until they reached 50-80% confluency. Cells were transfected using the gene porter 2 reagent (Gene Therapy Systems, California, USA). For each transfection 2μg of the desired plasmid and 0.4μg of the plasmid monitoring for transfection efficiency (β-galactosidase in pcDNA3) were diluted in 50μl Diluent B in an eppendorf tube. In a separate tube, 10μl of Gene Porter 2 reagent was diluted in 40μl of plain DMEM. Both tubes were incubated at room temperature for 3 minutes. The Gene Porter 2 mixture was then added to the DNA mix and left standing at room temperature for 10 minutes. Cells were washed twice with plain DMEM and subsequently the DNA mix was added to the plate. The plate was incubated for 4 to 5 hours at 37°C, 5% CO_2. After adding 2ml of 20% FBS in DMEM, the plate was incubated for a further 19 hours at 37° C, 5% CO_2. The cells were then cultured and treated as required for luciferase activity.

2.7.3 Transfection with siRNA

HEK293 cells were plated in 6 well dishes and grown to 60% confluency. 3.5μg siRNA against p53 (Upstate Cell Signaling Solutions, New York, USA) was diluted into 100μl of media. Six μl of RNAiFect Transfection reagent (Qiagen) was added to siRNA and incubated at room temperature for 10 minutes. The formed complexes between the reagent and siRNA were then added dropwise to the cells. The cells were then incubated with the transfection complexes under normal tissue culture conditions overnight. As controls, scrambled siRNA was used as described above. The cells were then treated and used for chromatin immunoprecipitation assays and western blots, as described in sections 2.9 and 2.10, respectively.

2.8 LUCIFERASE ASSAY

2.8.1 DR5-Luciferase Assay

Transfected cells were lysed in a passive lysis buffer (Promega Madison, WI, USA) for 15 minutes at room temperature with shaking. Cells were then removed from the plate and centrifuged for 10 minutes at maximum speed at room temperature in an eppendorf 5810R centrifuge. The supernatant was transferred to a fresh eppendorf tube and 20µl of this lysate was added to a 96 well plate. We used an Lmax luminometer (Molecular Devices Corporation, California, USA) and prepared it for measuring the lysate. We sterilized the machine by pumping 70% ethanol into the machine for 20 cycles and letting it sit for 30 minutes. We then washed the lines out with water 6 times for 99 cycles. We primed the line with substrate for 7 cycles and then the lysate in each well was measured for 10 seconds as relative light units (other settings were 100µL injector volume, do not pre-read wells, and a post-injection delay of 2 seconds). Luciferase activity was normalized to β-GAL activity and subsequently presented as luciferase units. After the measurements were taken the injectors were reversed for 7 cycles and then the lines were washed 6 times for 99 cycles with water.

2.8.2 β-galactosidase assay

Using transfected cells, added 50µl of lysate per well of a 96 well plate as well as 50µl of 2X assay buffer (200mM sodium phosphate buffer pH7.3, 2mM $MgCl_2$, 100mM β-mercaptoethanol, 1.33 mg/mL ONPG) . The plate is then incubated in the dark for 30 minutes at 37°C. The plate is then measure for β-GAL activity at 414nm on a Titertek Multiskan MCC/340 colorometer and the reading is used to normalize the luciferase activity readings.

2.9 CHROMATIN IMMUNOPRECIPITATION ASSAY (ChIPs)

2.9.1 Protein A Sepharose Bead Preparation

To begin, 0.1g of dry protein A sepharose beads (CL-4B, Amersham, Piscataway, New Jersey, USA) were resuspended in 10mL ddH_20 in a 15mL tube. The suspension was incubated for 30 minutes on an orbitron at room temperature and then centrifuged at 2000rpm for 5 minutes at room temperature in an Eppendorf 5810R centrifuge. The supernatant was removed and the beads were resuspended in 10mL dilution buffer (100µL of 10% SDS, 960µL of 0.5M EDTA, 1.67mL of 1M Tris pH8, 1.1mL of Triton X-100, 4.18mL of 4M NaCl, and ddH_20 to 100mL) and subsequently put on an orbitron for 10 minutes at room temperature. The suspension was then centrifuged at 2000 rpm for 5 minutes at room temperature, in the same centrifuge as previous step, and the supernatant again removed. The beads were resuspended in 100µL of 10 mg/mL BSA and 1mL dilution buffer and the suspension transferred to an eppendorf tube and put on an orbitron for 1 hour at room temperature. The tube was then centrifuged for 5 minutes at maximum speed at room temperature. The beads were then washed by resuspending them in 1ml of dilution buffer and left for half an hour at room temperature on an orbitron. The suspension was finally centrifuged for 5 minutes at maximum speed, room temperature, and the beads were resuspended in dilution buffer to a final volume of 1ml. The beads were stored at 4°C until being used.

2.9.2 Preparation of Cells for ChIPs

2.9.2.1 Cell Lines

Cell lines were grown in 100mm plates to 50-80% confluency before treatment. After treatment cells were fixed, in order to cross-link proteins bound to DNA, by adding formaldehyde to a final concentration of 1% and were put on shaker for 10 minutes at room temperature. The formaldehyde solution was then sucked off and the cells were washed three times with 1xPBS. The cells were removed from the plate in the PBS solution by pipetting and scraping and then transferred to a 15mL tube. The tube was then centrifuged at 1200 rpm for 5 minutes in an Eppendorf 5810R centrifuge and the supernatant was subsequently sucked off. The pellet was resuspended in 1.5mL of lysis buffer (10mL of 10% SDS, 8mL of 0.5M EDTA, 5mL of 1M Tris pH8, and ddH_20 to 100mL), 1.5μL PMSF (100mM), 10μL aprotinin, 10μL leupeptin (1mg/mL), and stored at -80°C for a minimum period of overnight but can remain at -80°C until they are sonicated. The frozen lysate of cross-linked protein was removed from the -80°C freezer and thawed at room temperature on ice. The cell lysate was sonicated at 30% output on ice for 4-20-second intervals on a Sonifier Cell Disruptor 350 (Branson Sonic Power Co., Conneticut, USA) with the end result being DNA fragments approximately 400-600bp in size. After sonication the 300μL of lysate was removed for DNA extraction to make input controls. The remaining lysate was centrifuged on Eppendorf 5810R for 8 minutes at 2000 rpm, 15°C and the supernatant was transferred to an eppendorf tube. The approximate DNA concentration of the supernatant was measured using a DU 640 Beckman Coulter spectrophotomer with UV light (260nm). The sample was diluted and

the machine was blanked in 5M urea/2M NaCl. This supernatant was used for subsequent ChIP assays but was stored at -20°C until time of use.

2.9.2.2 CLL PATIENT SAMPLES

Patient samples were added to 100mm plates at a concentration of 1 x 10^8 cells per plate with 10mL of hybridoma serum free media. After treatment, cells were fixed in order to cross-link proteins to bound DNA by adding formaldehyde to a final concentration of 1% and shaking the mixture for 10 minutes at room temperature. The cells were then removed from the plate in the formaldehyde-media solution by pipetting and scraping and then transferred to 15mL tube. The suspension was then centrifuged for 5 minutes at 1200 rpm and the supernatant was subsequently removed. The pellet was washed three times by resuspending in 8mL 1xPBS and centrifuging for 5 minutes at 1200 rpm in an Eppendorf 5810R centrifuge, replacing with fresh 1xPBS after each spin. After the last spin the pellet was resuspended in 1.5mL lysis buffer (see section 2.9.2.1), 1.5μL of 100mM PMSF, 10μL aprotinin, and 10μL leupeptin (1 mg/mL). It was stored at -80°C for a minimum overnight period. The frozen lysate of cross-linked protein was removed from the -80°C freezer and thawed at room temperature on ice. The cell lysate was sonicated at 30% output on ice for 4-20-second intervals (see section 2.9.2.1). After sonication the lysate was centrifuged for 8 minutes at 1200 rpm and the supernatant was transferred to an eppendorf tube. The approximate DNA concentration of the supernatant was measured using a DU 640 Beckman Coulter spectrophotomer with UV light. The sample was diluted and the machine was blanked in 5M urea/2M NaCl. This supernatant was used for subsequent ChIP assays but is stored at –20°C until time of use.

2.9.3 ChIP Protocol

To begin, 5μg of the prepared DNA lysate (determined by A_{260} units), cross-linked to protein, was precleared with protein A sepharose 4B by incubating at 4°C for 3 hours on an orbitron. The mixture was then centrifuged at maximum speed on a Heraeus Biofuge pico centrifuge for 5 minutes, at 4°C, and the supernatant was transferred to a new tube. The lysate was then precipitated with one of the following primary antibodies: p65 (3μg), p53 (2μg), acetylated histone 3 (3μg), HDAC1 (3.5μg), p300 (3μg), or no antibody (as negative control) overnight at 4°C on an orbitron. The next day the lysate was treated with precleared protein A sepharose 4B beads to bind the Ab-protein-DNA complexes for 3 hours at 4°C. The beads + complex were then washed with low salt buffer (1mL of 10% SDS, 1.6mL of 0.5M EDTA, 2mL of 1M Tris pH8, 1mL of Triton X-100, 3.75mL of 4M NaCl, and ddH_20 to 100mL), high salt buffer (same as low salt buffer except 12.5mL of 4M NaCl), and LiCl buffer (0.25M LiCl, 1% NP-40, 1% SDC, 1.2mM EDTA, 1.67mM Tris-Cl pH8, in ddH_20) for 1 hour each at 4°C on an orbitron. The beads were further washed twice with TE buffer (10mM Tris, 1mM EDTA, pH 8.0) for 5 minutes at 4°C on an orbitron. The protein+DNA complex was then eluted from the beads by twice treating with elution buffer for 15 minutes at room temperature on an orbitron, centrifuging for 5 minutes at maximum speed on a Spectrfuge 16M centrifuge after each wash and collecting the supernatant in a new sterilized eppendorf tube. The elutant was then treated with 4M NaCl overnight in a water bath set at 68°C. To degrade the protein from the protein + DNA complex, the elutant was treated with EDTA (10mM), Tris-HCl pH6.5 (40mM), and proteinase K (40μg/μL) for 2 hours in 55°C water bath. To degrade any RNA the elutant was then treated with RNase A for 1 hour in a 37°C water bath. An

equal volume of phenol-chloroform-isoamyl alcohol (25:24:1) (25mL buffer-saturated phenol, 24mL chloroform:isoamyl alcohol) was added and centrifuged at 13000rpm for 15 minutes at 4°C on a Heraeus Biofuge pico centrifuge. The top layer was carefully removed to a new eppendorf tube and was then treated with glycogen carrier (10μg) (GIBCO BRRL) and 100% cold ethanol and kept at -80°C for 2 hours. After pelleting the DNA, it was resuspended in 70% ethanol (1mL) and then pelleted again. The DNA pellet was then air-dried and resuspended in 10μL ddH_20. The DNA was analyzed using PCR (94°C, 58.5°C, 72°C, each for one minute for a total of 35 cycles) using primers (10pmol, Invitrogen) specific to exon-intron 1 of DR5 (5'ACCCTTGTGCTCGTTGTC3' and 5'TTCACGCAGCTTACTCGG3'). The PCR products were run on 1% agarose gels to view the product.

2.9.4 DNA Extraction

DNA was extracted from a 300μL sample of the sonicated lysate used for ChIP assays. The extracted DNA was used as input controls for the ChIP assays. To each 300μL sample, we added 10μL of RNase A (10 mg/mL) and incubated for 2 hours in a 37°C H_2O bath. We then added 15μL of proteinase K (10 mg/mL) and incubated overnight in a 55°C H_20 bath. The next day we extracted the DNA by phenol-chloroform extraction. We first added Buffer-saturated phenol in a 2:1 ratio (sample:phenol) and centrifuged for 15 minutes at maximum speed, 4°C, on a Heraeus Biofuge pico centrifuge. We then transferred the top layer to a new eppendorf tube and added chloroform in a 1:1 ratio. We again centrifuged for 15 minutes at maximum speed, 4°C, on a Heraeus Biofuge pico centrifuge, and transferred the resulting top layer to a new eppendorf tube. We added

20μL of 10M ammonium acetate and 1mL of 100% cold absolute ethanol and incubated at -20°C for 1 hour. After the incubation we centrifuged for 20 minutes at maximum speed, 4°C, on a Heraeus Biofuge pico centrifuge, and after decanting the supernatant, resuspended the pellet in 1mL of cold 70% ethanol. We centrifuged this for 10 minutes at maximum speed, 4°C, and sucked off the supernatant with gel tip. We let the pellet air dry right side up and resuspended it in 10μL of ddH_2O. The product was stored at -20°C.

2.10 WESTERN BLOT

2.10.1 Preparation of Protein Samples

Cells were lysed using a NP40 buffer containing 50mM HEPES pH 7.25, 150mM NaCl, 50μM NaF, 2mM EDTA, 1mM Na vanadate, 1% NP-40, 2mM phenylmethylsulfonyl fluoride. Cell debris was removed by centrifugation at 1200 rpm for 5 minutes on a Spetrafuge 16M centrifuge and protein concentration was determined by the Bradford assay. We mixed 2μL of sample with 2mL of Protein Assay Reagent (BioRad, Mississauga, Ontario, Canada) and based on a standard curve determined the protein concentration of the sample on a DU 640 spectrophotometer using visible light (595nm).

2.10.2 SDS-PAGE Gel and Transfer to Nitrocellulose Membrane

Western blot analysis by sodium dodecyl sulfate (SDS) polyacrylamide gel electrophoresis (PAGE) was used to identify proteins in cell lysates using specific antibodies. Each sample (5μg to 20μg) of cell lysate was separated using a Mini-PROTEAN 3 electrophoresis cell (BioRad, Mississauga, Ontario, Canada), running at 100V through a 5mm 10% SDS-polyacrylamide gel in running buffer. To transfer the

proteins to a nitrocellulose membrane , the gel, the membrane, and filter papers were soaked in transfer buffer (3.03g Tris Base, 14.4g glycine, 800mL ddH_2O, 200mL methanol), layered in a transfer apparatus, and run at one amp for 45 minutes.

2.10.3 Blocking of Membrane and Probing with Antibodies for Protein Detection

The membrane was then blocked with Tris buffered saline-Tween20 solution (TBST; 100mL TBS, 900mL ddH_2O, 1.5mL Tween 20) containing 5% powdered skim milk for 1 hour at room temperature. The membrane was incubated overnight at 4°C with the appropriate antibody diluted with blocking buffer. After the removal of the primary antibody solution, the membrane was washed for 30 minutes in TBST with agitation, changing the buffer every 5 minutes. The membrane was then incubated in blocking buffer containing the appropriate secondary antibody conjugated with alkaline phosphatase for 1 hour at room temperature. After removal of the secondary antibody solution, the membrane was washed for 30 minutes in TBST with agitation, changing the buffer every 5 minutes. The membrane was then developed using enhanced chemiluminescence as described by the manufacturer (ECL, Amersham Pharmacia Biotech). The membrane was exposed to X-ray film for desired length of time and processed in a tabletop automated developer (AGFA model# CP1000).

2.11 ACID-UREA GEL SEPARATION OF ACID-EXTRACTED HISTONES

2.11.1 Total Histone Preparation

Cells were taken off plate via pipetting and scraping and pelleted by centrifugation at 1200rpm, 8 minutes, 15°C in an Eppendorf 5810R centrifuge. Each pellet was resuspended in 1.5ml of TNM buffer (10mM Tris-HCl pH8.0, 100mM NaCl, 2mM $MgCl_2$, 300mM Sucrose, 1% Thiodiglycol v/v), 10µl of 100mM PMSF, 10µl of 1mg/ml leupeptin, and 10µl of aprotinin. The mixture was then homogenized by passing it through a 5mL syringe attached to a 22g needle (Becton Dickenson, Mississauga, Ontario, Canada) 5 times and the resulting mixture was split into 2 eppendorf tubes. Each tube was diluted with 19µl of NP-40 and centrifuged at 4000rpm, 10 minutes, 4°C. Each pellet was resuspended in 750µl of TNM buffer and 5µl of 100mM PMSF and then centrifuged at 4000rpm, 10 minutes, 4°C. Each resulting pellet was resuspended in 750µl of RSB buffer (10mM Tris-HCl pH7.4, 3mM $MgCl_2$, 10mM NaCl) and 5µl of 100mM PMSF and then 42µl of 4N H_2SO_4 was added. The samples were incubated on ice for 20 minutes and then centrifuged for 20 minutes at 10 000rpm, 4°C on a Heraeus Biofuge pico centrifuge. They were then dialyzed overnight in 6000-8000 molecular weight dialysis tubing against 4L of 0.1N glacial acetic acid. The next day the dialysis buffer was changed to ddH_20 and the water was subsequently changed for fresh ddH_20 twice over the next 36 hours. The samples were then removed from the tubing into eppendorf tubes and frozen at –80°C overnight. The samples were then lyophilized (Thermo Savant modulyo D) and resuspended in 50µl ddH_20, and the protein concentration was calculated using the Bradford assay.

2.11.2 Acid-Urea Gel Separation

2.11.2.1 SOLUTIONS

The following stock solutions were made ahead of time. They were stored in brown bottles at 4°C for up to 2 months.

TEMED/Acetic acid Stock: 4% TEMED, 43.1% Acetic acid

30% Acrylamide Stock (BioRad): 29.2% acrylamide, 0.8% bis-acrylamide

Riboflavin Stock: 0.004% riboflavin in ddH_2O

Potassium Acetate stock: 17.2mL glacial acetic acid, add ddH_2O to 90mL, titrate to pH 4.0 with KOH, and add ddH_2O to 100mL

The components of the stacking gel and separating gel are as follows:

Stacking Gel (8mL): 2.88g Urea , 1.6mL acrylamide stock, 2.33mL potassium acetate stock, 800μL riboflavin stock, 80μL thiodyglycol, 80μL TEMED, and ddH_2O to 8mL.

Separating Gel (19.4mL): 7.2g Urea, 10mL acrylamide stock, 2.5mL TEMED/acetic acid stock, 2mL riboflavin stock, 200μL thiodyglycol, and ddH_2O to 19.4mL.

2.11.2.2 POURING OF GEL

First, we prepare the separating gel as follows, we add the acrylamide stock to a 30mL beaker on a stir plate. We then add the urea slowly with constant stirring, along with TEMED/acetic acid, riboflavin stock, and a little ddH_2O. Once dissolved, we measure out the remaining ddH_2O to make the volume up to 19.4mL and add the thiodiethyleneglycol. We pour approximately 17.5mL of this separating gel solution in between glass plates of a large BioRad PROTEAN II xi electrophoretic cell set-up, using 0.75mm spacers. We overlay the separating gel with 70% ethanol and polymerize the gel between two light boxes for 3-4 hours. Once polymerized we pour off the ethanol and rinse the space

between the glass plates with water. We prepare the stacking gel by adding the ingredients in the same order as done in preparing the separating gel. We pour the stacking gel between the glass plates to the top of the plates and insert the comb (15 wells). We polymerize the gel between two light boxes for 3-4 hours. Once polymerized we cover the top of the gel apparatus with damp paper towels and wrap the entire apparatus with saran wrap. We stored the gel overnight at 4°C.

2.11.2.3 PREPARATION OF SAMPLES FOR GEL

The following solutions are used to prepare the samples and are stored at -20°C :

Sample Buffer: 6M urea, 5% acetic acid, 12.5mg/mL protamine sulfate, 0.2% pyronin Y, 30% sucrose, in ddH_2O.

Reducing Mix: All ingredients are in 1/1/1/1 ratio by volume, 2-mercaptoethanol, 20% (w/v) cysteamine, ddH_2O, and 1M Tris-HCl pH 8.8.

We prepare the samples the day we are going to run them on the gel, a good time is when the running apparatus is cooling down. We first add 4μL of reducing mix to 5μL of sample and incubate the mixture at room temperature for 20 minutes. We then added 6.7μL of sample buffer and 4.3μL of ddH_2O. We can adjust the volumes of reducing mix, sample buffer, and ddH_2O to the desired volume of sample but must keep the proportions the same as described above. We ran 25μg of sample and also ran a blank, as a control, which contained the only master mix; 9.3μL of ddH_2O, 4μL reducing mix, and 6.7μL sample buffer. Keep samples on ice until ready to load.

2.11.2.4 RUNNING AND TRANSFER OF ACID UREA GEL

We place 3L of running buffer (52mL of glacial acetic acid per 1L of ddH_2O) in the gel apparatus (PROTEAN II xi cell electrophoresis, BioRad, Mississauga, Ontario, Canada).

We remove the gel made the day before from the saran wrap and rinsed out the wells with running buffer. We placed the gel in the apparatus being careful to avoid bubbles and turned on the cooling system. We leave the entire system for 30 minutes to cool down. Once the samples are prepared, and the system cooled down, we load them into the wells using gel-loading tips. We run the gel at 250 volts for 36 hours.

Once the gel is finished running we transfer it to PVDF membrane, being careful when moving the gel from the apparatus because it is very thin. We submerge the PVDF membrane (BioRad) in methanol for 5-10 seconds, it will turn a grey color, and then place it in water until ready to use it. If the membrane loses its grey color you must re-submerge it in methanol. We set up the transfer apparatus and transfer the gel to the membrane as positive proteins, by reversing the electrodes (ie. black to red and red to black). We transfer the blot for 1 hour at 24 volts, 1 amp in transfer buffer (0.7% acetic acid, 10% methanol, 89.3% ddH_2O).

2.11.2.5 BLOCK THE MEMBRANE AND PROBE WITH ANTIBODIES

We disassemble the transfer apparatus and allow the PVDF membrane to air dry. We then block the membrane with Tris buffered saline-Tween20 (TBST) solution containing 5% powdered skim milk for 1 hour at room temperature on the orbitron. We probe the membrane with blocking buffer containing primary antibody overnight at 4°C on an orbitron. The next day we washed the membrane in 1xTBST for 15 minutes at room temperature on an orbitron. We continued to wash the blot three more times for 5 minutes each, changing the buffer after each wash. We then probed the blot with a secondary antibody, diluted in 5% skim milk, complimentary to the primary previously used. The membrane was then incubated in blocking buffer containing the appropriate secondary

antibody conjugated with alkaline phosphatase for 1 hour at room temperature on an orbitron. We then washed it in the same way we washed the blot after probing with the primary antibody. The membrane was then developed using enhanced chemiluminescence as described by the manufacturer (ECL, Amersham Pharmacia Biotech). The membrane was exposed to X-ray film for desired length of time and processed in a tabletop automated developer.

2.12 IMMUNOHISTOCHEMISTRY (IHC)

2.12.1 Cytospinning of CLL Patient Cells

CLL cells are initially plated in 100mm plates, see Section 2.9.2.2., and treated, see Section 2.5.2. We then remove the cells from the plate by pipetting up and down as little as possible, without scraping, and transfer the cells to a 50mL Corning tube. We centrifuge the cells for 5 min at 1200rpm, on an Eppendorf 5810R centrifuge, at room temperature and suck off the supernatant. We resuspend the pellet in fresh hybridoma media and then count the cells on the coulter counter (Beckman Coulter Z2). Once we determine the concentration of cells in the media we want to load 3-4 x 10^6 cells into the cytospin apparatus (ThermoShandon Cytospin 4). We spin the cells for 3 minutes at 200 rpm, room temperature, onto glass slides. We disassemble the apparatus and place the slides in room temperature fixing solution (100mL 37% formaldehyde, 900mL 1xPBS). We then store the cells in the fixing solution in the 4°C fridge.

2.12.2 Staining of Slides

We remove the slides from the fixing solution and wash them 3 times for 5 minutes in washing buffer (1xPBS, 0.1% NP-40) on an orbitron, changing to fresh buffer after each wash. We diluted our primary antibody in 10% FBS, 0.1% NP-40, in 1xPBS, and kept this on ice until we were ready to use it. We removed the slides from the washing buffer and tapped off the excess buffer. We laid them in a humid chamber with wet blotting paper and added 100 μL of the primary antibody dilution followed by a coverslip. We let the slides incubate for 1 hour at room temperature. We then washed the slides 4 times for 5 minutes in fresh washing buffer, removing the coverslip after the first wash, on an orbitron. We removed the slides from the washing buffer and tapped off the excess buffer. We placed the slide in the same humid chamber used for the primary antibody. We diluted our secondary antibody in 10% FBS, 0.1% NP-40, in 1xPBS, and added 100μL of this dilution to the slide followed by a coverslip. We incubated the slides for 1 hour at room temperature in the dark. We again washed the slides 4 times for 5 minutes in fresh washing buffer, removing the coverslip after the first wash, on an orbitron in the dark. We removed the slides from the washing buffer, tapped off the excess buffer, and laid them in a cardboard chamber. We added 10μL of DAPI + Antifade (Vectashield) to the cells on each slide and covered with a small coverslip. We stored the slides in the cardboard case at 4°C for no more than 4 weeks.

2.12.3 Fluorescence Microscopy and Deconvolution Analysis

Fluorescence images were captured on an AxioPhot II microscope (Carl Zeiss) with an AxioHRm camera. The stack images of 80 optical sections with a step size of 200nm were then deconvolved in three dimensions with the AxioVision 4.1 constrained Iterative Algorithm (Carl Zeiss) (116).

3. PROJECT HYPOTHESIS

1. The expression of death receptor 5 (DR5) is regulated by NF-kappa B (NFκB) and histone acetylation.
2. NFκB and histone acetylation may play an important role in regulating DR5 expression in chronic lymphocytic leukemia (CLL) cells.
3. Treatment of CLL cells with fludarabine (FLU) or lysophosphatidic acid (LPA) lead to the expression of different histone modifications.

4. RESULTS

4.1 DR5 transcriptional activity requires NFκB activation:

Our lab has previously determined that blocking NFκB activation with ΔIκB cells prevents etoposide induced DR5 expression. These ΔIκB cells sequester NFκB in the cytosol thereby preventing them from translocating into the nucleus and being activated. A putative NFκB binding site has been found in the first intronic region of the human DR5 gene and we therefore wanted to determine whether NFκB activation regulates DR5 transcriptional activity through this binding site. To do so we expressed the DR5 luciferase reporter gene containing the promoter and first intron region into HEK293 cells stably expressing ΔIκB or in HEK293 cells expressing vector alone. The transcriptional activity of the DR5 promoter in the ΔIκB expressing cells was repressed to near background levels compared to that of the vector alone expressing cells which measured above 30 relative luciferase units (Figure 7). To support these results, HEK293 cells were transiently transfected with the DR5 promoter and either vector alone or ΔIκB and subsequently treated with etoposide for 4 hours. In the cells transfected with vector alone, the DR5 promoter activity was increased 2.5 fold but the promoter activity failed to significantly increase in cells transfected with ΔIκB with only a 1.3 fold increase (Figure 8). To ensure the specificity of the ΔIκB cells in blocking NFκB activity we also measured the transcriptional activity of a p53 responsive BAX promoter. We found that expression of ΔIκB did not block the increase of activity following etoposide treatment, as compared to vector alone cells (Figure 9).

DR5 transcriptional activity requires NFκB activation

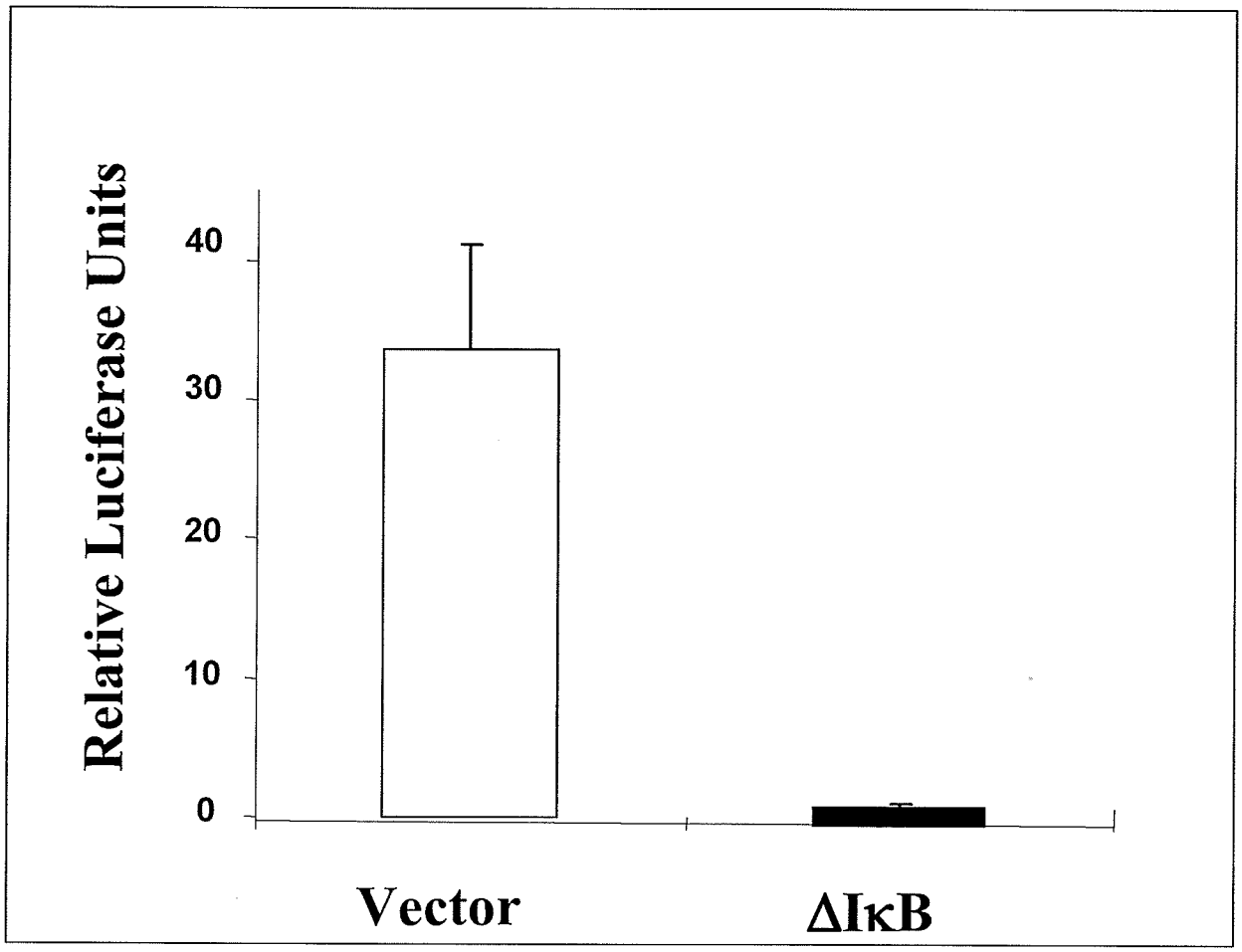

Figure 7

HEK293 cells were stably transfected with either vector alone or ΔIκB and both were transiently transfected with wild-type DR5 promoter-intron region luciferase reporter plasmid. β-gal reporter plasmid was used as a control for transfection efficiency. Twenty-four hours after transfection the cells were harvested, lysed, and a luciferase assay was performed as described in the Materials and Methods section. Error bars represent the standard deviation for three independent experiments. Relative luciferase units represent DR5 promoter activity.

DR5 transcriptional activity requires NFκB activation

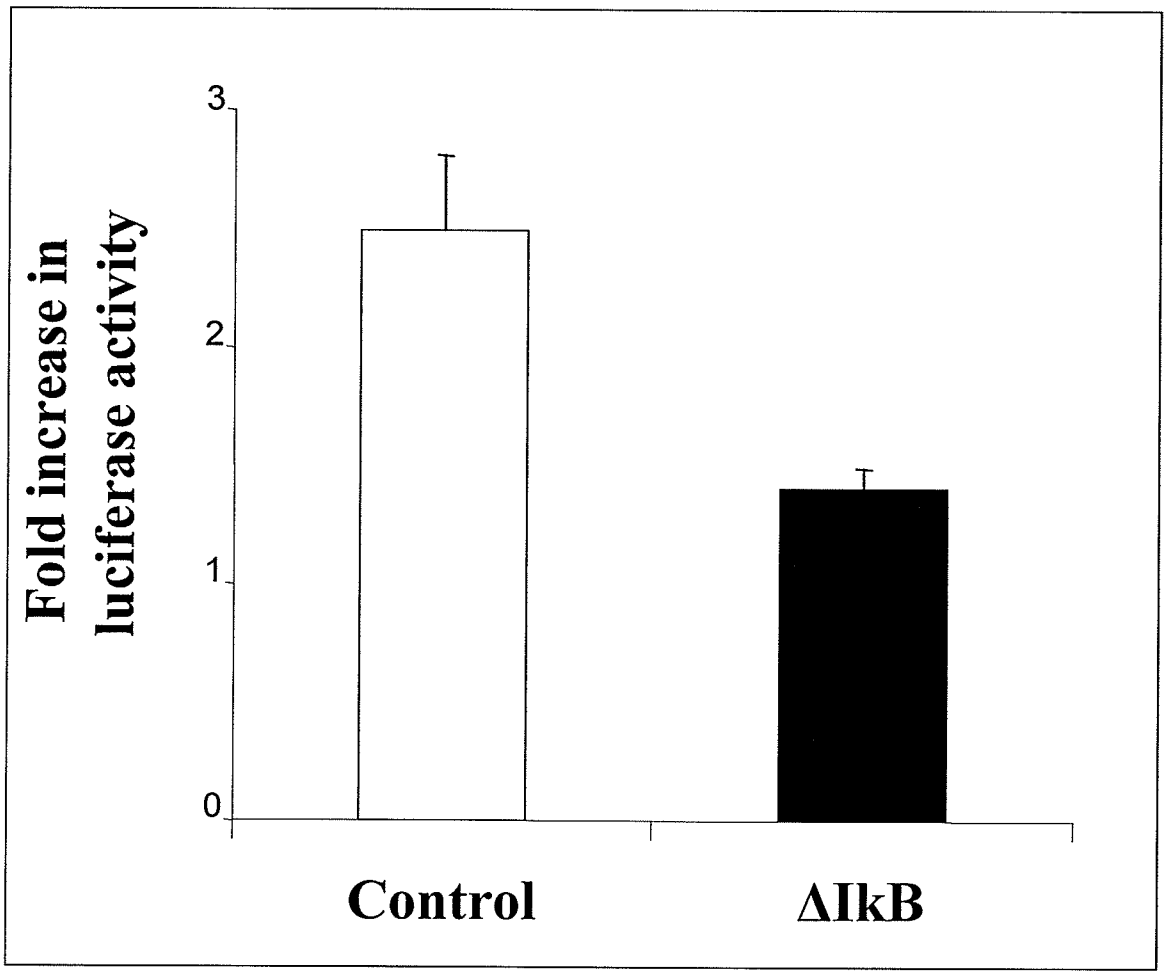

Figure 8

HEK293 cells were transiently transfected with wild-type DR5 promoter-intron region luciferase reporter plasmid and either vector alone (control) or ΔIκB. β-gal reporter plasmid was used as a control for transfection efficiency. Twenty-four hours after transfection the cells were treated with etoposide (100μM) for 4 hours, lysed, and a luciferase assay was performed as described in the Materials and Methods section. Error bars represent the standard deviation for three independent experiments.

Bax promoter activity does not require NFκB activation

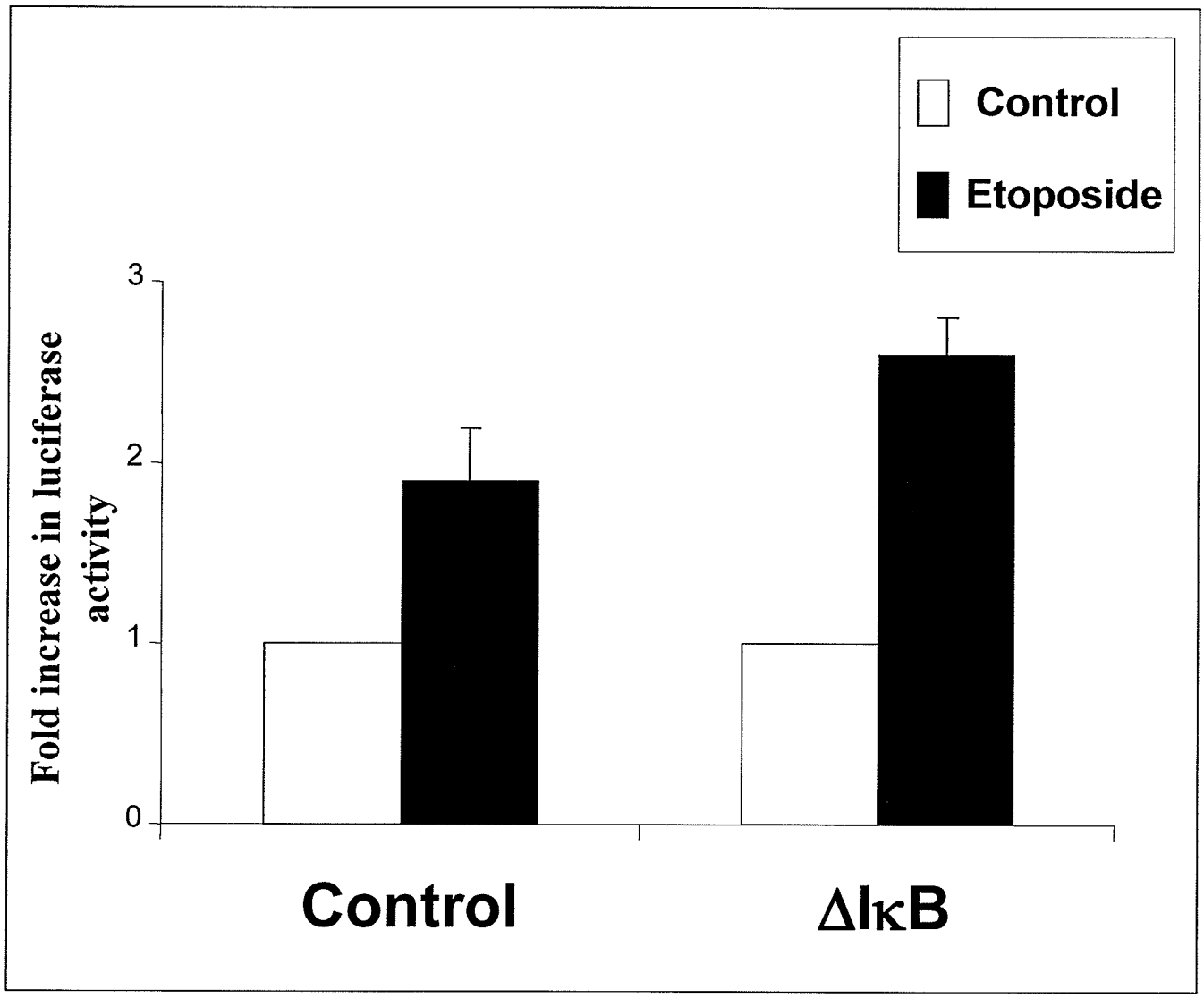

Figure 9

HEK293 cells were transfected with a Bax promoter luciferase construct and either empty vector (control) or ΔIκB. B-gal reporter plasmid was used as a control for trasnfection efficiency. Twenty-four hours after transfection the cells were treated with etoposide (100μM) for 16 hours, lysed, and a luciferase assay was performed as described in the Materials and Methods section. Error bars represent the standard deviation for three independent experiments.

Next, we wanted to determine whether this site-specific NFκB site within the first intronic region of the DR5 gene was responsible for the NFκB dependent transactivation of the DR5 gene. Point mutations were introduced within the NFκB consensus sequence (GGGAGTATCGCTTG), in the first intron of the DR5 gene, by Dr. Shashi Shetty. These mutations would prevent NFκB from binding to this site. A dramatic reduction in DR5 transcriptional activity was observed when this mutated promoter construct was transiently transfected into MCF-7 and HEK293 cells, compared to cells transfected with the wild-type promoter. HEK293 and MCF-7 cells transfected with the wild-type promoter exhibited over 3000 and 1000 relative luciferase units, respectively, whereas both cell types with mutated NFκB site exhibited less than 200 relative luciferase units (Figure 10). Dr. Shashi Shetty also made a promoter construct with the putative NFκB binding site deleted and similar results were observed. Even when the cells were transfected with a p65 over-expressing vector in combination with either the wild-type DR5 promoter-intron, the promoter with mutated p53, or the promoter with mutated NFκB DR5 plasmids, the mutated sites failed to show DR5 transcriptional activity (Figure 11). The wild-type promoter showed an 8 fold increase in activity, whereas the promoter with the mutated p53 site only showed a 2.5 fold increase and the promoter with the mutated NFκB site only showed a 2 fold increase. Furthermore, upon treating transfected HEK293 cells with etoposide for 16 hours, those transfected with the mutated NFκB site construct failed to increase DR5 transcriptional activity above the background level, as compared to the wild-type construct which showed a two-fold increase (Figure 12).

DR5 promoter activity requires NFκB and p53

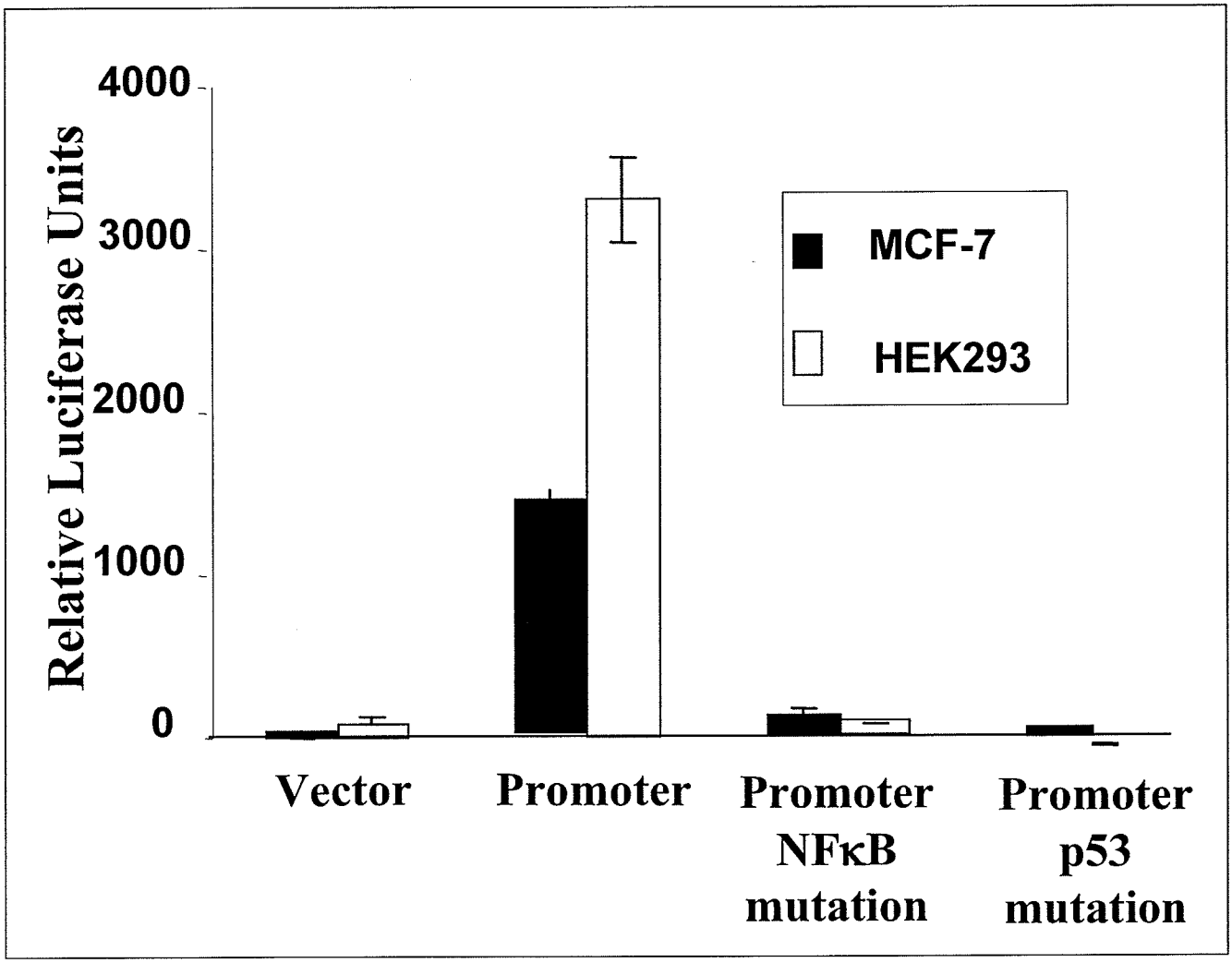

Figure 10

The NFκB putative binding site was mutated at GGGAGTATCGC, where nucleotides underlined represent point mutations. The p53 site was mutated at GGGAATATCCGGGCAAGACG, where nucleotides underlined represent point mutations. HEK293 cells and MCF-7 cells were transfected with luciferase reporter plasmid alone (vector), containing wild type DR5 promoter-intron region (Promoter), containing mutations in the NFκB binding site in the DR5 promoter-intron region (Promoter NFκB mutation), or containing mutations in the p53 binding site in the DR5 promoter-intron region (Promoter p53 mutation). β-gal reporter plasmid was used as a control for transfection efficiency. The cells were harvested after 24 hours, lysed, and a luciferase assay performed as described in the Materials and Methods section. Relative luciferase units represent DR5 promoter activity. Error bars represent the standard deviation for three independent experiments.

Overexpression of NFκB subunit p65 induces DR5 transcriptional activity

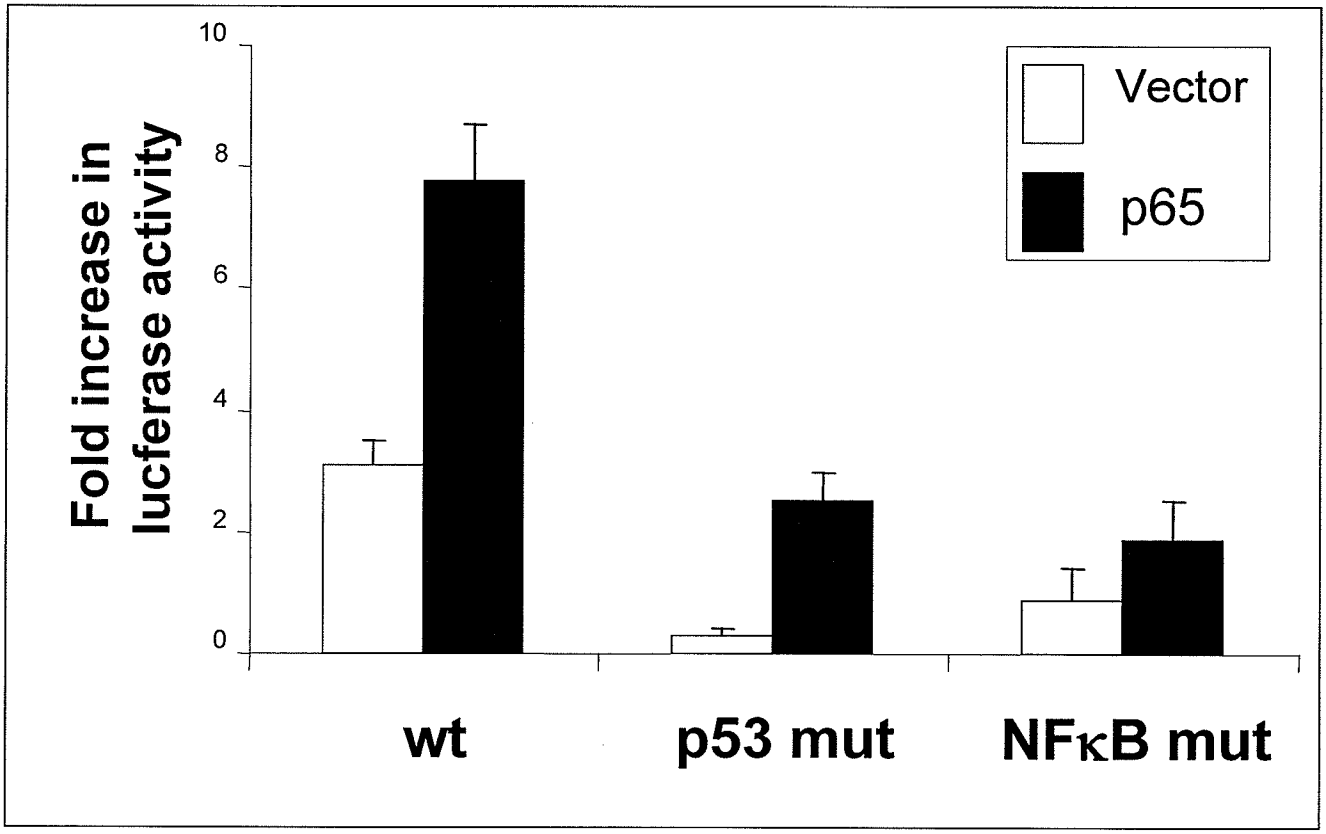

Figure 11

HEK293 cells were transiently transfected with either vector alone (vector) or p65 over-expressing vector (p65) in combination with either wild-type DR5 promoter-intron region luciferase reporter plasmid (wt), DR5 promoter-intron region luciferase reporter plasmid with mutated p53 binding site (p53 mut), or DR5 promoter-intron region luciferase reporter plasmid with mutated NFκB binding site. β-gal reporter plasmid was used as a control for transfection efficiency. Twenty-four hours after transfection the cells were treated with etoposide (100μM) for 6 hours, lysed, and a luciferase assay was performed as described in the Materials and Methods section. Error bars represent the standard deviation for three independent experiments.

DR5 transcriptional activity requires NFκB activation

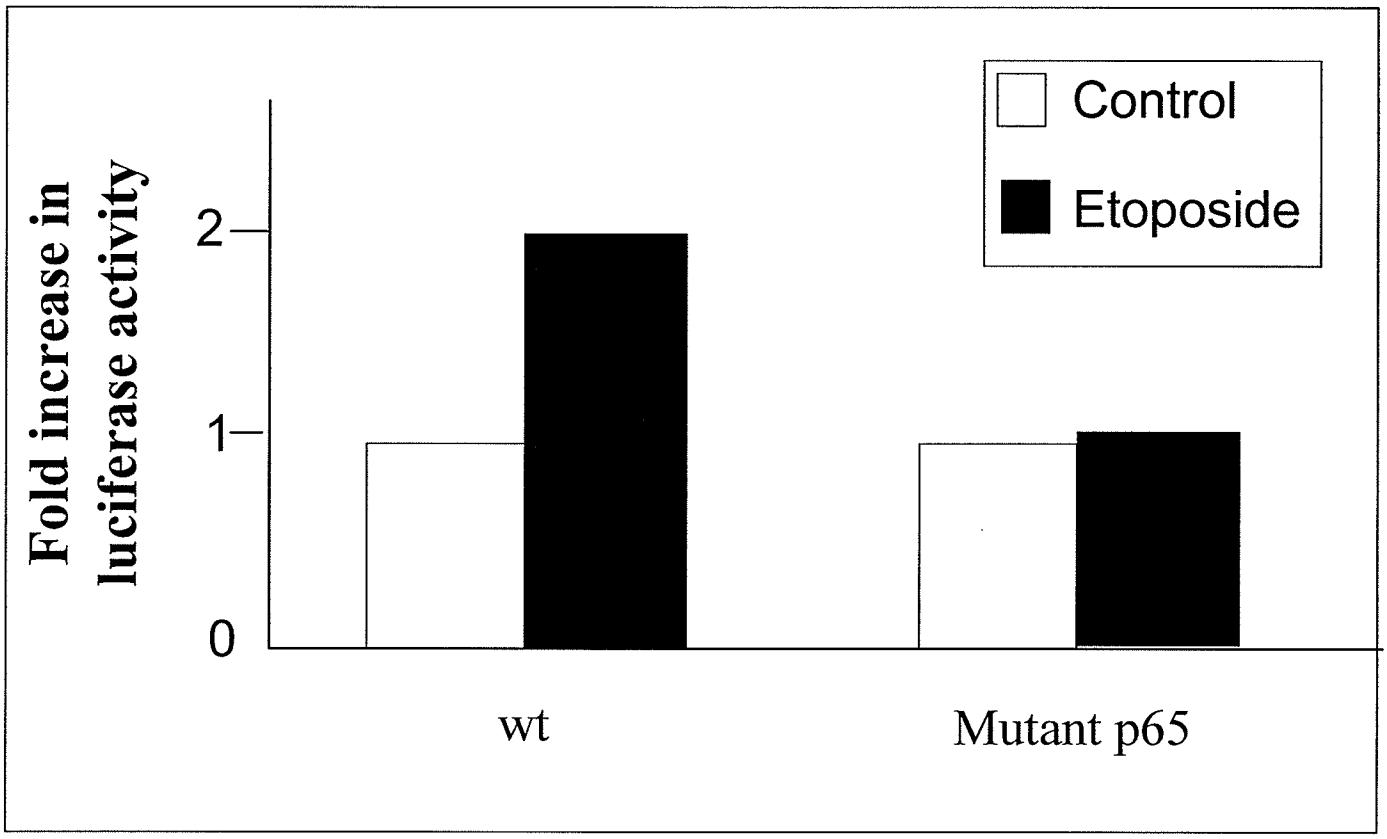

Figure 12

The NFκB putative binding site was mutated at GGGAGTATCGC, where nucleotides underlined represent point mutations. HEK293 cells were transfected with luciferase reporter plasmid containing either wild type DR5 promoter-intron region (wt) or containing mutations in the NFκB binding site in the DR5 promoter-intron region (Mutant p65). β-gal reporter plasmid was used as a control for transfection efficiency. Twenty-four hours after transfection the cells were left untreated (Control) or treated with etoposide (100μM) for 16 hours. The cells were then harvested, lysed, and a luciferase assay performed as described in the Materials and Methods section.

Finally, we used 3T3 murine fibroblast cells that lack p65 expression. Upon treatment with etoposide for 16 and 24 hours, these cells showed a significant reduction in DR5 transcriptional activity when compared to wild type cells expressing p65. Wild-type 3T3 cells showed a 5-fold increase after 16 hours of treatment and a 6.5-fold increase following 24 hours of treatment with etoposide. 3T3 cells lacking p65 expression, however, only showed a 2-fold increase after 16 hours of treatment and only a 4-fold increase after 24 hours of treatment (Figure 13). All of these results together suggest that the NFκB binding site within the first intronic region of the DR5 gene is involved in its expression.

4.2 NFκB binds to the first intronic region of the DR5 gene

To determine whether NFκB binds to the first intronic region of the DR5 gene we performed chromatin immunoprecipitation (ChIP) assays in HEK293 cells where the first intronic region of the DR5 gene was amplified. We treated HEK293 cells with etoposide over an 8 hour time course. We observed that binding of the p65 subunit of NFκB to the first intronic region of the DR5 gene increased over the 8 hours, peaking 4 hours post-treatment (Figure 14). For each time point, we used amplified input DNA from the intronic region of the DR5 gene as our loading control and lysate with no antibody as our negative control.

DR5 transcriptional activity requires NFκB activation

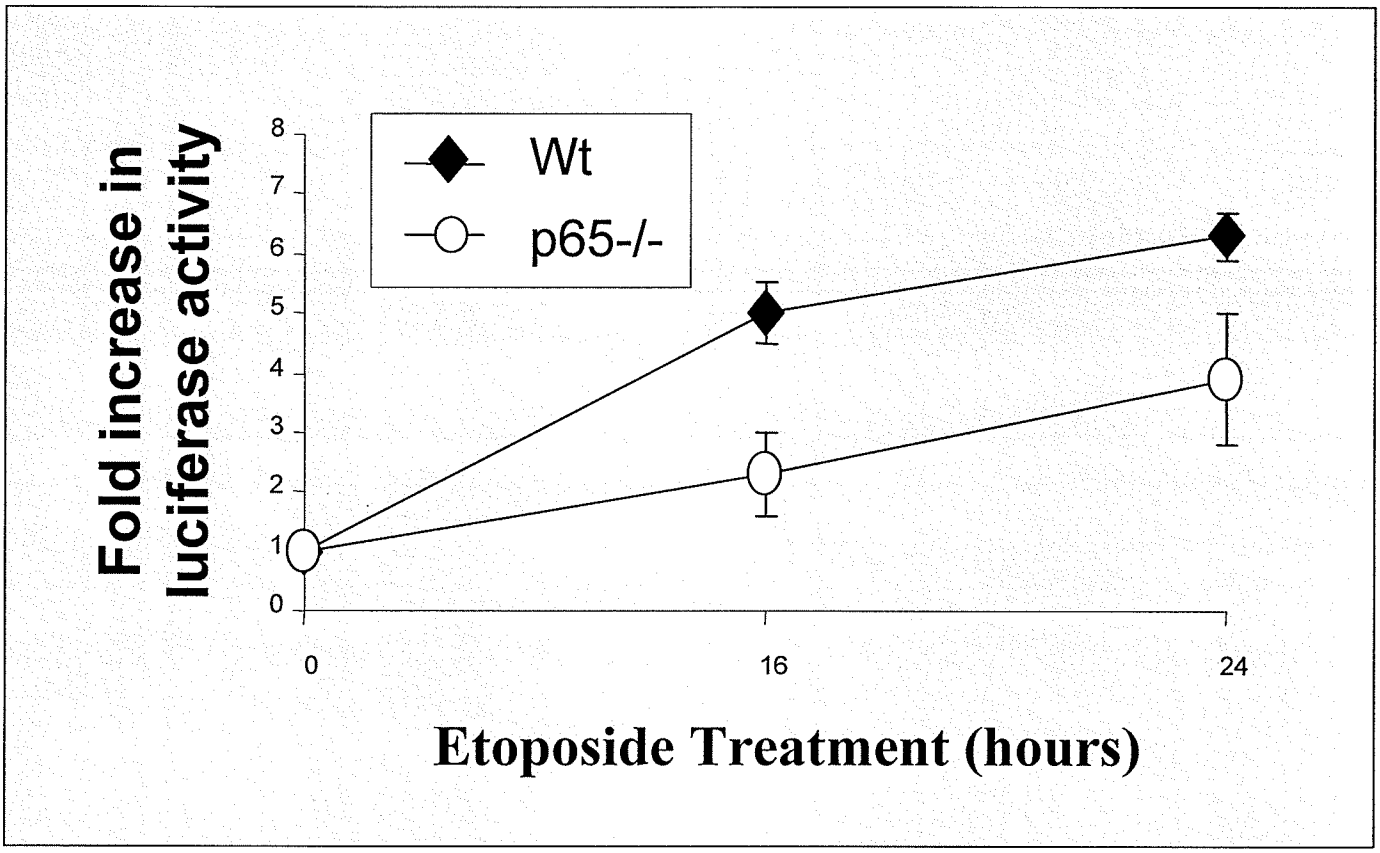

Figure 13

3T3 murine fibroblast cells, parental (wt) or lacking p65 expression (p65 -/-), were transfected with the wild-type DR5 promoter-intron region luciferase reporter plasmid. β-gal reporter plasmid was used as a control for transfection efficiency. Twenty-four hours after transfection the cells were treated with etoposide (100μM) and lysed after 16 and 24 hours. A luciferase assay was performed as described in the Materials and Methods section. Error bars represent the standard deviation for three independent experiments.

NFκB subunit p65 binds to the DR5 gene in the first intron

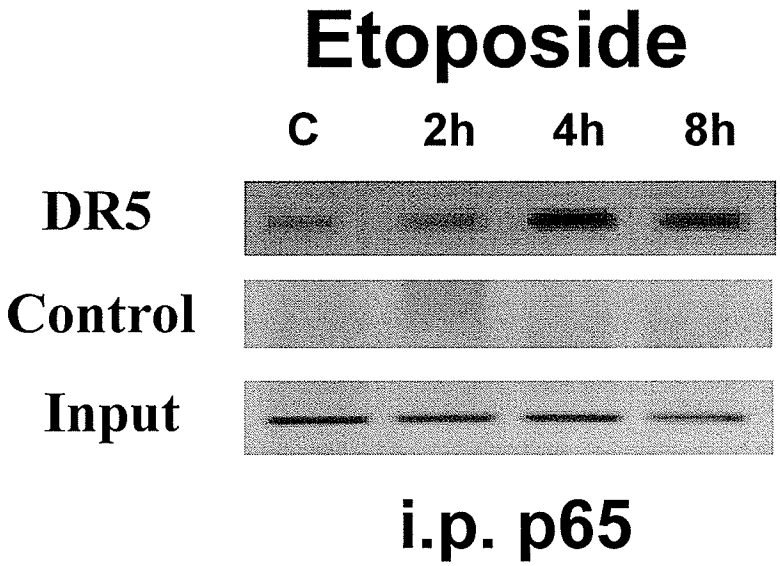

Figure 14

HEK 293 cells untreated (C) or treated with etoposide (100μM) were used in a ChIP assay with anti-p65 antibodies. No antibody added was used as a negative control whereas genomic DNA was used as an input control. Precipitated DNA was analyzed by PCR using primers specific for the DR5 exon 1 and intron 1 region. Each experiment was repeated three times.

4.3 Tumor suppressor p53 required for DR5 promoter activity

It has already been determined that there is also a p53-like consensus site within the first intronic region of the DR5 gene. Since it is thought that NFκB may cooperate with p53 in inducing expression of pro-apoptotic genes we wanted to determine whether p53 is important for DR5 transcriptional activity following etoposide treatment. We used a DR5 promoter construct with point mutations within the p53 consensus-binding site (GGGAATATCCGGGCAAGACG) in the first intronic region of the DR5 gene. We transiently transfected the mutant construct and the wild-type construct, separately, into HEK293 and MCF-7 cells. We observed a significant reduction in DR5 promoter activity with those cells transfected with the mutant construct compared to the wild-type construct (Figure 10). HEK293 and MCF-7 cells transfected with the wild-type promoter exhibited over 3000 and 1000 relative luciferase units, respectively, whereas both cell types with mutated p53 site exhibited less than 100 relative luciferase units. These results suggest that the p53 binding site within the first intronic region of the DR5 gene is involved in its expression.

4.4 p53 binds to the first intronic region of the DR5 gene and is required for the binding of p65 to the DR5 gene

To determine whether p53 binds to the first intronic region of the DR5 gene we performed ChIP assays in HEK293 cells where the DR5 gene was amplified. We observed that p53 binds to the DR5 gene both in untreated cells as well as those treated with etoposide over an 8 hour time course. The binding of p53 to the DR5 gene peaked at 4 hours (Figure 15).

p53 binds to the DR5 gene in the first intron

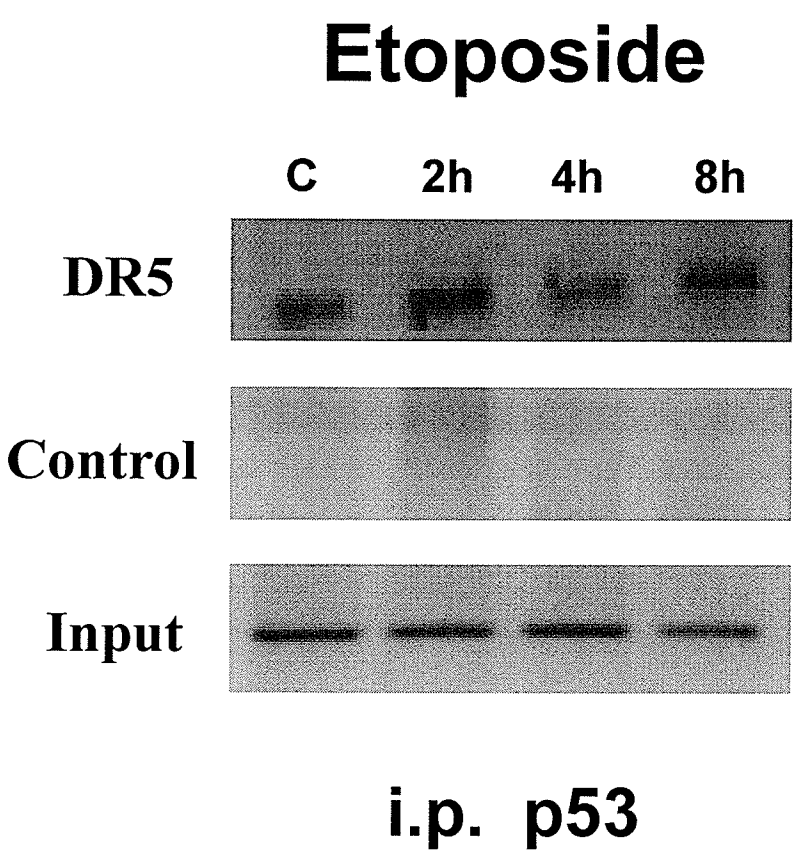

Figure 15

HEK 293 cells untreated (C) or treated with etoposide (100μM) were used in a ChIP assay with anti-p53 antibodies. No antibody added was used as a negative control whereas genomic DNA was used as an input control. Precipitated DNA was analyzed by PCR using primers specific for the DR5 exon 1 and intron 1 region. Each experiment was repeated three times.

The ChIP assay was also performed in MCF-7 cells with similar results (Figure 16). We observed p53 binding only after treatment with etoposide for 2 hours or 4 hours.

To determine whether p53 binding to the DR5 gene affects the binding of p65 we used siRNA against p53. We transfected HEK293 cells with siRNA directed against p53, thereby reducing the expression of p53, or scrambled siRNA as a control (Figure 17). We then used these cells in a ChIP assay to determine the effect of p65 binding to the DR5 gene. Upon treatment with etoposide for 4 hours, those cells transfected with scrambled siRNA showed binding of both p53 and p65 to the DR5 gene (Figure 17). However, those cells transfected with p53 siRNA failed to show binding of either p53 or p65 to the DR5 gene following etoposide treatment for 4 hours (Figure 17). These results along with the previous ChIP assay and luciferase results suggest that p53 is required for DR5 expression and cooperates with NFκB.

4.5 Epidermal Growth Factor (EGF) induces NFκB and p53 binding to the DR5 gene

Our lab has previously determined that DR5 mRNA expression and protein levels are induced following treatment with etoposide. In contrast, EGF treatment shows no induction of DR5 mRNA expression and no increase in DR5 protein levels. To determine whether p65 and p53 bind to the first intronic region of the DR5 gene we performed ChIP assays in HEK293 cells where the DR5 gene was amplified. We observed that p65 binds to the DR5 gene both in untreated cell as well as those treated with EGF (Figure 18). The binding of p65 to the DR5 gene peaked at 1 hour and was reduced to basal levels after 4 hours of treatment. In contrast, we observed that p53 binds to the intronic region of the

p53 binds to the DR5 gene in the first intron

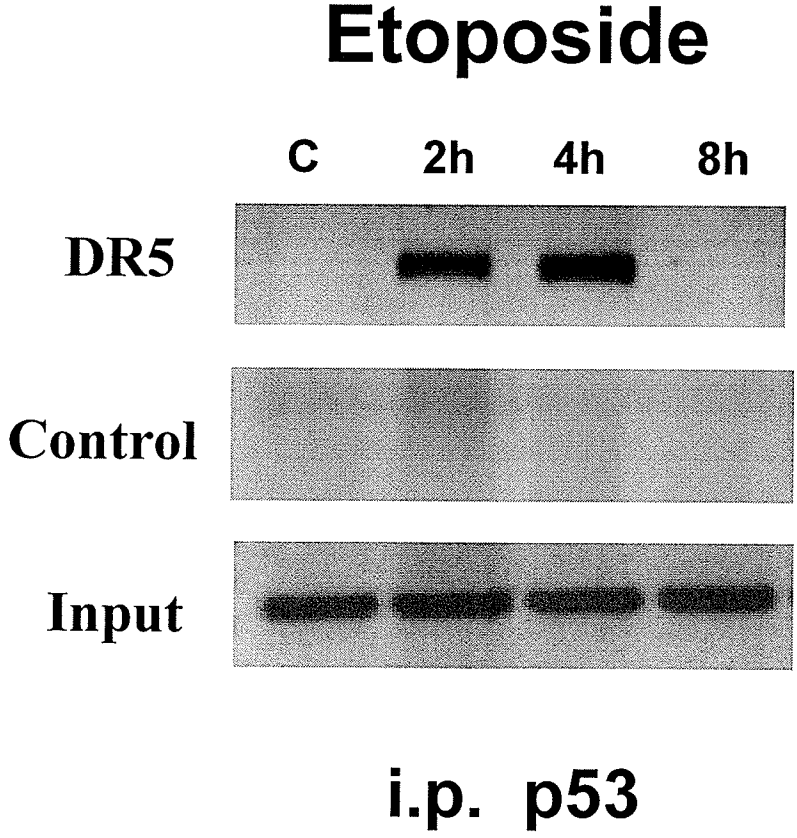

Figure 16

MCF-7 cells untreated (C) or treated with etoposide (100μM) were used in a ChIP assay with anti-p53 antibodies. No antibody added was used as a negative control whereas genomic DNA was used as an input control. Precipitated DNA was analyzed by PCR using primers specific for the DR5 exon 1 and intron 1 region. Each experiment was repeated three times.

p53 is required for NFκB to bind to DR5 gene upon treatment with etoposide

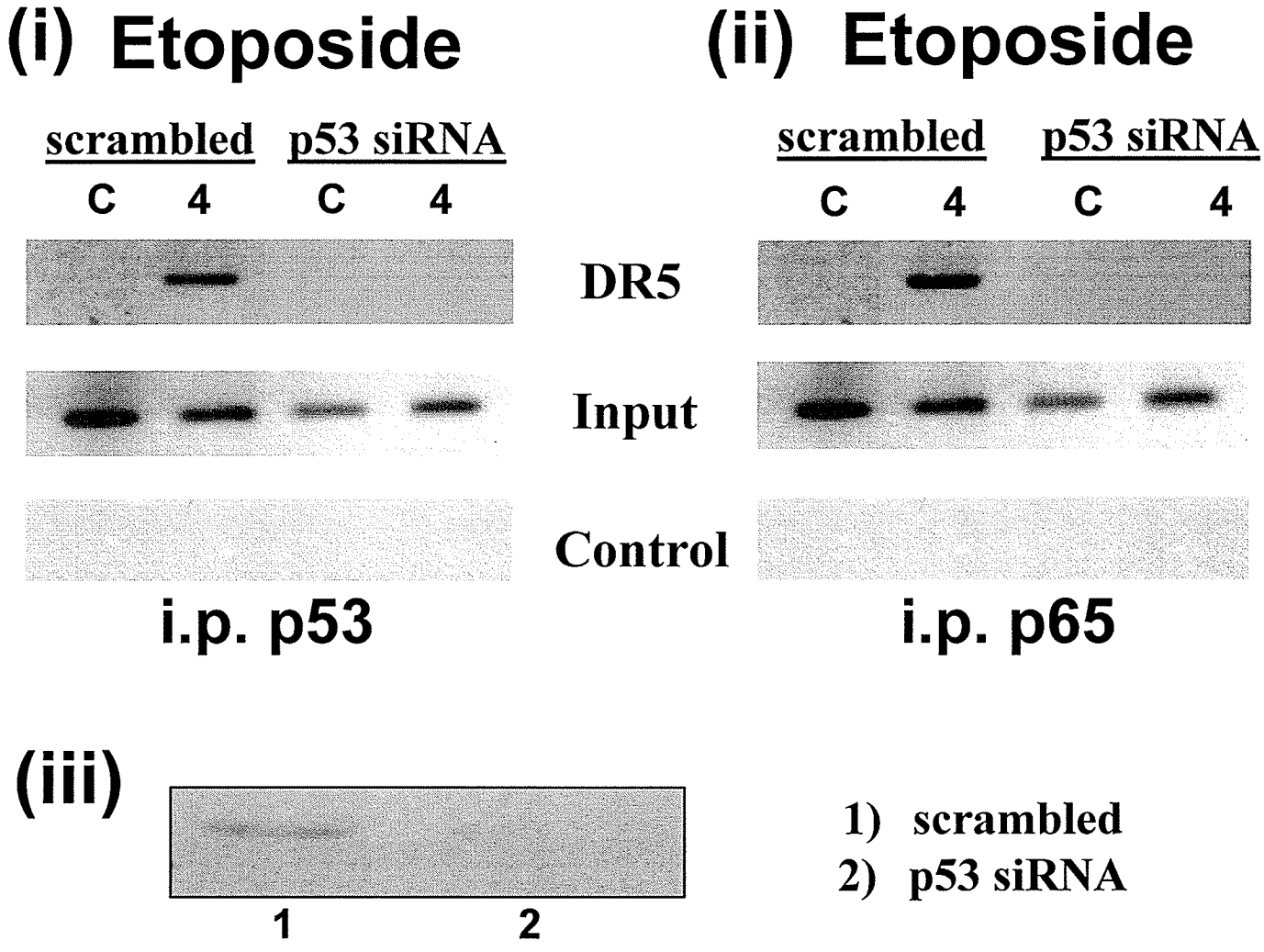

Figure 17

HEK293 cells were transfected with siRNA against p53 or scrambled siRNA and left untreated (C) or treated with etoposide (100μM) for 4 hours. The cells were lysed and used in a ChIP assay with either (i) anti-p53 antibody or (ii) anti-p65 antibody. No antibody added was used as a negative control whereas genomic DNA was used as an input control. Immunoprecipitated DNA was analyzed by PCR using primers specific for DR5 exon 1 and intron 1 regions. (iii) Transfected cells were lysed and western blotted for p53 expression.

NFκB subunit p65 binds to the DR5 gene in the first intron

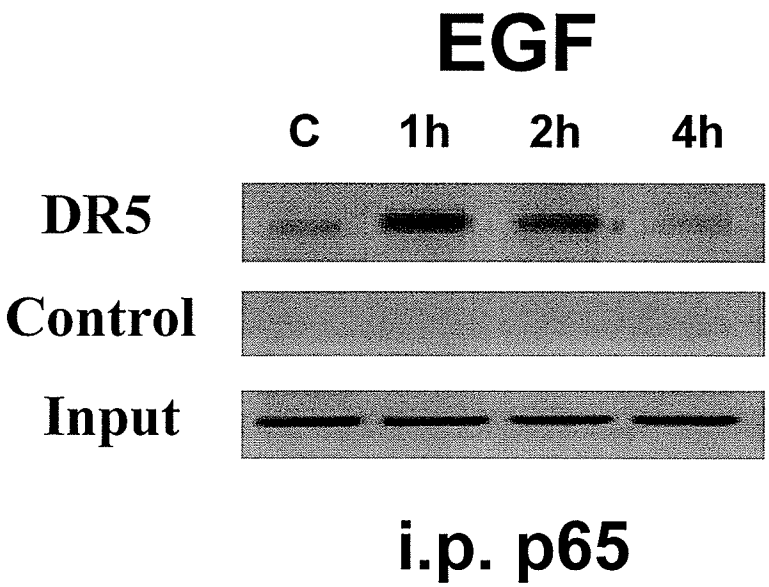

Figure 18

HEK 293 cells untreated (C) or treated with EGF (1μg/mL) were used in a ChIP assay with anti-p65 antibodies. No antibody added was used as a negative control whereas genomic DNA was used as an input control. Precipitated DNA was analyzed by PCR using primers specific for the DR5 exon 1 and intron 1 region. Each experiment was repeated three times.

DR5 gene but fails to increase following EGF treatment (Figure 19). These results suggest that EGF induces the binding of NFκB but it does not induce the binding of p53 however it does not inhibit the binding of p53 either. Since NFκB seems to be induced under both survival and apoptotic conditions we wanted to determine if there was a difference between the NFκB induced upon etoposide treatment and the NFκB induced upon EGF treatment. To do so we performed a western blot with HEK293 cells treated with either etoposide or EGF and looked at the expression levels of NFκB p65 subunit phosphorylated at serine 529. We observed that there was no phosphorylation of NFκB at serine 529 following an 8 hour time course of etoposide. There was, however, p65 phosphorylation following EGF treatment for an 8 hour time course, with levels peaking around 0.5 hours. The peak at 8 hours could be due to over-loading (Figure 20). These results suggest that the binding of NFκB to the DR5 gene following EGF and etoposide treatment could be differentiated by the modifications on p65 subunit of NFκB.

4.6 HDAC1 recruitment to the DR5 gene following EGF treatment but not etoposide treatment is mediated by NFκB

Histone acetylation allows for transcription of genes. The ability of etoposide or EGF to increase histone acetylation in the DR5 gene is unknown. To determine if histone acetylation within the DR5 gene occurred under etoposide or EGF treatment, a ChIP assay was performed on untreated and treated HEK293 cells using an anti-acetyl histone H3 antibody (Figure 21). We observed that treatment with etoposide induced histone acetylation after 16 hours of treatment. This time course corresponds with that of DR5

p53 binds to the DR5 gene in the first intron

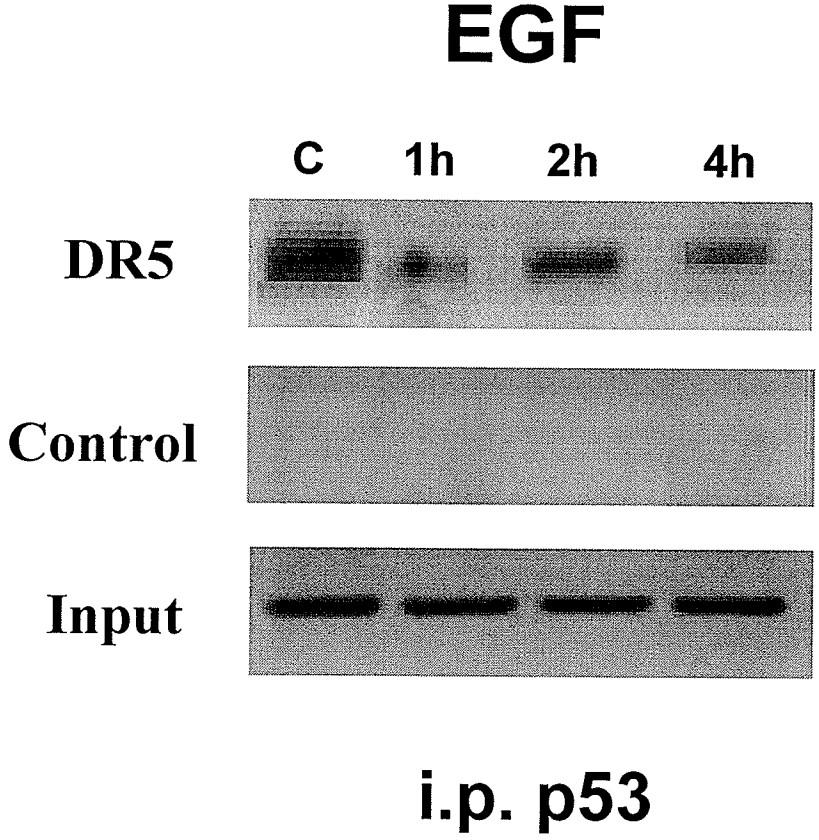

Figure 19

HEK 293 cells untreated (C) or treated with EGF (1μg/mL) were used in a ChIP assay with anti-p53 antibodies. No antibody added was used as a negative control whereas genomic DNA was used as an input control. Precipitated DNA was analyzed by PCR using primers specific for the DR5 exon 1 and intron 1 region. Each experiment was repeated three times.

NFκB is phosphorylated following treatment with EGF but not Etoposide

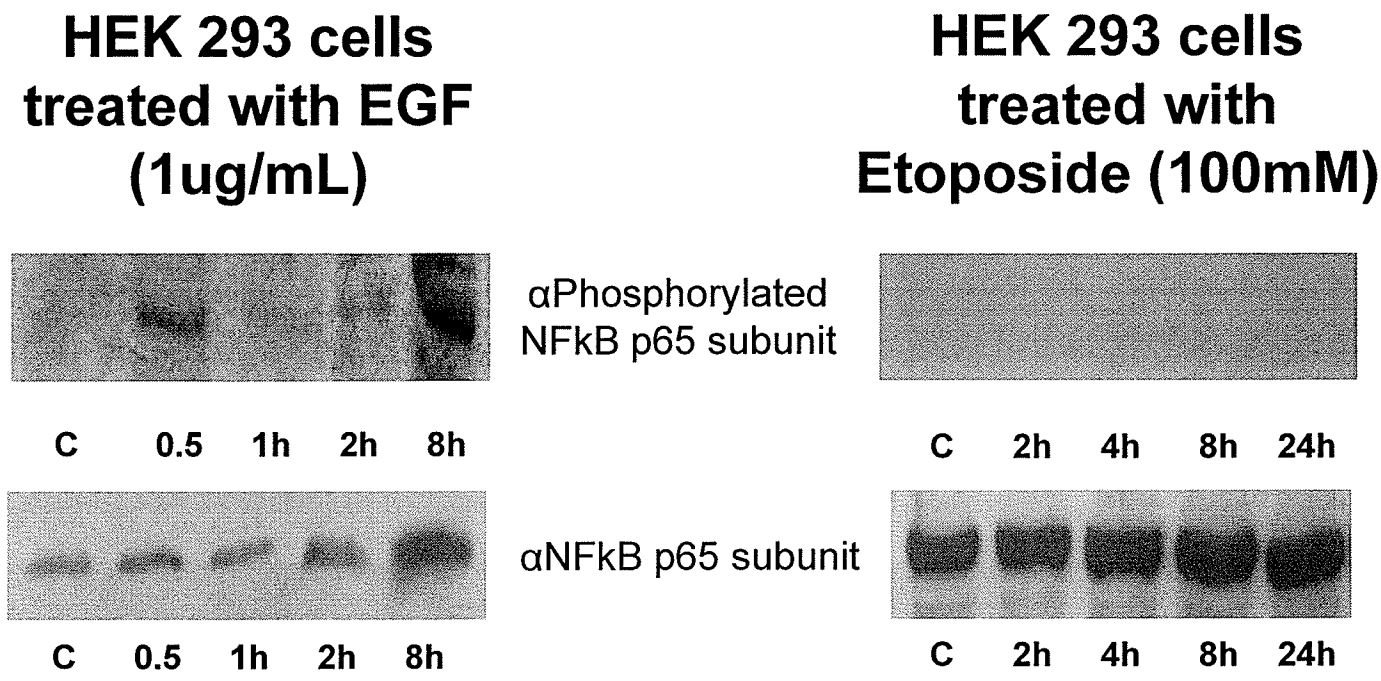

Figure 20

HEK293 cells were treated with etoposide (100μM) or EGF (1μg/mL) over the indicated times. The cells were then lysed and Western blotted for phosphorylated NFκB p65 subunit (serine 529) and NFκB p65 subunit (loading control).

DR5 gene is acetylated following etoposide but not EGF treatment

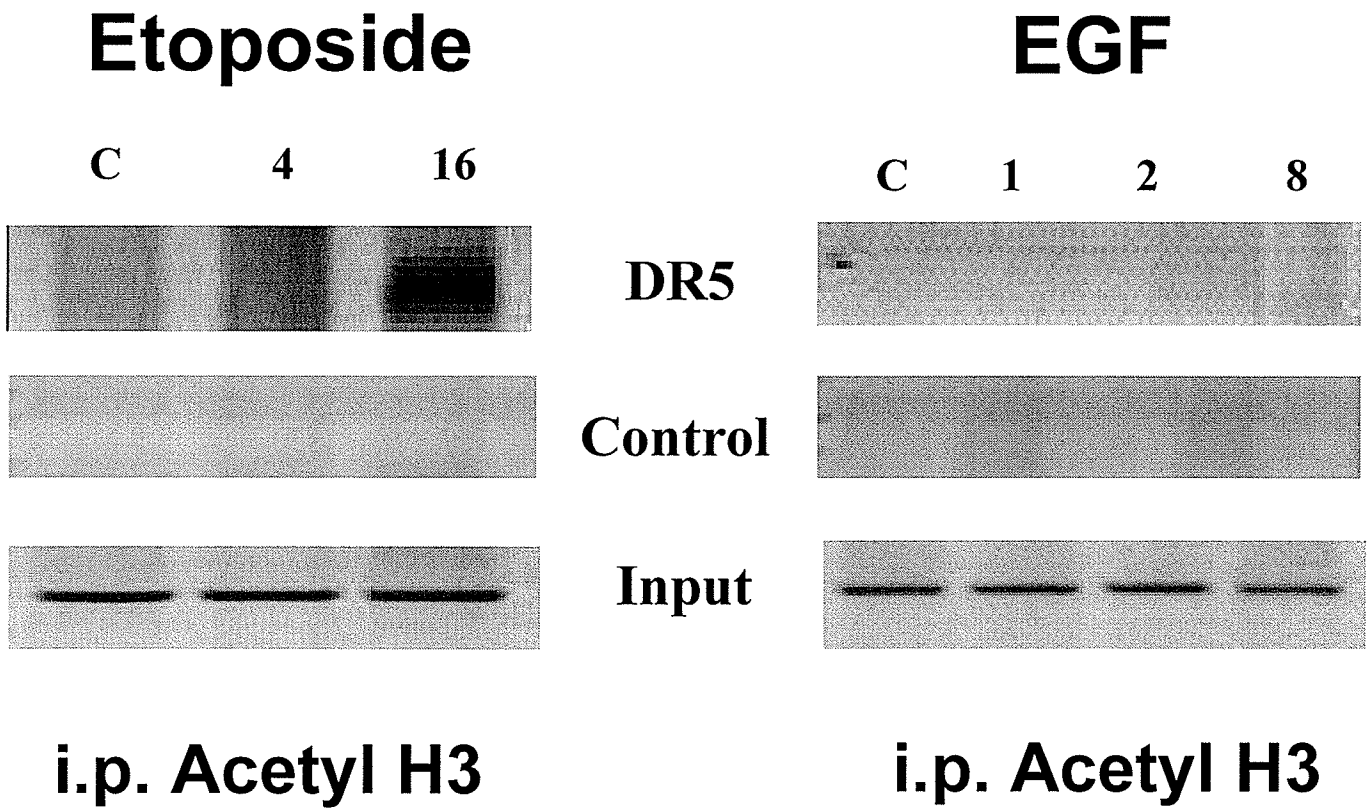

Figure 21

HEK293 cells untreated (C) or treated with either etoposide (100μM) or EGF (1μg/mL) were used in a ChIP assay with anti-acetyl histone H3 antibody. No antibody added was used as a negative control whereas genomic DNA was used as an input control. Immunoprecipitated DNA was analyzed by PCR using primers specific for DR5 exon1 and intron 1 regions.

expression. In contrast, we observed no increase in histone acetylation following EGF treatment within the time course of NFκB binding to the DR5 gene. This indicates that etoposide but not EGF treatment induces histone acetylation required for transcription. Histone deacetylases (HDACs) repress transcription of genes. To determine whether HDAC1 associates with the DR5 gene following treatment with either etoposide or EGF, a ChIP assay was performed on untreated and treated HEK293 cells using HDAC1 antibodies (Figure 22). We observed that treatment with EGF resulted in HDAC1 binding to the DR5 gene after 2 and 4 hours of treatment. In contrast, we observed that treatment with etoposide failed to recruit HDAC1 to the DR5 gene. This suggests that following EGF treatment the DR5 gene is actively repressed by HDAC1.

NFκB has been shown to associate with HDAC1 and has been implicated in transcriptional repression of target genes. To determine whether NFκB interacts with HDAC1 following EGF or etoposide treatment, Dr. Jennifer Brown immunoprecipitated NFκB with anti-p65 over a time course in HEK293 cells and western blotted for HDAC1. It was observed that the interaction between p65 and HDAC1 increased following EGF treatment but no increase was observed following etoposide treatment. To demonstrate that HDAC1 recruitment to the DR5 gene requires NFκB, we performed a ChIP assay on HEK293 cells stably expressing ΔIκB as well as HEK293 cells stably expressing vector alone, both treated with EGF (Figure 23). We observed that the ability of HDAC1 to associate with the DR5 gene following EGF treatment was blocked in ΔIκB expressing HEK293 cells whereas HDAC1 was shown to bind to the DR5 gene following 2 and 4 hours treatment with EGF in vector alone expressing HEK293 cells. This suggests that

HDAC1 is recruited to the DR5 gene following EGF but not Etoposide treatment

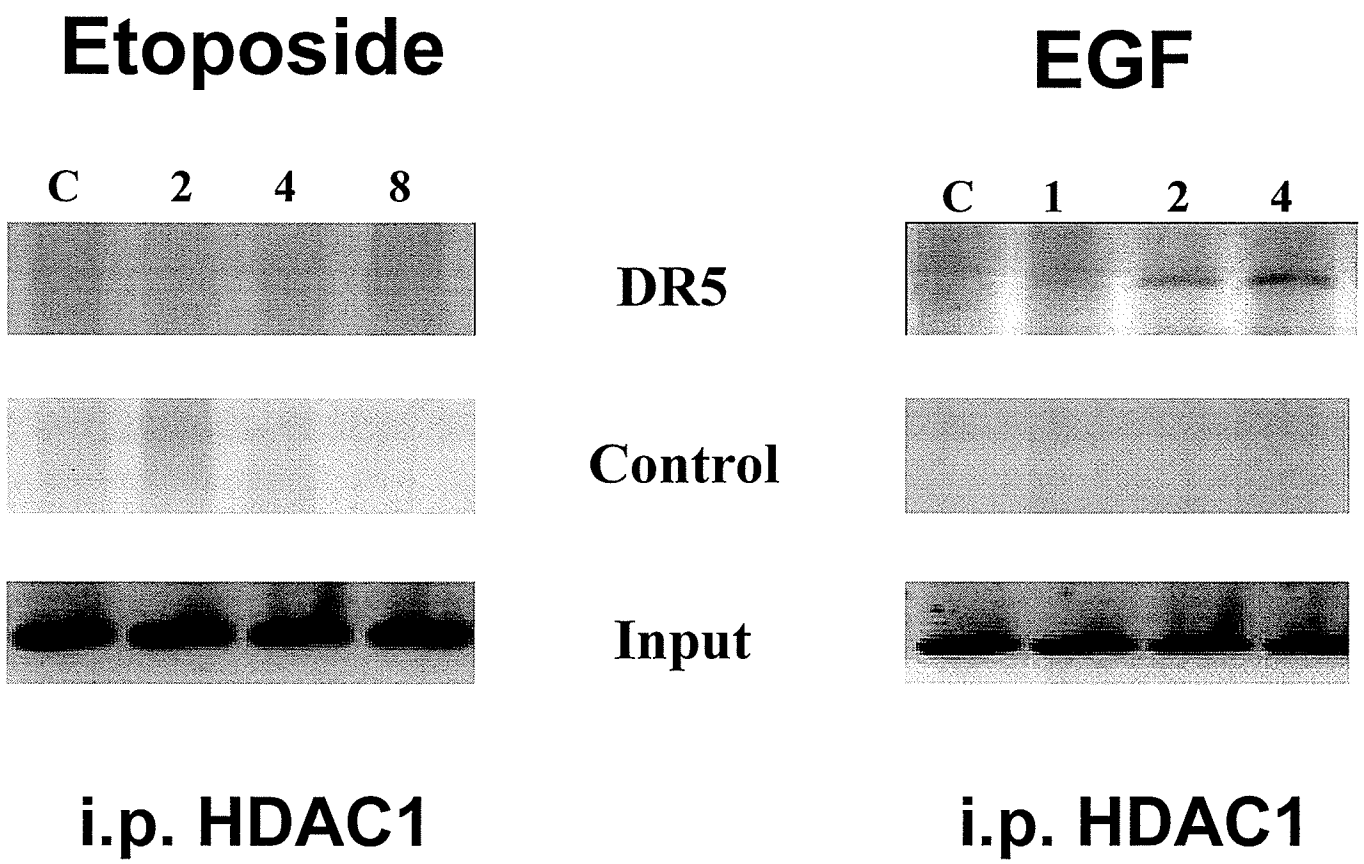

Figure 22

HEK293 cells untreated (C) or treated with either etoposide (100μM) or EGF (1μg/mL) were used in a ChIP assay with anti-HDAC1 antibody. No antibody added was used as a negative control whereas genomic DNA was used as an input control. Immunoprecipitated DNA was analyzed by PCR using primers specific for DR5 exon 1 and intron 1 regions.

p65 is required to recruit HDAC1 to the DR5 gene

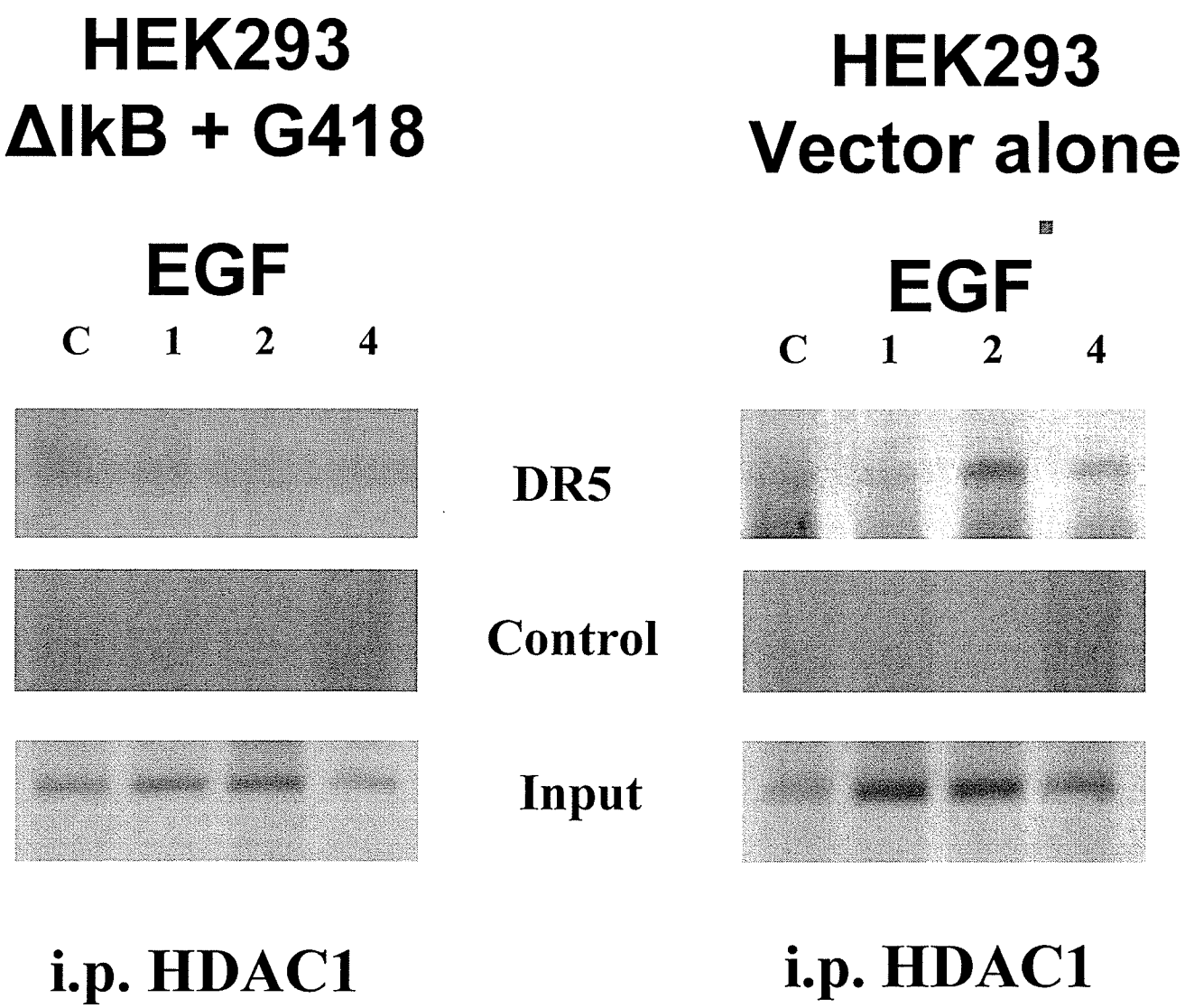

Figure 23

HEK293 cells were stably transfected with either vector alone or ΔIκB plasmids and left untreated (C) or treated with EGF (1μg/mL). The cells were lysed and then used in a ChIP assay with anti-HDAC1 antibody. No antibody added was used as a negative control whereas genomic DNA was used as an input control. Immunoprecipitated DNA was analyzed by PCR using primers specific for DR5 exon 1 and intron 1 regions.

NFκB is involved in the recruitment of HDAC1 to the DR5 gene following EGF treatment.

4.7 Inhibition of HDAC activity causes increased DR5 expression

The association of HDAC1 with the DR5 gene suggests that HDACs repress DR5 expression. Our lab has previously determined that treatment with HDAC inhibitors trichostatin A (TSA) or valproic acid (VPA) , increased DR5 mRNA level by 2.0 and 2.5 fold respectively. TSA has been previously demonstrated to activate both p53 and NFκB through acetylating these proteins. To demonstrate this we transfected HEK293 cells with either NFκB luciferase plasmid or p53 luciferase plasmid and treated the cells with TSA (Figure 24). Using luciferase reporter assays, we observed that TSA activated both p53 and NFκB by 1.5 and 1.75 fold, respectively.

To determine whether p53 and p65 are bound to the DR5 intronic regions similar to etoposide treatment, we performed ChIP assays on HEK293 cells treated with TSA for 16 hours (Figure 25). We observed that treatment with TSA lead to the binding of both p53 and p65 to the intronic region of the DR5 gene whereas HDAC1 failed to bind to this region. These results suggest that HDAC inhibitors induce DR5 expression mediated by p53 and NFκB activation.

Inhibition of HDAC activity leads to an increase in DR5 expression

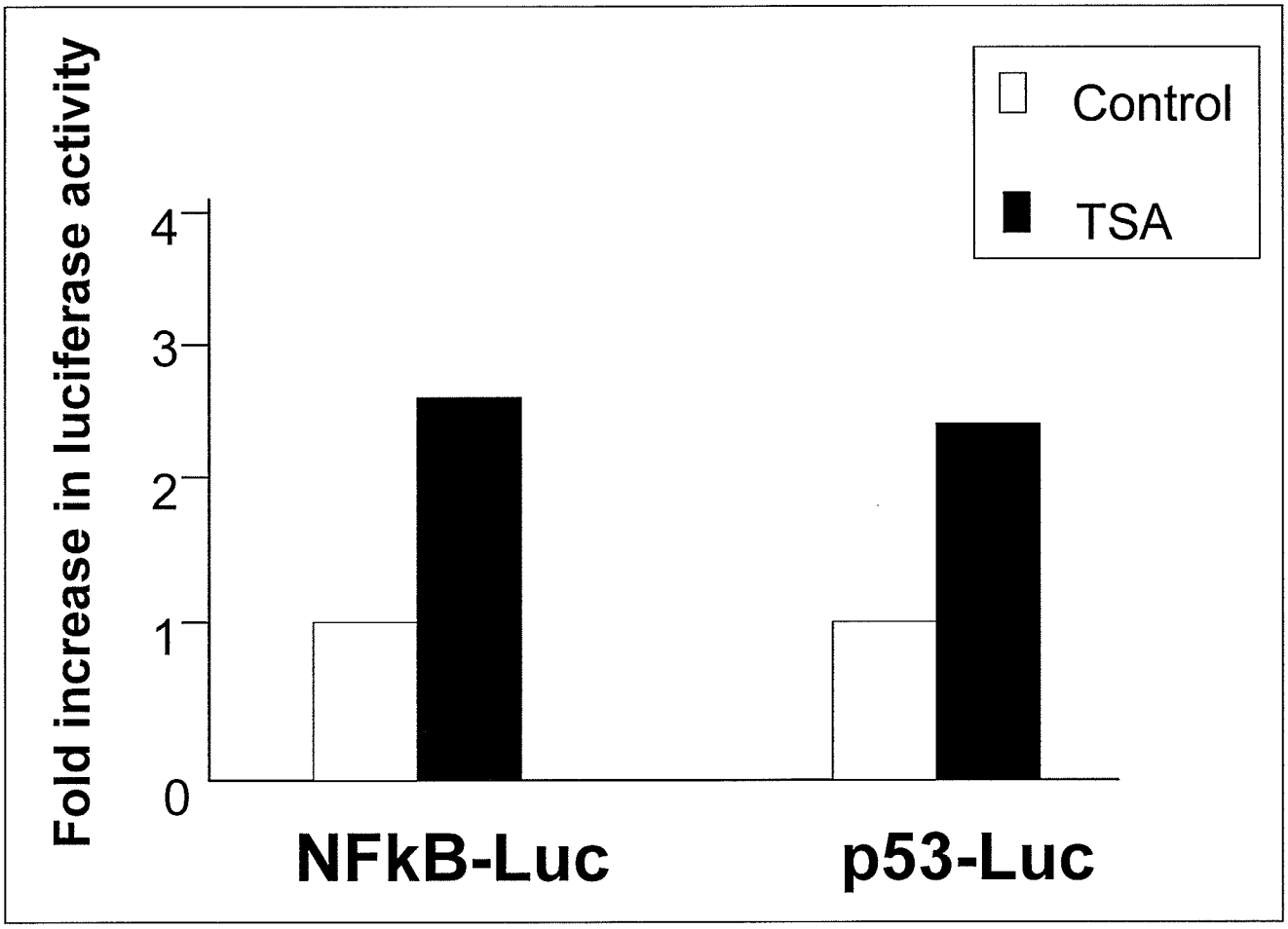

Figure 24

HEK293 cells were transfected with a Bax promoter luciferase construct (p53-Luc) or an NFκB luciferase construct (NFκB-Luc). β-gal reporter plasmid was used as a control for transfection efficiency. Twenty-four hours after transfection the cells were lysed (control) or treated with TSA (45nM) and lysed after 16 hours (TSA). A luciferase assay was performed as described in the Materials and Methods section. Error bars represent the standard deviation for three independent experiments.

Treatment with TSA enhances the binding of p53 and NFκB to the first intron of DR5

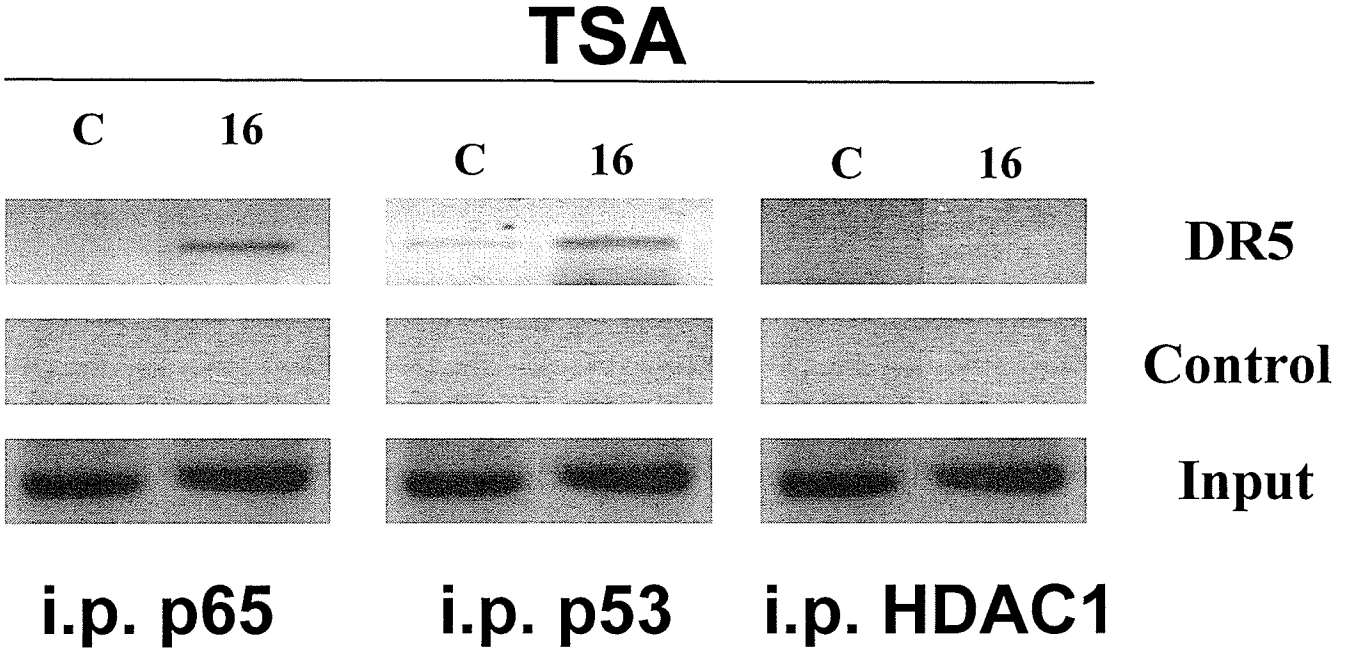

Figure 25

HEK293 cells untreated (C) or treated with TSA (45nM) were used in a ChIP assay with either anti-p65 antibody, anti-p53 antibody, or anti-HDAC1 antibody. No antibody was used as a negative control whereas genomic DNA was used as an input control. Immunoprecipitated DNA was analyzed by PCR using primers specific for DR5 exon 1 and intron 1 regions.

4.8 Chlorambucil and Fludarabine induce binding of p65 and p53 to the DR5 gene in primary CLL cells

CLL is generally thought to be an incurable disease and therefore new therapies are desperately needed to aid in the treatment of this disease. One new therapy being considered is TRAIL. Although CLL cells are resistant to TRAIL alone, they are made sensitive when treated in combination with such drugs as HDAC inhibitors. Death receptor 5 is one of the receptors that bind TRAIL leading to the activation of apoptosis and therefore a better understanding of the mechanism of DR5 expression could lead to more efficient treatment of CLL. Our lab has previously determined that DR5 mRNA expression, protein levels, and cell surface expression are induced following treatment with either FLU or CLB. Since we showed that p65 and p53 play a role in the regulation of DR5 using HEK 293 cells we wanted to see whether this would hold true for primary CLL cells. To determine whether p65 and p53 bind to the first intronic region of the DR5 gene we performed ChIP assays in primary CLL cells. We observed that p65 binds to the DR5 gene both in untreated cells as well as those treated with either CLB or FLU (Figure 26). The binding of p65 to the DR5 gene peaked at approximately 18 hours post-treatment and was reduced to basal levels after 24 hours of treatment. In contrast, we observed that p53 binds to the intronic region of the DR5 gene only after treatment (Figure 27). p53 binding peaked around 18 hours with FLU treatment and around 5 hours with CLB treatment. These results suggest that FLU- and CLB-induced DR5 gene expression is mediated in part by p53 and NFκB.

The p65 subunit of NFkB is bound to the DR5 gene

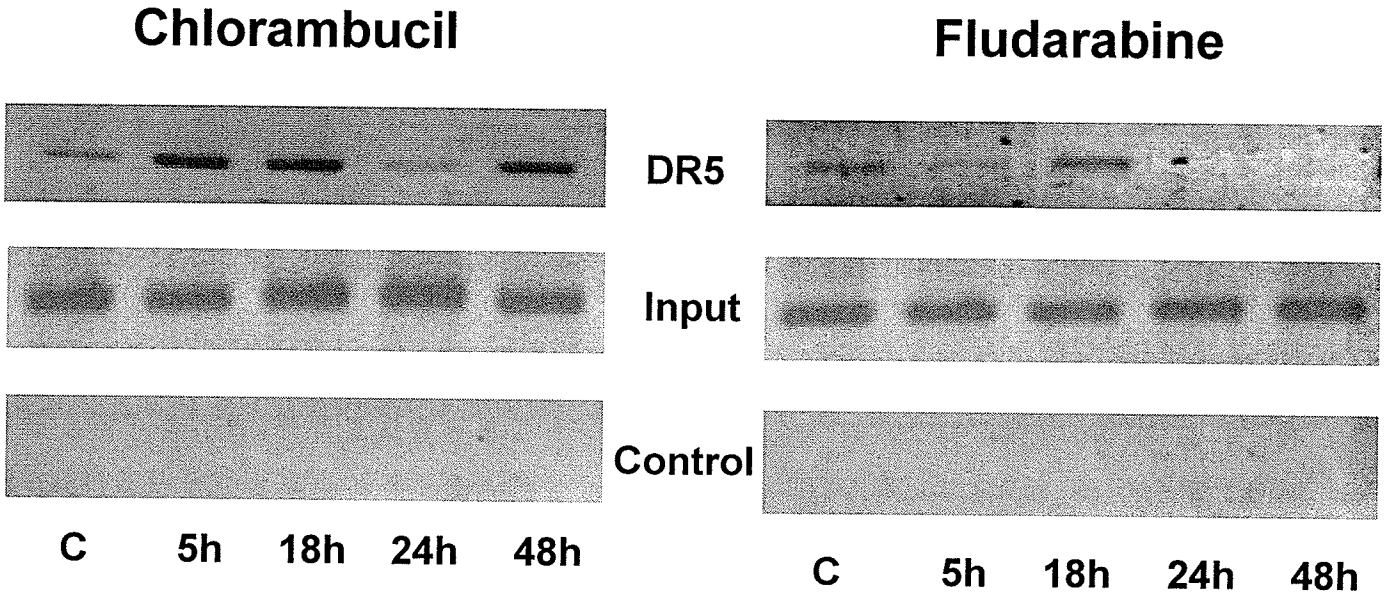

i.p. p65

Figure 26

CLL patient samples untreated (C) or treated with either CLB (10μM) or FLU (10μM) were used in a ChIP assay with anti-p65 antibodies. No antibody added was used as a negative control whereas genomic DNA was used as an input control. Precipitated DNA was analyzed by PCR using primers specific for the DR5 exon 1 and intron 1 regions. Each experiment was repeated on 3 different patients with similar results.

p53 is bound to the DR5 gene with FLU or CLB

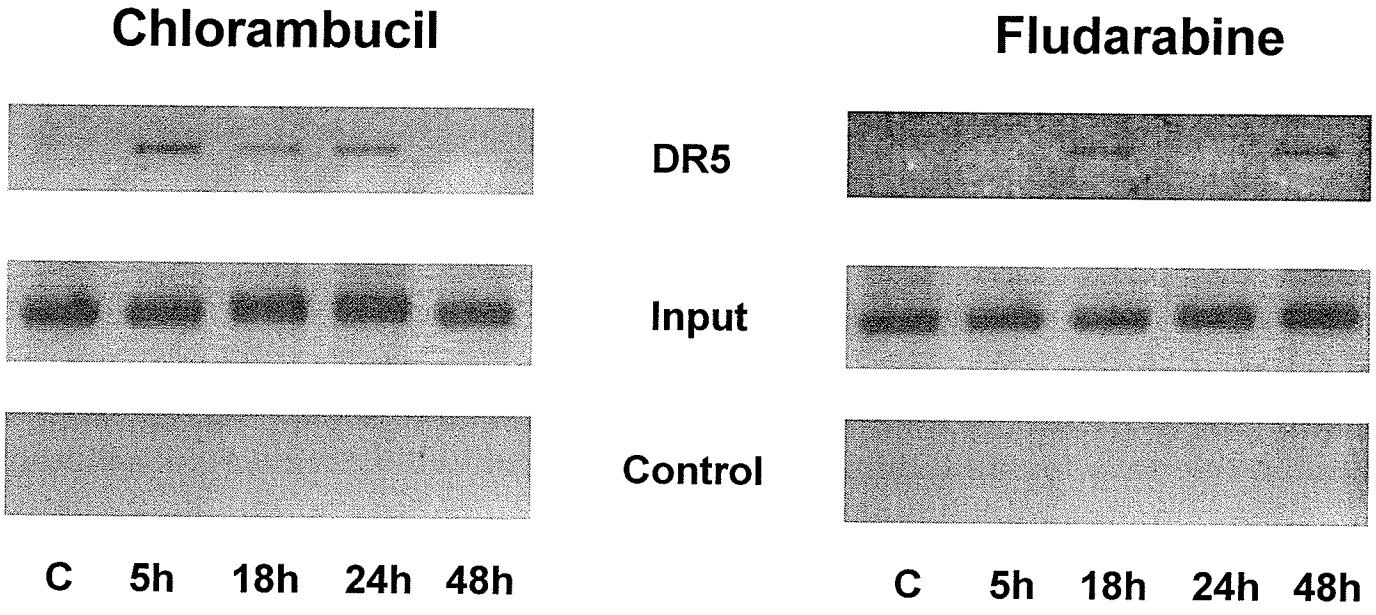

i.p. p53

Figure 27

CLL patient samples untreated (C) or treated with either CLB (10μM) or FLU (10μM) were used in a ChIP assay with anti-p53 antibodies. No antibody added was used as a negative control whereas genomic DNA was used as an input control. Precipitated DNA was analyzed by PCR using primers specific for the DR5 exon 1 and intron 1 regions. Each experiment was repeated on 3 different patients.

4.9 Chlorambucil and Fludarabine induce acetylation of histone H3 and binding of p300 to the DR5 gene but not binding of HDAC1 in primary CLL cells

Our lab has previously determined that DR5 mRNA expression is induced following treatment with either FLU or CLB. It is widely known that acetylated histones are found in areas of transcription. We therefore wanted to show that the DR5 gene was acetylated following treatment with CLB or FLU. To show this we performed ChIP assays in primary CLL cells treated with FLU or CLB and immunoprecipitated with antibodies against acetylated histone H3. We observed that the DR5 gene was acetylated following treatment with both CLB and FLU with levels peaking at 5 hours with FLU and 24 hours with CLB (Figure 28). HATs are involved in the acetylation of histones as well as transcription factors and the HAT p300 has been shown to complex with p53 and NFκB. We therefore wanted to determine if the HAT p300 was present on the DR5 gene following treatment with FLU or CLB. We performed ChIP assays on primary CLL cells using p300 antibody and observed that following treatment with FLU p300 was bound following 5 hours of treatment (Figure 29). We also observed binding of p300 to the gene following 5-24 hours of CLB treatment (Figure 29). This supports the expression pattern of the DR5 gene in CLL cells following treatment with either FLU or CLB. After observing the acetylation and presence of p300 on the DR5 gene we wanted to check to make sure that HDAC1 was not present. We performed ChIP assay on primary CLL cells using HDAC1 antibody and observed that following treatment with FLU there was no binding of HDAC1 to the DR5 gene (Figure 30).

The DR5 gene is acetylated following treatment with FLU or CLB

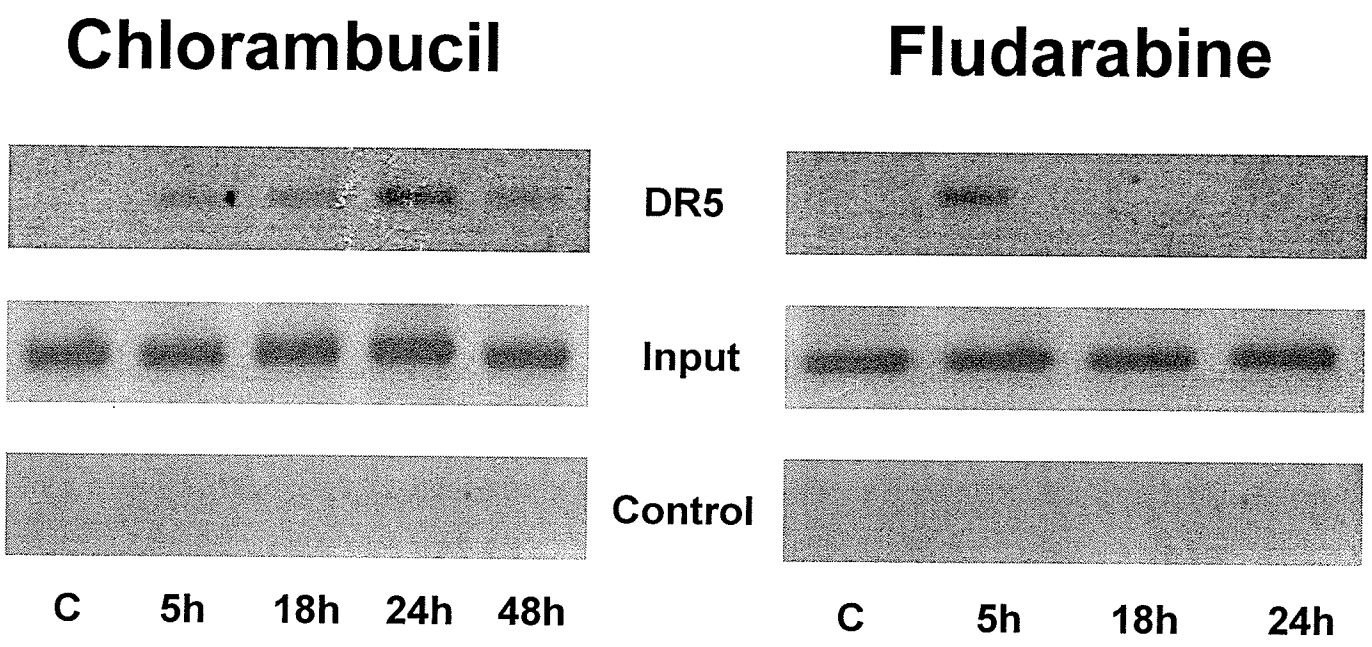

i.p. AcH3

Figure 28

CLL patient samples untreated (C) or treated with either CLB (10μM) or FLU (10μM) were used in a ChIP assay with anti-p53 antibodies. No antibody added was used as a negative control whereas genomic DNA was used as an input control. Precipitated DNA was analyzed by PCR using primers specific for the DR5 exon 1 and intron 1 regions. Each experiment was repeated on 3 different patients.

p300 binds the DR5 gene following treatment with FLU or CLB

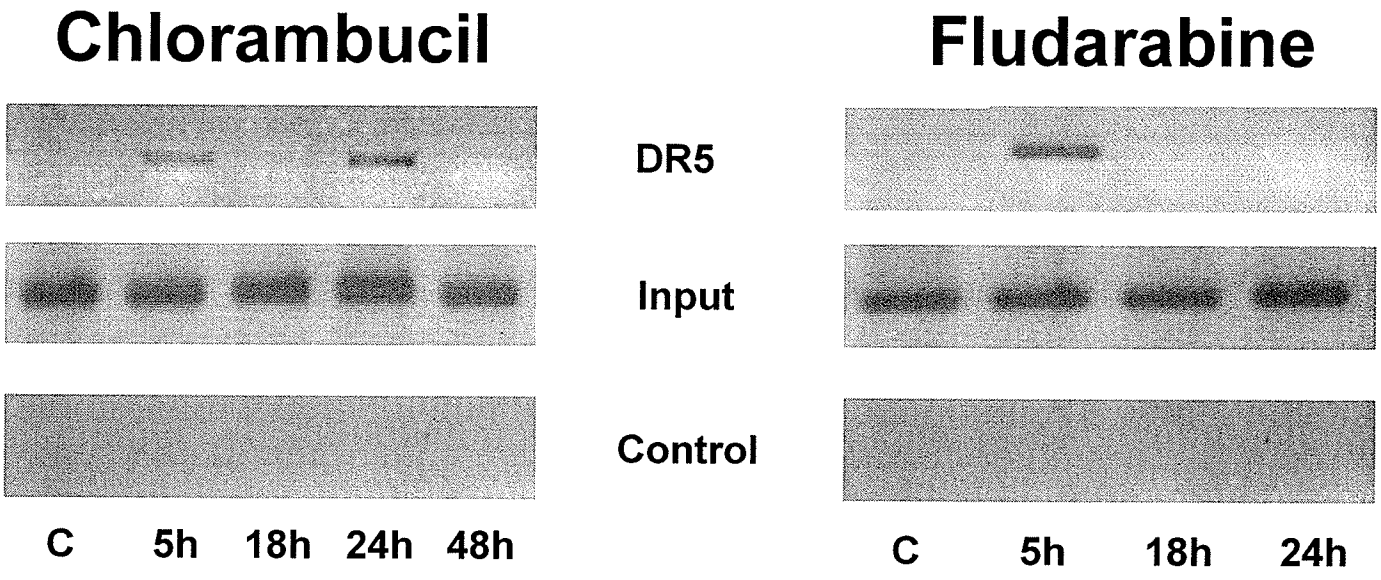

i.p. p300

Figure 29

CLL patient samples untreated (C) or treated with either CLB (10μM) or FLU (10μM) were used in a ChIP assay with anti-p300 antibodies. No antibody added was used as a negative control whereas genomic DNA was used as an input control. Precipitated DNA was analyzed by PCR using primers specific for the DR5 exon 1 and intron 1 regions. Each experiment was repeated on 3 different patients.

HDAC1 does not bind DR5 gene following FLU or CLB treatment

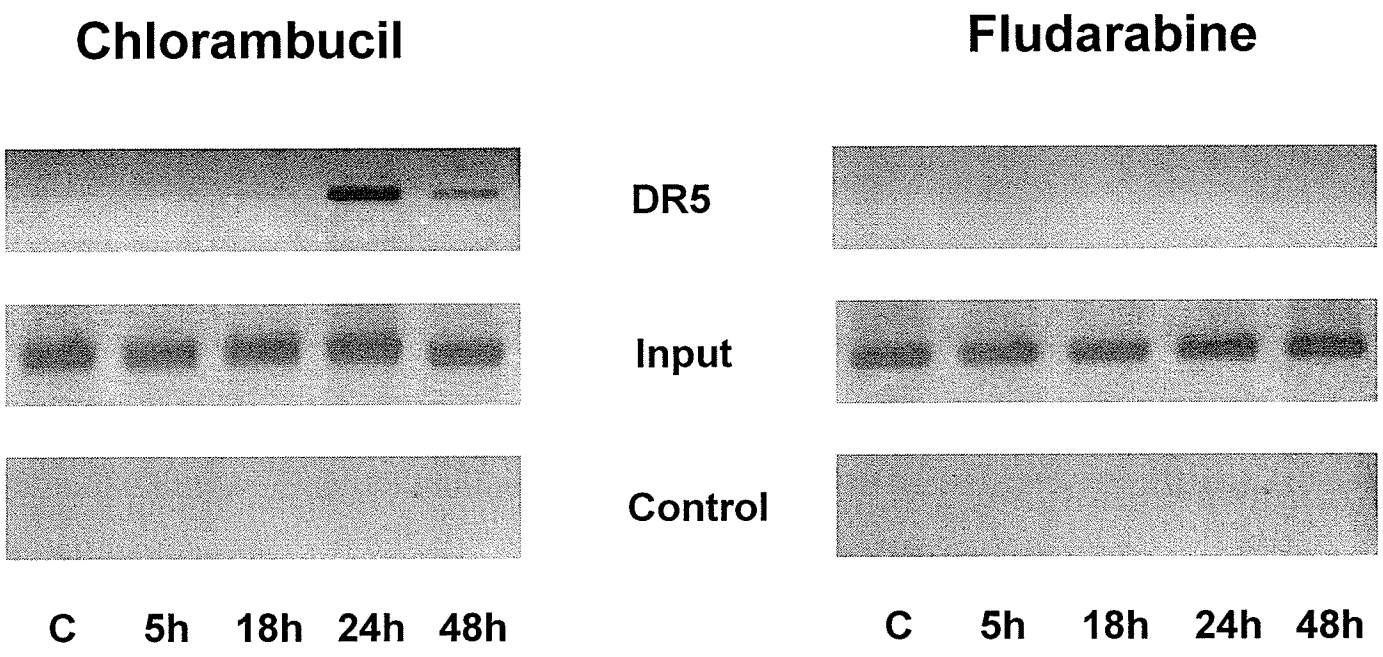

Figure 30

CLL patient samples untreated (C) or treated with either CLB (10μM) or FLU (10μM) were used in a ChIP assay with anti-HDAC1 antibodies. No antibody added was used as a negative control whereas genomic DNA was used as an input control. Precipitated DNA was analyzed by PCR using primers specific for the DR5 exon 1 and intron 1 regions. Each experiment was repeated on 3 different patients.

We did observe binding of HDAC1 to the DR5 gene following CLB treatment but it was at later time points, 24 and 48 hours (Figure 30). CLB is a very fast acting drug and so it is not surprising to find that the drug loses its affect at the later time points.

4.10 Lysophosphatidic acid (LPA) treatment induces binding of p65 and HDAC1 to the DR5 gene in primary CLL cells

LPA is a survival factor that our lab has determined does not induce protein levels of DR5. We used it to mimic the experiments performed with EGF treated HEK 293 cells. We could not use EGF because CLL cells do not express EGF receptors. We found using ChIP assays that LPA induces the binding of p65 to the first intronic region of the DR5 gene in CLL cells whereas it does not seem to induce the binding of p53 (Figure 31). We also found that the DR5 gene is not acetylated following treatment with LPA and, in accordance with this result, p300 is not observed to bind to DR5 (Figure 32). We did, however, observe the binding of HDAC1 to the DR5 gene following LPA treatment (Figure 33). The binding peaked around 16 hours and returned to basal levels after 48 hours. These results suggest that LPA prevents the expression of DR5 by inducing the binding of HDAC1 and p65, thereby inhibiting acetylation of the gene by preventing the binding of p300 and p53.

The p65 subunit of NFκB but not p53 is bound to the DR5 gene following LPA treatment

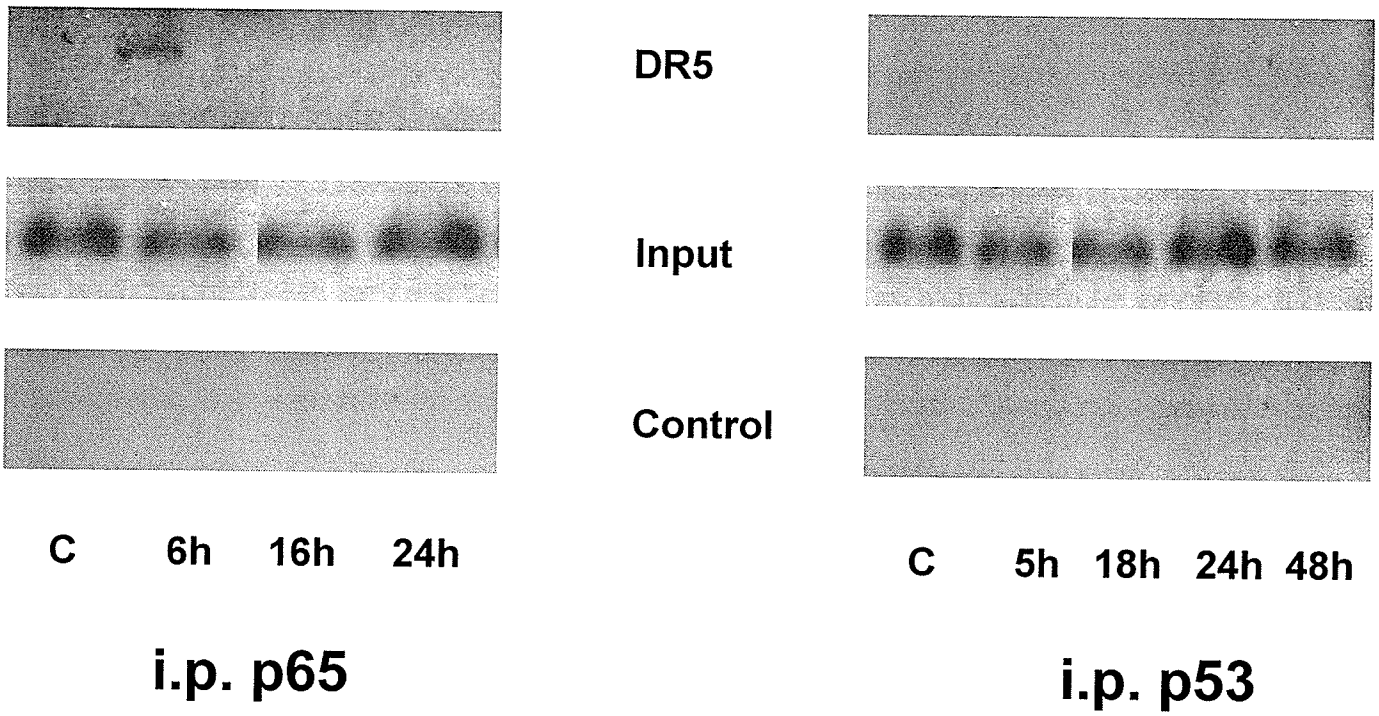

Figure 31

CLL patient samples untreated (C) or treated with LPA (10μM) were used in a ChIP assay with either anti-p65 antibodies or anti-p53 antibodies. No antibody added was used as a negative control whereas genomic DNA was used as an input control. Precipitated DNA was analyzed by PCR using primers specific for the DR5 exon 1 and intron 1 regions. Each experiment was repeated on 3 different patients.

p300 does not bind the DR5 gene and the DR5 gene is not acetylated following treatment with LPA

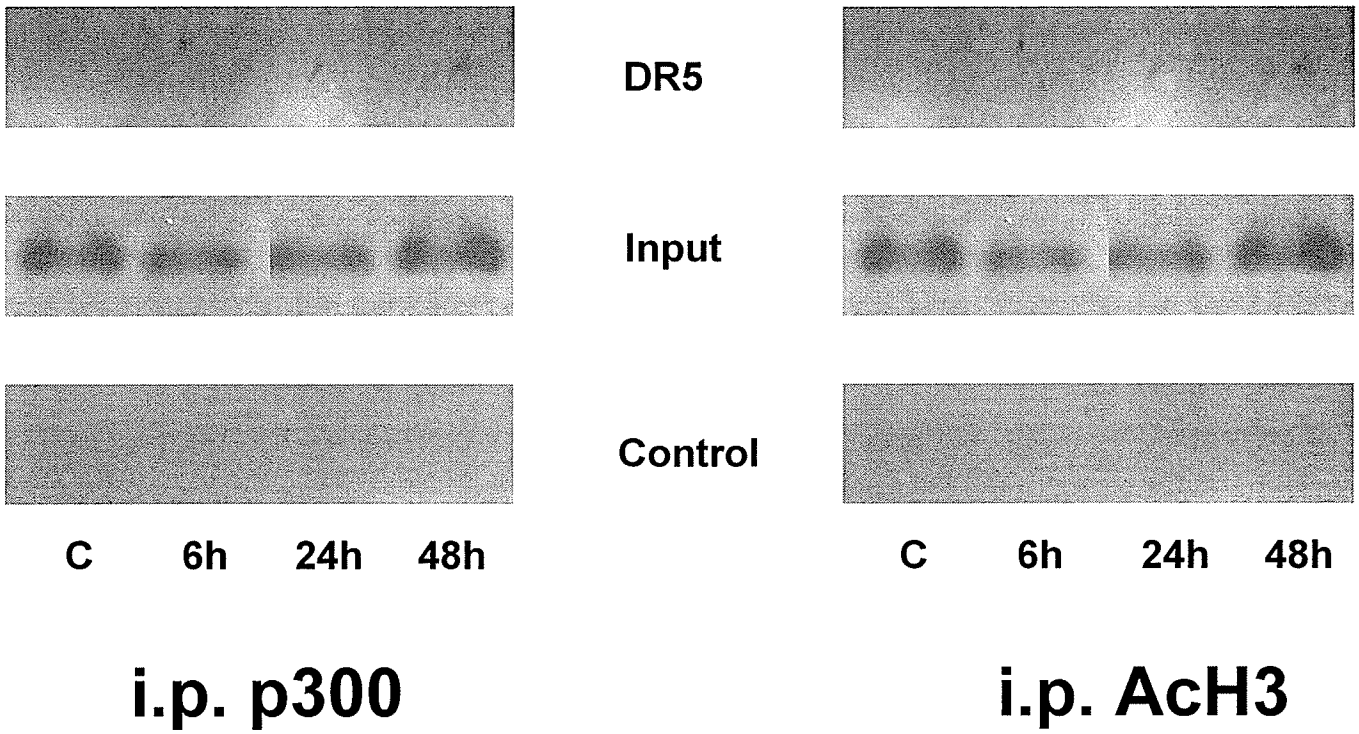

Figure 32

CLL patient samples untreated (C) or treated with LPA (10μM) were used in a ChIP assay with either anti-p300 antibodies or anti-acetylated histone H3 antibodies. No antibody added was used as a negative control whereas genomic DNA was used as an input control. Precipitated DNA was analyzed by PCR using primers specific for the DR5 exon 1 and intron 1 regions. Each experiment was repeated on 3 different patients.

HDAC1 binds DR5 gene with LPA treatment

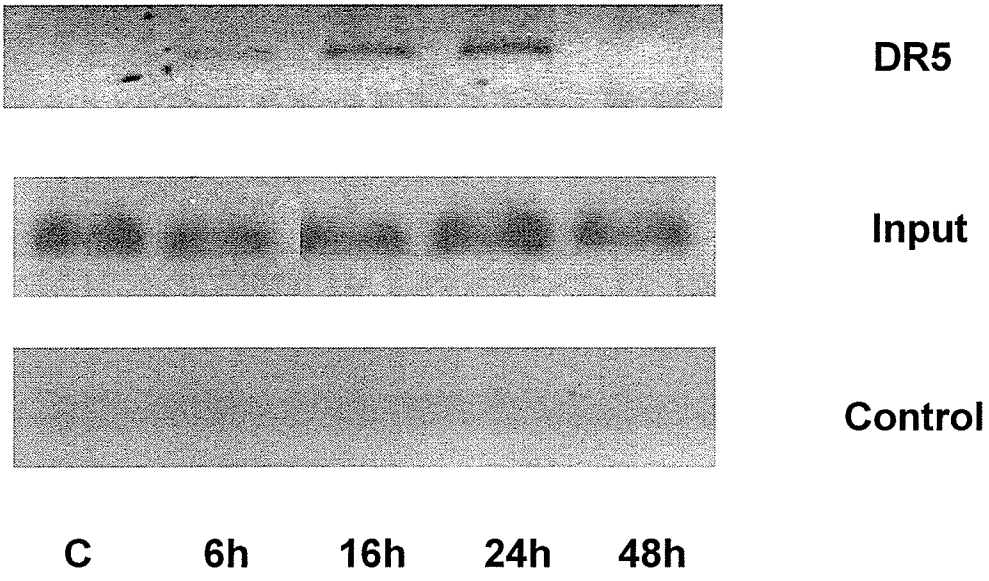

Figure 33

CLL patient samples untreated (C) or treated with LPA (10μM) were used in a ChIP assay with anti-HDAC1 antibodies. No antibody added was used as a negative control whereas genomic DNA was used as an input control. Precipitated DNA was analyzed by PCR using primers specific for the DR5 exon 1 and intron 1 regions. Each experiment was repeated on 3 different patients.

4.11 Level of H3 acetylation is increased in CLL patient cells

Based on the results from the ChIP assays we showed that the DR5 gene was acetylated following treatment with FLU or CLB but not LPA. Due to the small amount of cells we were able to get from normal blood donors we were unable to perform ChIP assays with them. To compare normals to CLL patients we used western blots and immunohistochemistry. We isolated histones from both normal human B lymphocytes and CLL cells, either untreated or treated with FLU. We first ran the histones on an SDS page gel and performed a western, probing for acetylated H3. We observed that total acetylation was increased in untreated CLL patients compared to untreated normal human lymphocytes and HEK293 cells (Figure 34). We used histone H3 as the loading control. To confirm these results we also performed immunohistochemistry on normal human B lymphocytes and CLL patient samples, using an acetylated histone H3 antibody. We observed the same results, that CLL patient cells are more highly acetylated than normal human lymphocytes (Figure 35).

4.12 Histone acetylation is increased following treatment with fludarabine and decreased following treatment with LPA

We next wanted to determine the levels of acetylation following treatment with either FLU or LPA. We first isolated histones from CLL patient cells and separated them using SDS page gels. Using a western blot we probed for acetylated histone H3 and found elevated levels following treatment with FLU and decreased levels following LPA treatment (Figure 36a). We also ran the isolated histones on an acid urea gel. This gel separates the histones according to size and charge.

Difference in Level of H3 Acetylation in CLL cells

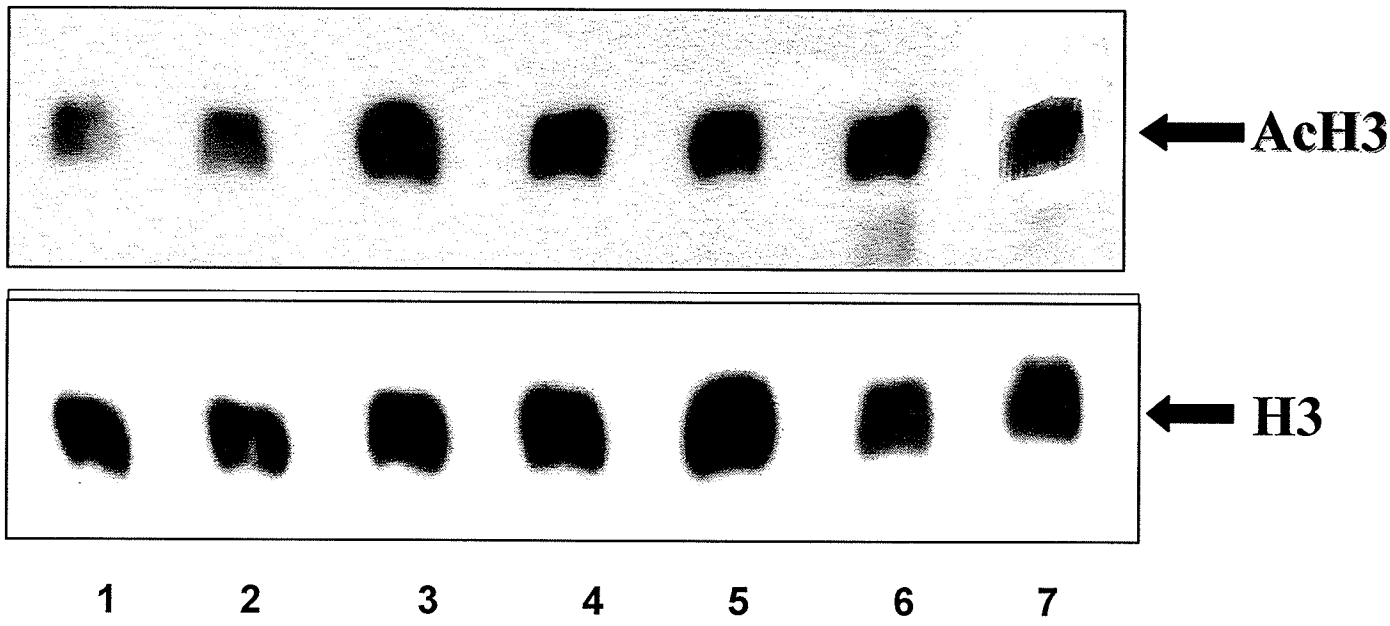

1) HEK293
2) Normal human lymph
3) CLL patient #1
4) CLL patient #2
5) CLL patient #3
6) CLL patient #4
7) CLL patient #5

Figure 34

Western blot analysis of the expression of acetylated histone H3 and histone H3 (loading control). Histones were isolated, run on an SDS-PAGE gel, and western blotted with anti-acetylated histone H3 antibody as described in the Materials and Methods section. The blot was stripped and re-probed with anti-histone H3 antibody as a loading control. Lane 1: HEK293 cells, Lane2: Normal human lymphocytes, Lane 3: CLL patient #1, Lane 4: CLL patient #2, Lane 5: CLL patient #3, Lane 6: CLL patient #4, and Lane7: CLL patient #5.

Histone Acetylation is increased in CLL patient samples compared to normal human lymph

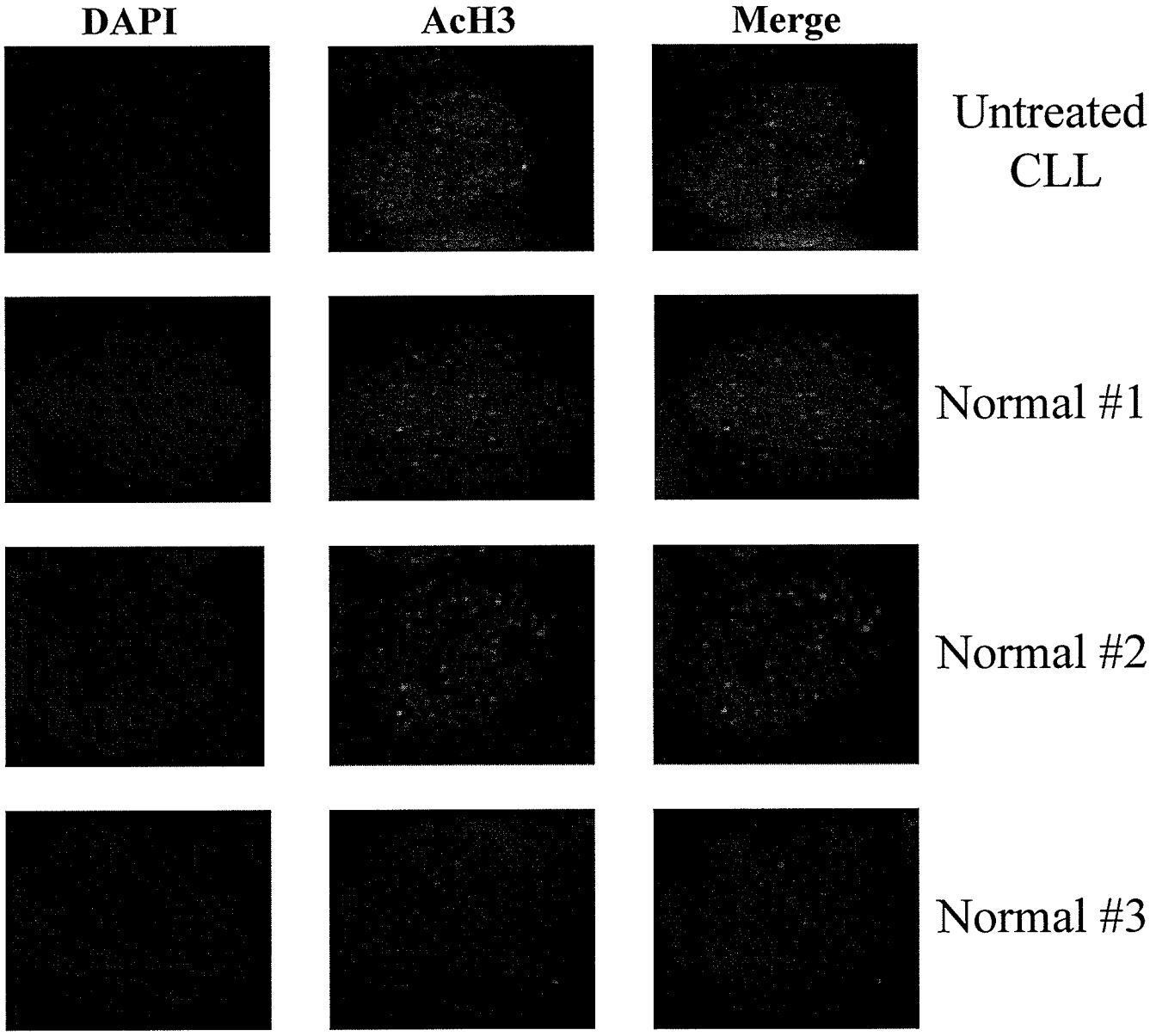

Figure 35

CLL patient samples or normal human lymphocytes samples were cytospun onto slides as described in Materials and Methods. The slides were stained with acetylated histone H3 Ab (FITC, green). The DNA was stained blue with DAPI. The slides were viewed using a Carl Zeiss AxioPhot II microscope and the pictures deconvolved in three dimensions with the AxioVision 4.1 constrained iterative algorith.

Overall histone aceylation is increased in CLL cells

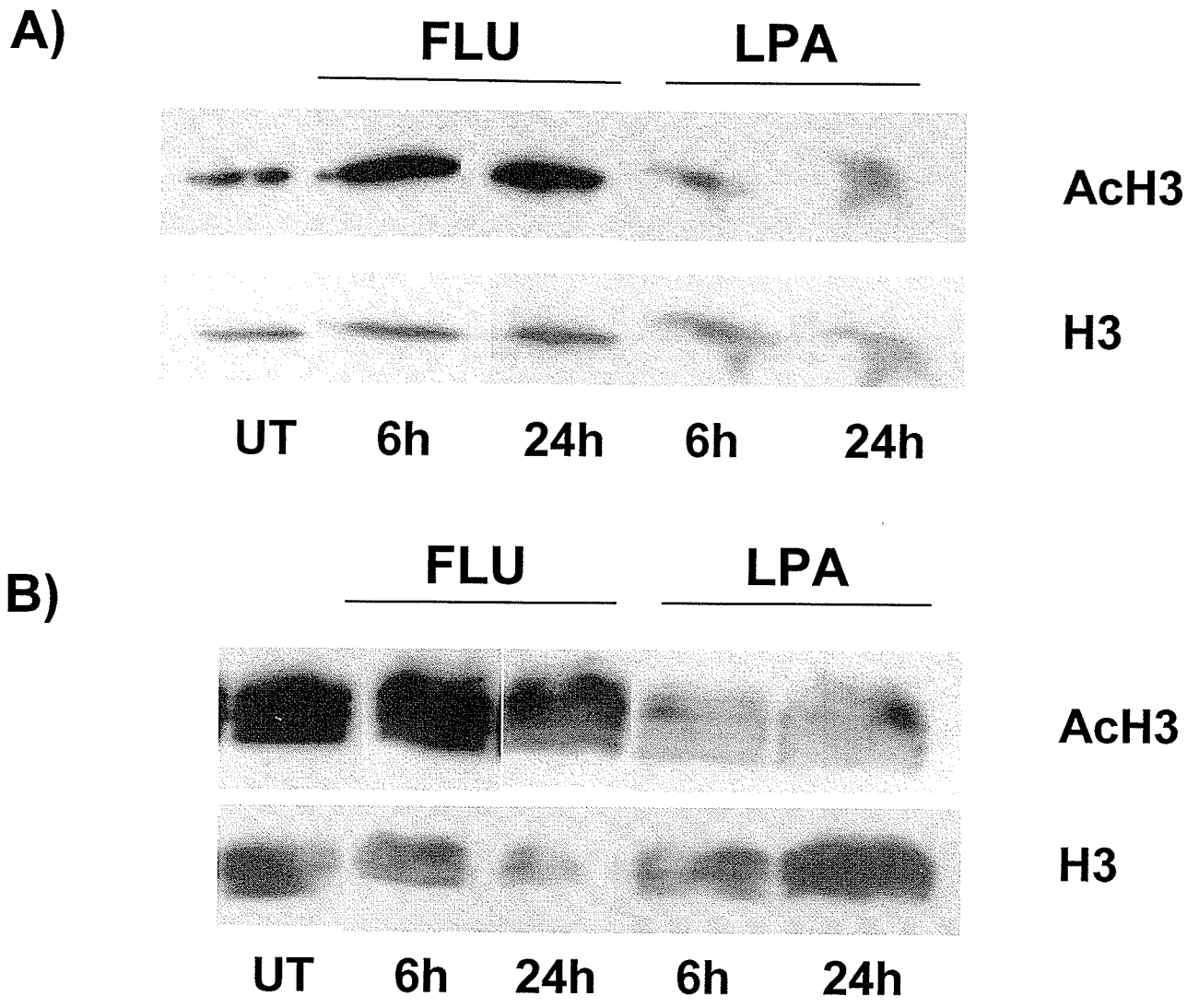

Figure 36

CLL patient samples were left untreated (UT) or treated with either fludarabine (FLU) (10μM) or lysophosphatidic acid (LPA) (10μM) for 6 or 24 hours. The histones were then isolated from these cells as described in the Materials and Methods section. The isolated histones were run on either an SDS-Page gel (A) or an acid urea gel (B) and western blotted for acetylated histone H3 (AcH3). The blots were stripped and re-probed for histone H3 (H3) as a loading control.

This allows you to separate the histones based on their modifications, due to the reduction in net positive charge caused by acetylation and phosphorylation of the histone. After separating the histones with the acid urea gel we performed a western blot and probed with acetylated histone H3. We observed that treatment with FLU lead to an increase in multiple modifications (Figure 36b). We can only say multiple modifications because of the nature of the gel. The lowest band on the gel indicates a single modification, in this case acetylation, however, each band above it indicates another modification but they are not necessarily acetylation. In contrast, treatment with LPA lead to a decrease in the expression of acetylated histone H3 and a lower level of modification (Figure 36). To confirm these results we again performed immunohistochemistry experiments. We used CLL patient cells untreated or treated with either FLU or LPA and probed the cells with antibody against acetylated histone H3. We observed that treatment with FLU lead to an increase in overall acetylation of histone H3 following 6 hours of treatment and the level of acetylation seemed to return to untreated levels 24 hours post-treatment (Figure 37). In contrast, we observed that treatment with LPA lead to a decrease in the overall acetylation of histone H3 following 6 hours of treatment, with the return to untreated levels 24 hours post-treatment (Figure 38). All of these results suggest that treatment of CLL cells with FLU leads to an increase in the overall acetylation levels in the cell whereas treatment with LPA leads to a decrease in the overall acetylation levels.

Histone Acetylation is increased in CLL cells following treatment with FLU

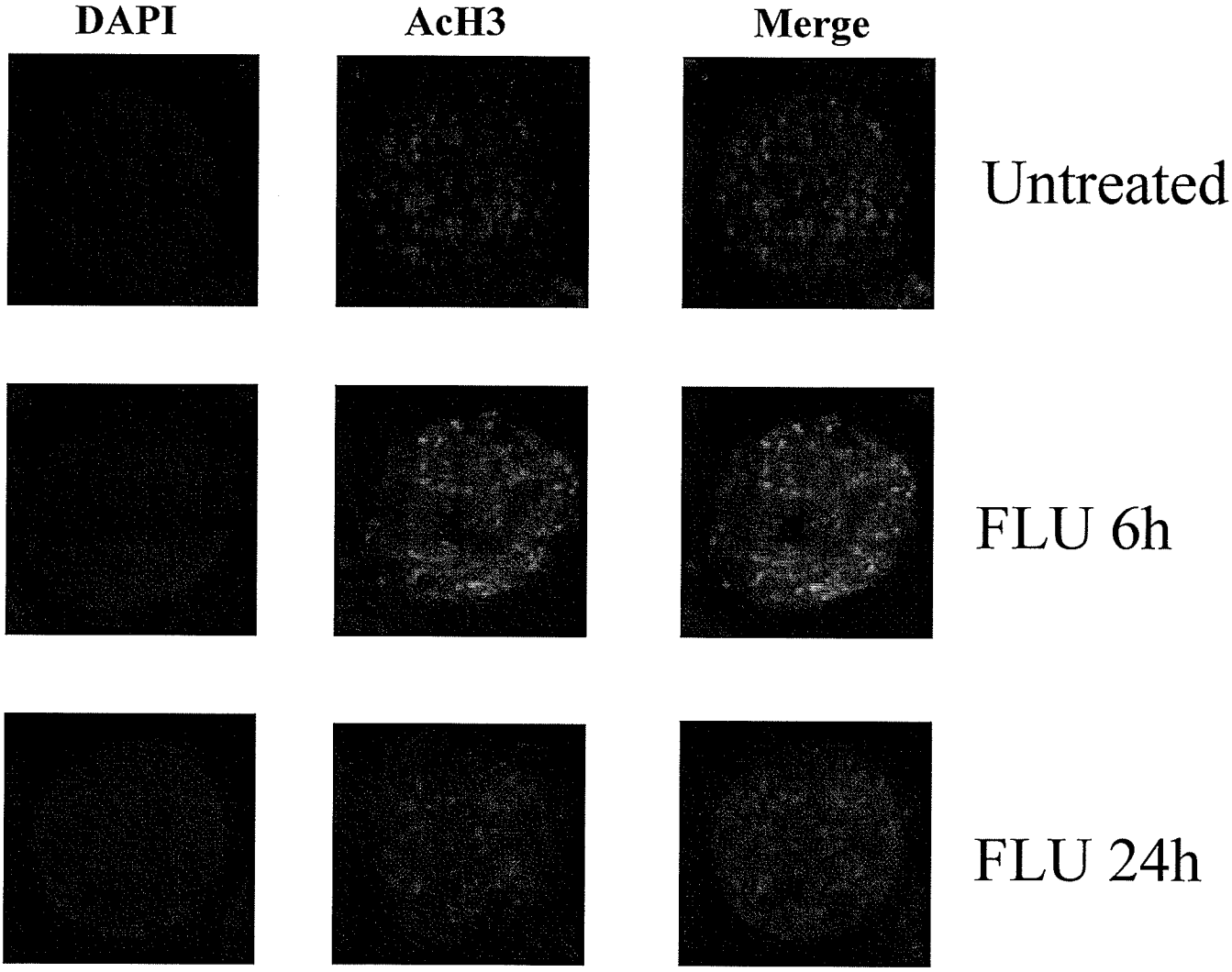

Figure 37

CLL patient samples were left untreated or were treated with fludarabine (FLU) (10μM) for 6 or 24 hours. All of the cells were then cytospun onto slides as described in Materials and Methods. The slides were stained with acetylated histone H3 Ab (FITC, green). The DNA was stained blue with DAPI. The slides were viewed using an Carl Zeiss AxioPhot II microscope and the pictures deconvolved in three dimensions with the AxioVision 4.1 constrained iterative algorith.

Histone acetylation is decreased in CLL cells following treatment with LPA

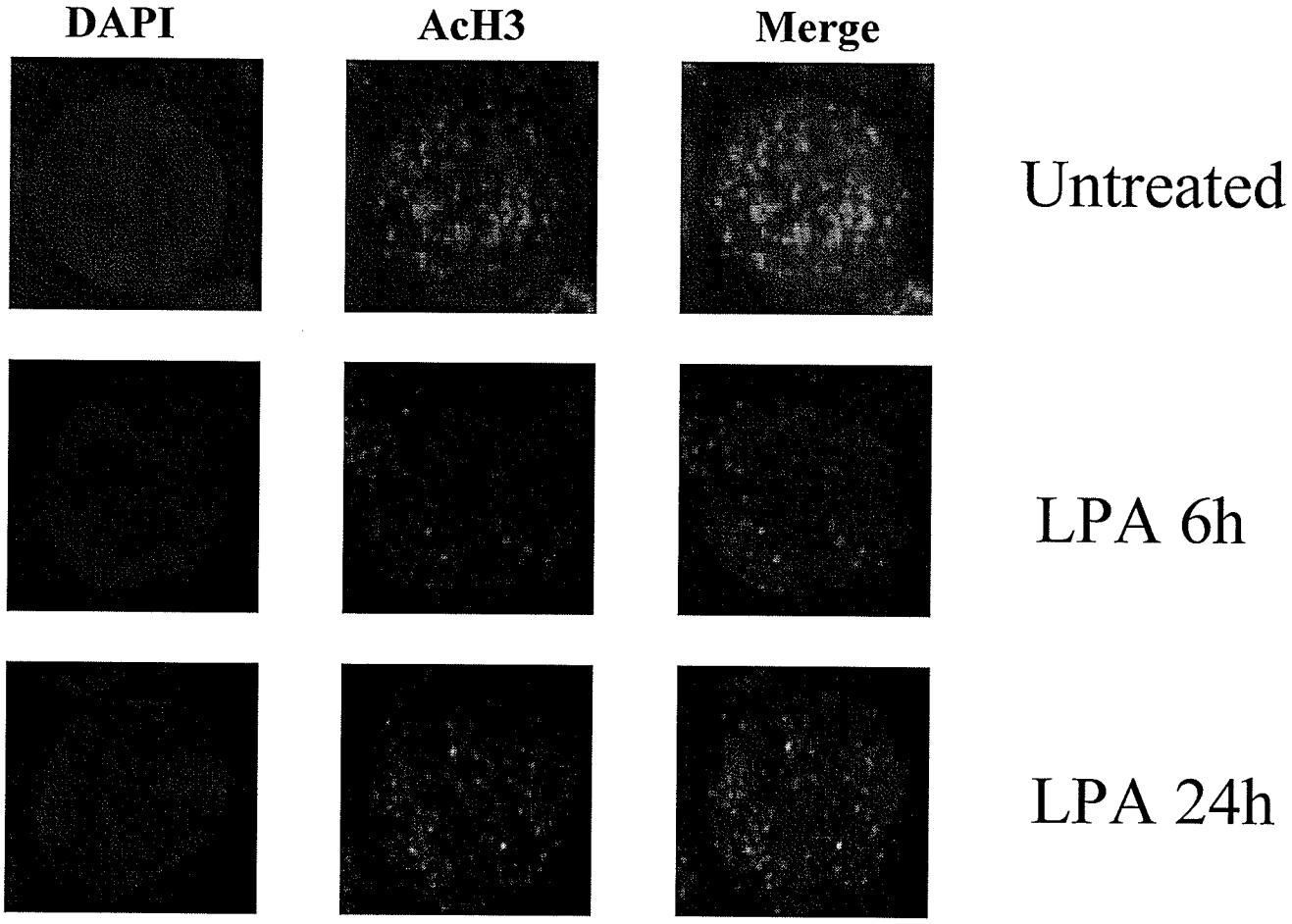

Figure 38

CLL patient samples were left untreated or were treated with lysophosphatidic acid (LPA) (10μM) for 6 or 24 hours. All of the cells were then cytospun onto slides as described in Materials and Methods. The slides were stained with acetylated histone H3 Ab (FITC, green). The DNA was stained blue with DAPI. The slides were viewed using an Carl Zeiss AxioPhot II microscope and the pictures deconvolved in three dimensions with the AxioVision 4.1 constrained iterative algorith.

4.13 LPA protects CLL cells against FLU-induced histone acetylation

Since we have shown that FLU increases the level of histone acetylation and LPA decreases histone acetylation, we wanted to determine whether the effect of one drug could silence the effect of the other. We therefore pre-treated CLL cells with LPA for 1 hour and then treated them with FLU. We observed that after 24 hours LPA prevented the normal induction of histone acetylation following FLU treatment (Figure 39). These results suggest that LPA protects CLL cells against FLU-induced histone acetylation.

4.14 Histone phosphorylation is decreased in CLL cells following treatment with FLU and LPA

To look at the effect of FLU and LPA on histone phosphorylation we first isolated histones from CLL patient cells treated with LPA or FLU. We ran them on an SDS page gel and performed a western blot, probing for phosphorylated histone H3 (Ser28). We observed no major difference in the levels of phosphorylation between untreated CLL cells and those treated with either FLU or LPA (Figure 40). There is perhaps a slight decrease in phosphorylation after 6 hours of LPA treatment and after 24 hours of FLU treatment. To support these observations we used immunohistochemistry. We first looked at whether there was any difference in the level of histone phosphorylation between normal cells and CLL cells. We observed that histone phosphorylation levels show a slight increase in CLL patient cells compared to normal human lymphocytes (Figure 41). We then wanted to look at the effect that treatment with LPA or FLU would have on the level of phosphorylation in CLL cells.

LPA protects against FLU-induced increase in histone acetylation

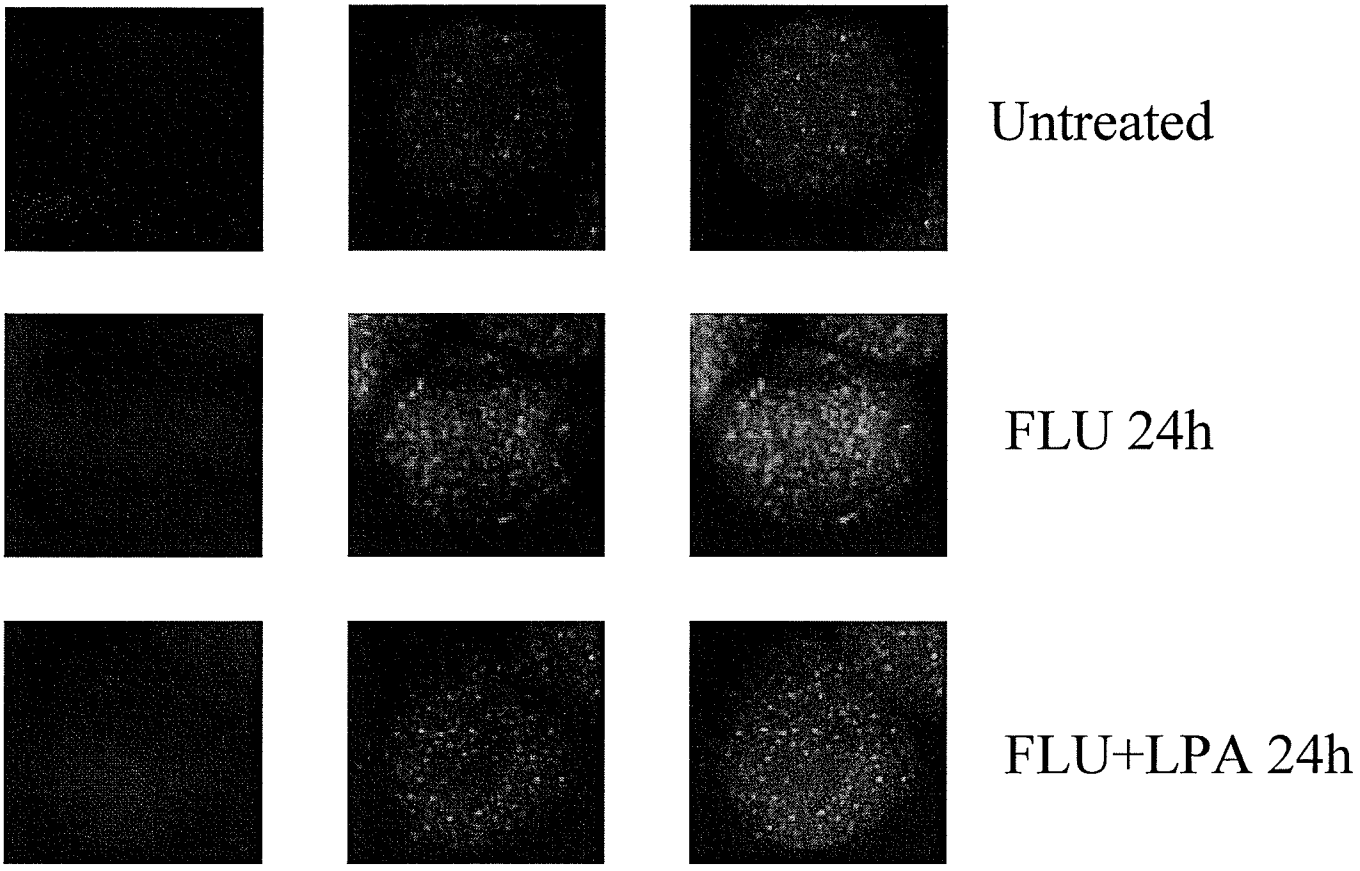

Figure 39

CLL patient samples were left untreated or were treated with first lysophosphatidic acid (10μM) and then fludarabine (FLU) (10μM) for 24 hours. All of the cells were then cytospun onto slides as described in Materials and Methods. The slides were stained with acetylated histone H3 Ab (FITC, green). The DNA was stained blue with DAPI. The slides were viewed using an Carl Zeiss AxioPhot II microscope and the pictures deconvolved in three dimensions with the AxioVision 4.1 constrained iterative algorith.

No difference in overall H3 phosphorylation in CLL cells

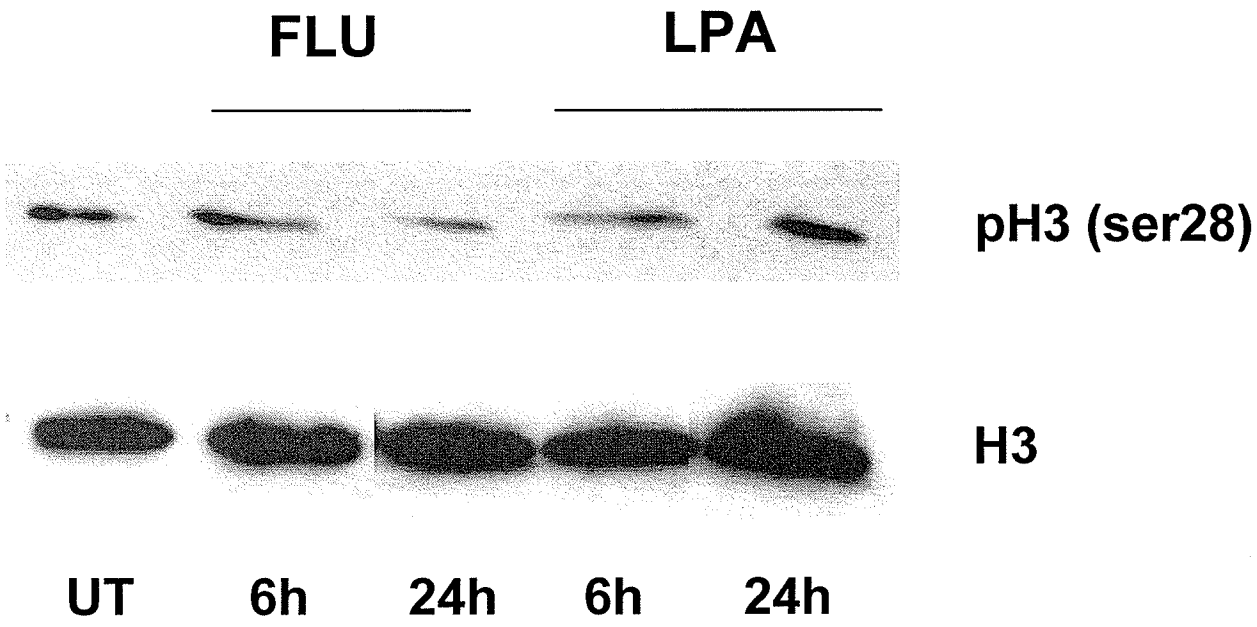

Figure 40

CLL patient samples were left untreated (UT) or treated with either fludarabine (FLU) (10μM) or lysophosphatidic acid (LPA) (10μM) for 6 or 24 hours. The histones were then isolated from these cells as described in the Materials and Methods section. The isolated histones were run on an SDS-PAGE gel and western blotted for phosphorylated histone H3 on serine 28 (pH3). The blots were stripped and re-probed for histone H3 (H3) as a loading control.

Histone phosphorylation is increased in CLL patient samples compared to normal human lymph

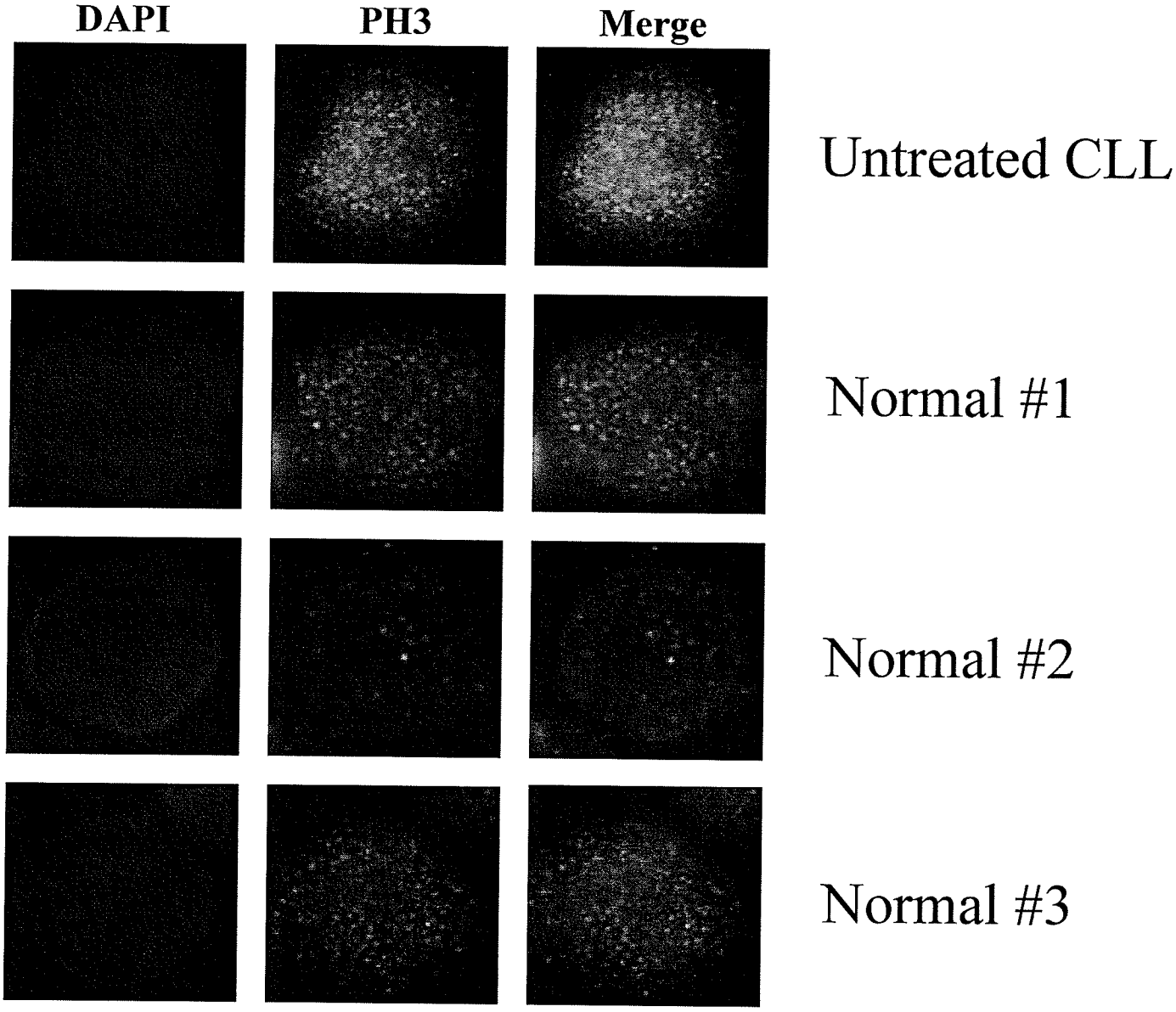

Figure 41

CLL patient samples or normal human lymphocyte samples were cytospun onto slides as described in Materials and Methods. The slides were stained with phosphorylated (serine28) histone H3 Ab (FITC, green). The DNA was stained blue with DAPI. The slides were viewed using a Carl Zeiss AxioPhot II microscope and the pictures were deconvolved in three dimensions with the AxioVision 4.1 constrained iterative algorith.

We observed that FLU treatment did not affect the levels of histone phosphorylation after 6 hours or 24 hours of treatment (Figure 42). However, following 6 hours of LPA treatment we observed a decrease in histone phosphorylation (Figure 43). After 24 hours of treatment the levels of phosphorylation began to increase but not to the levels of untreated cells. When we treated the CLL cells with both LPA and FLU we did not see a reduction in histone phosphorylation indicating that LPA does not affect the level of FLU-induced histone phosphorylation (Figure 44).

4.15 Levels of histone methylation are similar between normal cells and CLL cells and treatment of CLL cells with FLU or LPA do not affect histone methylation levels

We performed immunohistochemistry to determine the effect that CLL and treatment had on the levels of methylation. We observed no major changes in the levels of methylation between normal cells and treated CLL cells (Figure 45,46). It also appears that treatment with FLU has no effect on the level of methylation in the CLL cells. Treatment with LPA seems to induce a slight decrease in the levels of histone methylation, however the levels of methylation are so low to begin with that it is hard to make any clear conclusions. The low levels could be due to the antibody used and further experiments are required to investigate this modification.

Histone phosphorylation is not affected by FLU treatment

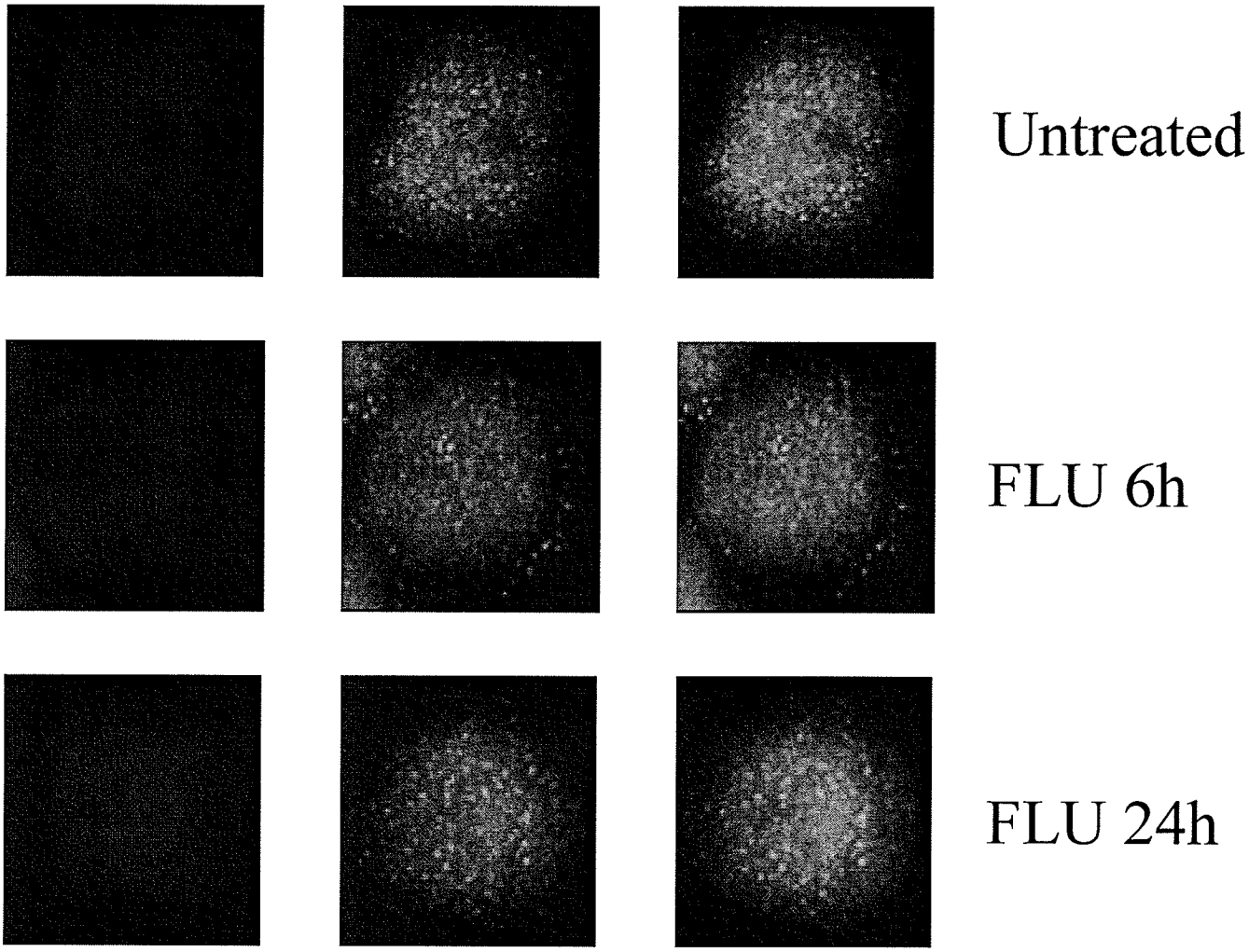

Figure 42

CLL patient samples were left untreated or were treated with fludarabine (FLU) (10μM) for 6 or 24 hours. All of the cells were then cytospun onto slides as described in Materials and Methods. The slides were stained with phosphorylated (serine 28) histone H3 Ab (FITC, green). The DNA was stained blue with DAPI. The slides were viewed using an Carl Zeiss AxioPhot II microscope and the pictures deconvolved in three dimensions with the AxioVision 4.1 constrained iterative algorith.

Histone phosphorylation is decreased following LPA treatment

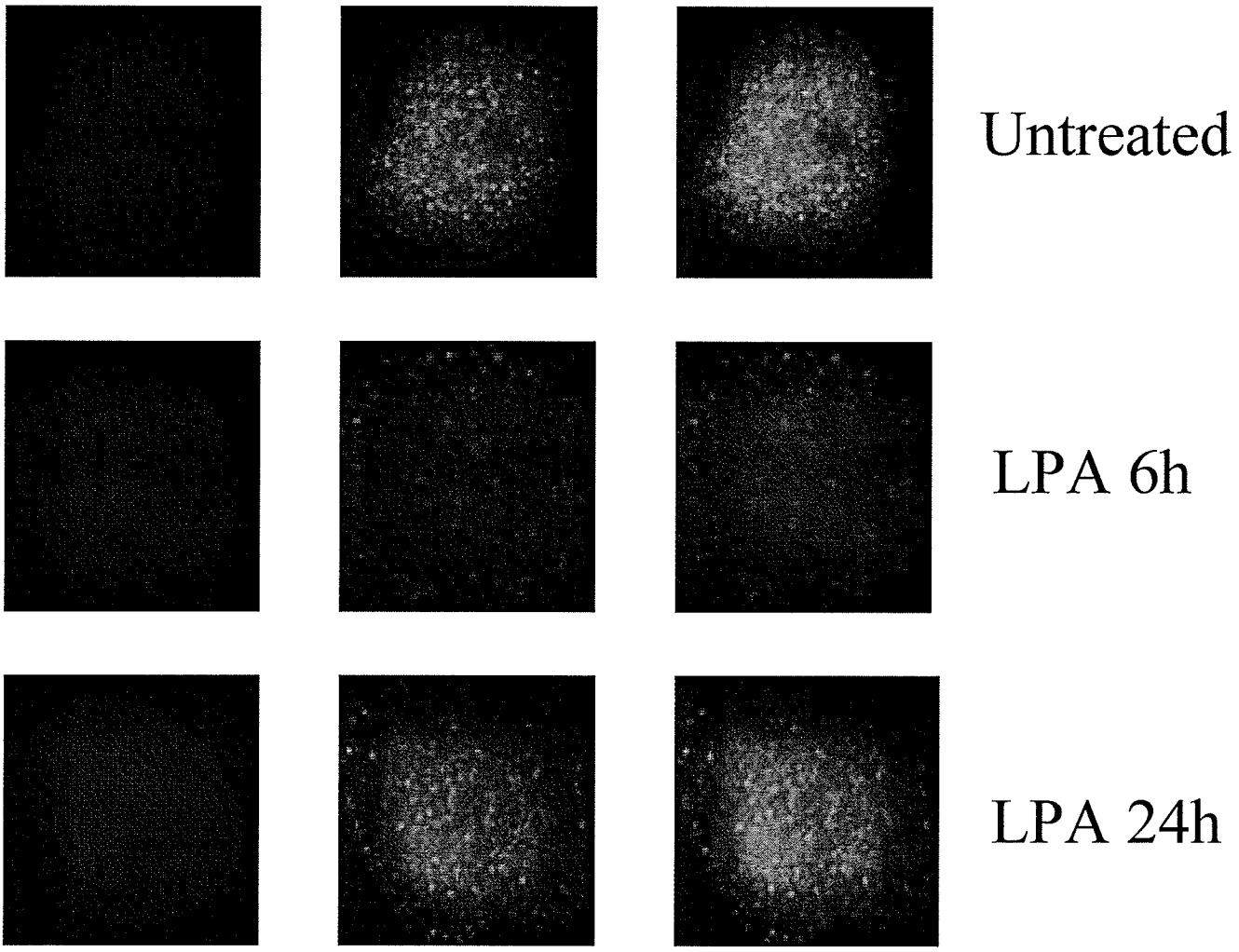

Figure 43

CLL patient samples were left untreated or were treated with lysophosphatidic acid (LPA) (10μM) for 6 or 24 hours. All of the cells were then cytospun onto slides as described in Materials and Methods. The slides were stained with phosphorylated (serine 28) histone H3 Ab (FITC, green). The DNA was stained blue with DAPI. The slides were viewed using an Carl Zeiss AxioPhot II microscope and the pictures deconvolved in three dimensions with the AxioVision 4.1 constrained iterative algorith.

LPA does not inhibit FLU-induced histone phosphorylation

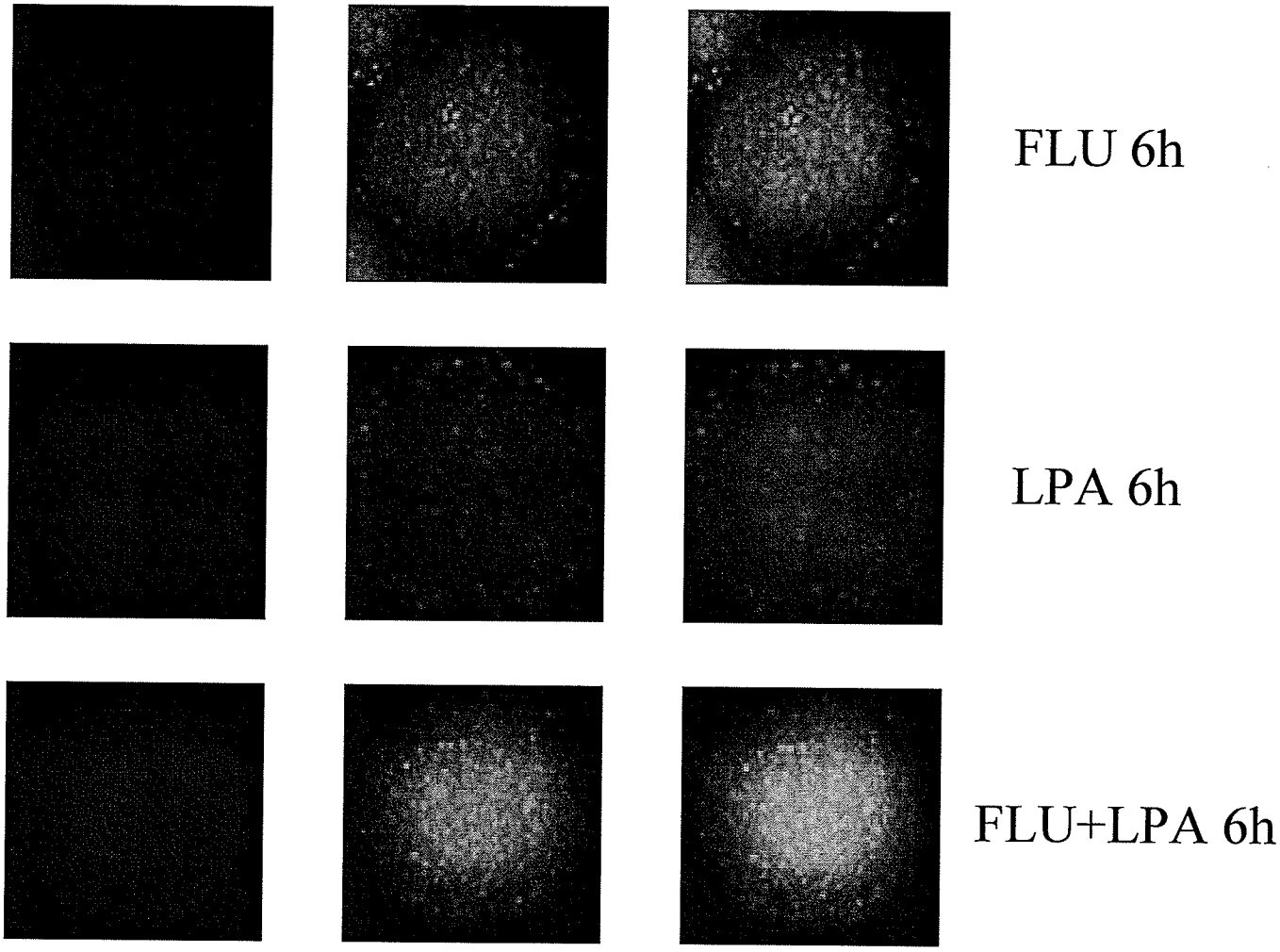

Figure 44

CLL patient samples were left untreated or were treated with first lysophosphatidic acid (10μM) and then fludarabine (FLU) (10μM) for 6 hours. All of the cells were then cytospun onto slides as described in Materials and Methods. The slides were stained with phosphorylated (serine 28) histone H3 Ab (FITC, green). The DNA was stained blue with DAPI. The slides were viewed using an Carl Zeiss AxioPhot II microscope and the pictures deconvolved in three dimensions with the AxioVision 4.1 constrained iterative algorith.

No difference in the level of histone methylation with FLU treatment

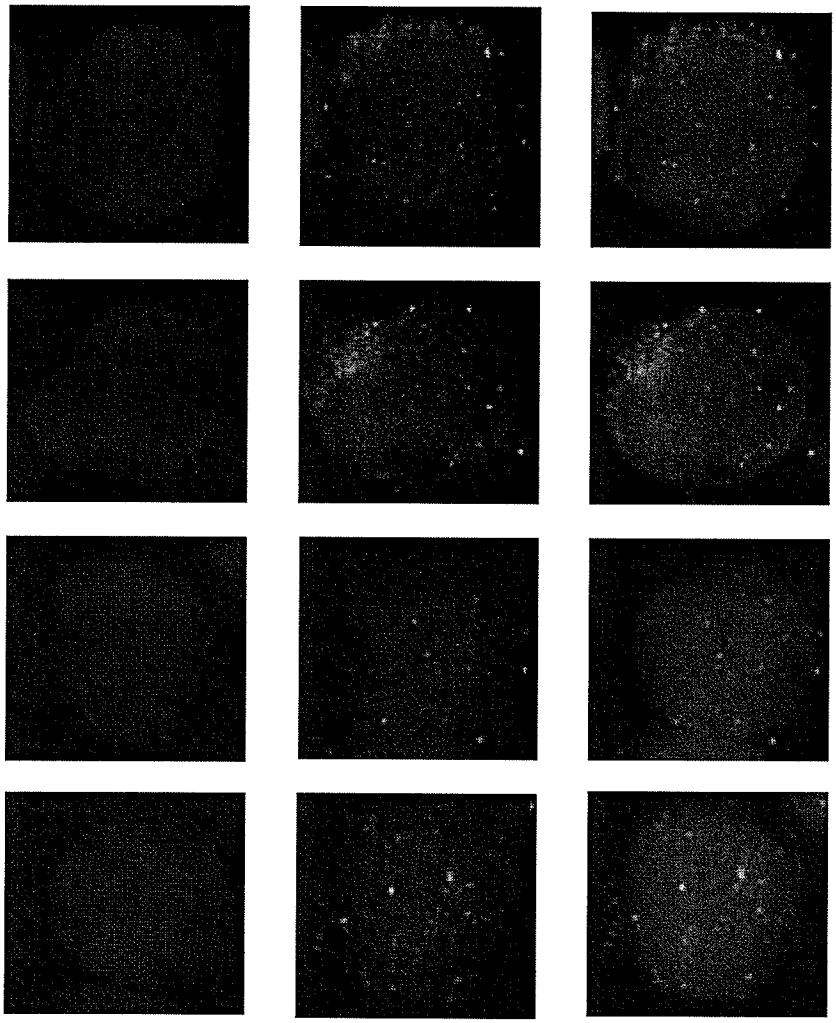

Figure 45

Normal human lymphocyte cells were left untreated and CLL patient samples were treated with fludarabine (FLU) (10μM) for 6 or 24 hours. All of the cells were then cytospun onto slides as described in Materials and Methods. The slides were stained with dimethylated histone H3 Ab (FITC, green). The DNA was stained blue with DAPI. The slides were viewed using an Carl Zeiss AxioPhot II microscope and the pictures deconvolved in three dimensions with the AxioVision 4.1 constrained iterative algorith.

Histone methylation is decreased in CLL cells with LPA treatment

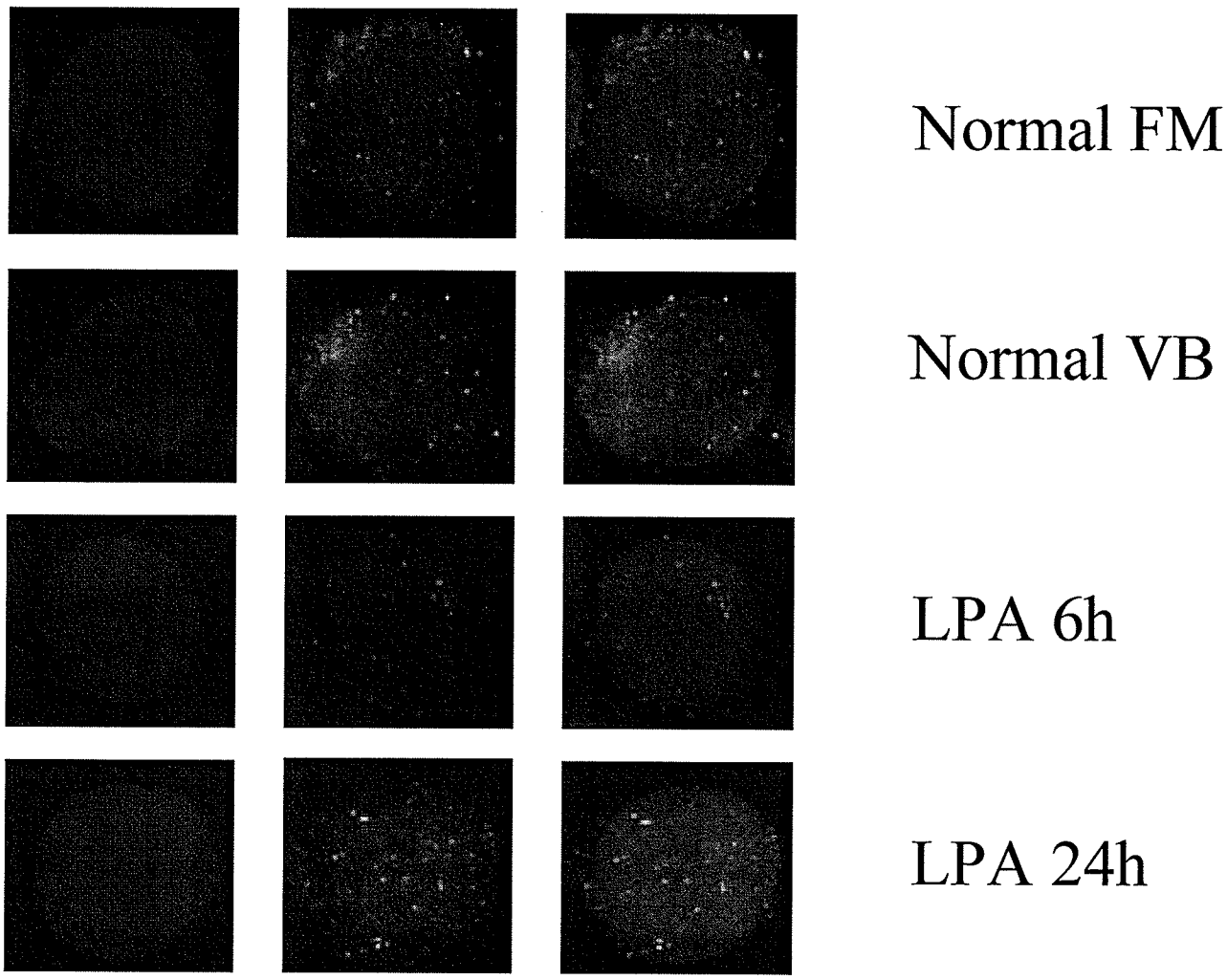

Figure 46

Normal human lymphocyte cells were left untreated and CLL patient samples were treated with lysophosphatidic acid (LPA) (10μM) for 6 or 24 hours. All of the cells were then cytospun onto slides as described in Materials and Methods. The slides were stained with dimethylated histone H3 Ab (FITC, green). The DNA was stained blue with DAPI. The slides were viewed using an Carl Zeiss AxioPhot II microscope and the pictures deconvolved in three dimensions with the AxioVision 4.1 constrained iterative algorith.

6. DISCUSSION

Apoptotic stimuli including genotoxins upregulate DR5 levels sensitizing cells to undergo programmed cell death. This increased expression makes DR5 a potential target for molecular based cancer therapy (12). In accordance with this, TRAIL and antibodies directed against DR5 have been developed for anti-cancer therapy (72, 80, 117, 118). Understanding the regulation of DR5 expression would therefore increase the effectiveness of these therapies.

6.1 NFκB Regulation of DR5

It has been demonstrated by our lab, and others, that genotoxins increase DR5 expression through the activation of transcription factors p53 and NFκB (10, 12, 13). A possible mechanism for NFκB transactivation of the DR5 gene is through the binding of NFκB to the intronic region of the DR5 gene. This binding along with p53 binding induces DR5 expression following etoposide treatment. It is well established that there is transcriptional crosstalk between NFκB and p53 (119). These transcription factors could mutually repress each other's transcriptional activity by competing for a limited pool of histone acetyltransferase p300/CBP or by directly associating with each other (120, 121). In contrast, NFκB activation could increase p53 levels and p53 could activate NFκB transcriptional activity contributing to apoptosis (37). We found that both endogenous p53 and NFκB bind to the DR5 gene leading to the up-regulation of DR5 and apoptosis following genotoxin treatment. Eliminating p53 binding to the intronic region by siRNA also prevented the binding of p65. This suggests that p53 and NFκB cooperate to induce DR5 expression. It has been shown that when p53 is bound to its target gene it recruits

the CBP-PCAF coactivator complex leading to the acetylation of nucleosomal histones (57). This promotes the access of DNA to RNA polymerase II and other basal transcriptions factors, such as NFκB. Besides these transcription factors, other proteins could be sufficient to induce DR5 expression. For example, bile acid induced apoptosis increases DR5 expression mediated by the c-Jun N-terminal kinase (JNK) and interferon-γ induced DR5 expression involves the transcription factor STAT1 (122, 123). Our results indicate that both p53 and NFκB in epithelial derived cells are required for etoposide induced DR5 expression and cross-talk between NFκB and p53 in the regulation DR5 expression will be the focus for future investigations.

NFκB is involved in both cell survival and apoptosis (25, 31, 124). It has been reported that this contradictory function of NFκB could be due to differentially regulated subunits of NFκB (125, 126). The p65 subunit was shown to be required for expression of the anti-apoptotic gene Bcl-x_L and the c-Rel subunit was shown to be required for upregulation of DR5 (125, 126). In contrast, we found that the p65 subunit of NFκB was capable of increasing DR5 expression and over expression of p65 was sufficient to induce DR5 expression. This difference could be due to the specific cell type used. Mouse embryonic fibroblasts lacking c-Rel expression failed to induce DR5 expression (125) whereas human epithelial derived cell lines were able to induce DR5 expression in a p65 dependent manner. The c-Rel subunit was observed to be a minor component of the NFκB activity induced upon apoptosis in HEK293 cells (125). In 3T3 murine fibroblasts lacking p65, the ability of etoposide to induce DR5 transcriptional activity was attenuated indicating a role of p65 in DR5 expression. Thus, it is unlikely that the subunits of NFκB are responsible for differential regulation of gene expression leading to cell survival or

apoptosis. It could however be a result of the modifications present on NFκB, such as phosphorylation.

6.2 Histone Acetylation Regulation of DR5

It has been demonstrated in the nucleus of resting cells that NFκB is complexed with the histone deacetylase HDAC1 and represses NFκB transcriptional activity (24). Upon NFκB activation, HDAC1 is released from the complex, freeing NFκB to target genes for expression (127). Under apoptotic conditions, p65 has been demonstrated to bind to Bcl-x_L and XIAP promoters decreasing their expression. This was accomplished through recruitment of HDACs to these promoters mediated by p65 (128). We have demonstrated that upon EGF treatment, HDAC1 recruitment to the DR5 gene is mediated by NFκB. The mechanism by which HDAC proteins repress the transcriptional activity of NFκB is through their deacetylase activity, since treatment with HDAC inhibitors TSA or VPA activate NFκB and induce DR5 expression. However, the mechanisms regulating the interactions between NFκB and HDAC proteins are unknown. It is possible that in the case of EGF stimulation, NFκB is activated early as opposed to etoposide treatment, which is a late activator of NFκB. Another determinant for NFκB involvement in apoptosis could be how long NFκB is activated. Growth factors activate NFκB transcriptional activity transiently, whereas genotoxin induced NFκB activation is prolonged. This could influence the binding of HDACs to NFκB, defining whether a gene is expressed or repressed. Modification of the NFκB subunit could also be a possibility, as we have shown that NFκB is phosphorylated with EGF and not with etoposide treatment. Furthermore, the lack of p53 recruitment to the DR5 gene following

EGF treatment could influence HDAC binding to this gene. Nevertheless, NFκB activation under survival stimulation (EGF) mediates HDAC1 recruitment to the DR5 gene likely preventing DR5 expression, whereas both NFκB and p53 are recruited to the DR5 gene under apoptotic stimuli (etoposide) inducing DR5 expression. This could be a mechanism controlling NFκB mediated expression of pro-apoptotic genes under apoptotic conditions.

HDAC inhibitors have been shown to have anti-tumor activity (92-94). Death receptor apoptotic signaling pathways have been shown to be activated following treatment with HDAC inhibitors (129). Our lab has previously shown that treatment with HDAC inhibitors TSA and VPA increases DR5 expression and that treatment with both HDAC inhibitors and TRAIL gives a synergistic apoptotic response (36). We also showed that blocking TRAIL from binding to DR5 effectively reduced HDAC inhibitor induced apoptosis (36). In leukemia cells, HDAC inhibitors increase DR5 expression and activation of the TRAIL apoptotic pathway occurs (130). This contributed to HDAC inhibitor induced apoptosis in these cells. As well, several groups have shown that activation of the TRAIL apoptotic signaling pathway occurs following treatment with HDAC inhibitors in various cell types (81, 131). It has been shown that p53 and p300, a HAT, colocalize within the nucleus and co-exist as a stable DNA-binding complex (60). p300 has been shown to enhance the binding of p53 to its site-specific binding sites through acetylation of p53 (58). Treatment of cells with TSA has been shown to increase the level of acetylated p53 and lead to an increase in p53 binding to an endogenous target promoter (58, 61). We have shown that the binding of p53 to the DR5 gene is increased following treatment with TSA, as is its expression level. It has been shown that NFκB

associates with p300 as well, leading to the acetylation of p65. It has been shown that treatment with TSA blocks the association of NFκB with HDAC and increases the binding of NFκB to DNA (132). It has also been shown that treatment with TSA leads to an increased basal and inducible expression level of the NFκB-regulated IL-8 gene (24). We have shown this with the DR5 gene. Treatment with TSA leads to an increase in NFκB binding to the DR5 gene, as well as an increase in DR5 expression levels. Another possible role for acetylation of p53 and NFκB is nuclear localization. Both p53 acetylation sites are located within nuclear localization signals and therefore might affect nuclear import and export (60). It has been shown that acetylation of Rel A blocks the ability of IκBα to assemble with Rel A and therefore prevents the nuclear export of NFκB (56). This regulation of export involves HDAC3. Treatment of cells with HDAC3 deacetylates RelA allowing IκBα to associate with Rel A and return it to the cytoplasm thereby terminating the NFκB transcriptional response (132). This also serves to replenish the pool of NFκB-IκBα complexes for the next induced NFκB response (132). Taken together, this provides a mechanism for HDAC inhibitor induced up-regulation of DR5 involving NFκB and p53 contributing to the cytotoxicity of these inhibitors. It is therefore promising that DR5 induced expression could be an effective target for synergistic chemotherapeutic treatment for cancer.

6.3 CLL as Model System

Based on the results from the cell lines we have demonstrated a possible mechanism for DR5 expression wherein following etoposide treatment the gene is acetylated as a result of the binding of p65, p53, and possibly a HAT to the first intron of the gene thereby promoting transcription of the gene (Figure 47).

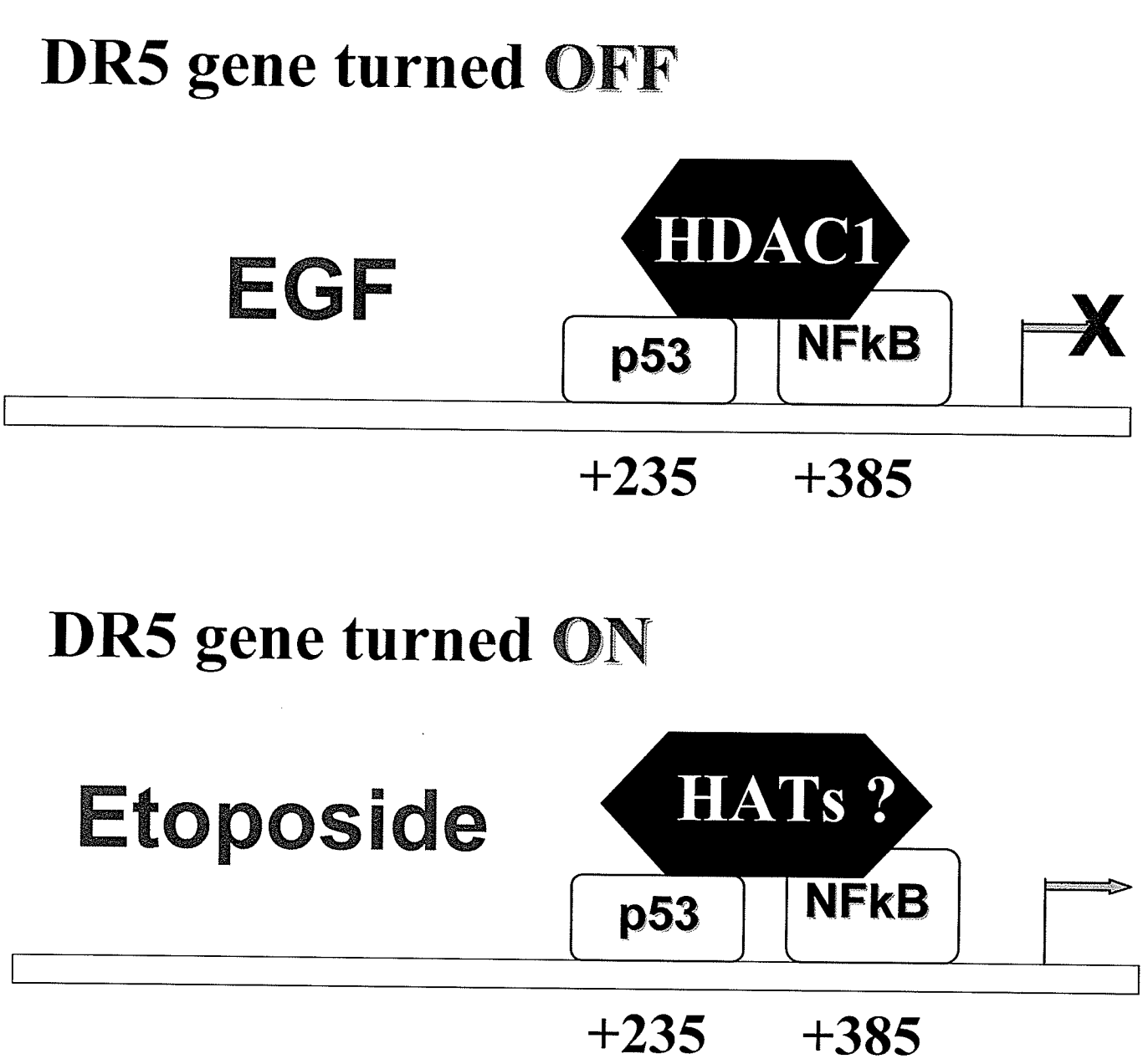

Figure 47

Model of the regulation of DR5 gene expression.
The DR5 gene is expressed after treatment with genotoxins such as etoposide. This expression is regulated by p53, NFκB, and likely HATs.
The DR5 gene is not expressed after treatment with EGF. This lack of expression is regulated by p53, NFκB, and HDAC1.

However, following EGF treatment the gene is deacetylated as a result of the binding of p65, HDAC1, and p53 to the first intron of the gene thereby preventing the transcription of the gene. To prove this in an in vivo model we used primary CLL cells. Our lab has previously shown that treatment of primary CLL cells with either chlorambucil or fludarabine leads to an increase in the expression of DR4 and DR5 at the mRNA, protein, and cell membrane levels (11). In contrast, treatment of normal lymphocytes with either chlorambucil or fludarabine does not affect the expression of DR4 or DR5 (11). Based on these results it was suggested that part of the antitumor activity of CLB and FLU is related to the upregulation of DR4 and DR5 expression on the cell surface and this sensitizes the cells to TRAIL. For this reason we evaluated the roles of the transcription factors involved in CLB and FLU induction of DR4 and DR5 expressions in primary CLL cells. Due to the difficulty of transfecting primary CLL cells we relied on the ChIP assays to determine which transcription factors were involved in the regulation of DR5 expression. Similar to experiments with cell lines p65 was found to bind under both chemotherapeutic and survival treatments and differences between the two treatments could therefore be due to the modifications occurring on the p65 subunit. Aberrations of the p53 gene, such as mutations and functional inactivation of the protein, are one of the most predictive molecular markers for drug resistance and an inferior overall survival rate in patients with CLL (101). It was, therefore, not surprising to see it binding to the DR5 gene only under treatment with chemotherapy drugs as it presumably plays an important role in initiation of apoptosis and success of treatment in CLL. In accordance with our cell line model we saw acetylation of the DR5 gene and the binding of p300 to the gene following treatment with FLU or CLB and saw binding of HDAC1 to the gene following

treatment with LPA. HDAC inhibitors such as depsipeptide and MS-275 have been shown to induce caspase-dependent apoptosis in CLL cells, presumably through the extrinsic pathway (129, 133, 134). Also, it has been shown that treatment with HDAC inhibitors leads to an increase in acetylation of histone H3 and H4 and aids in overcoming TRAIL resistance (110, 129). Since HDAC inhibitors have been shown to function through the induction of the extrinsic pathway and induce the upregulation of DR5 as well as histone acetylation, this supports our data in suggesting that acetylation likely plays an important role in the regulation of the DR5 gene. TRAIL induces apoptosis preferentially in cancer cells as opposed to normal cells and is therefore thought to be a promising new treatment for cancer. The preferential induction of apoptosis in cancer cells versus normal cells may be due to the levels of histone modifications, specifically acetylation. In our studies so far acetylation seems to be the most important modification as it shows the most differential expression between normal, untreated CLL, and treated CLL cells. Many tumors and leukemias are thought to result, in part, from a dysequilibrium of histone acetylation, leading to the abherrant expression and repression of genes (23). This holds true for CLL cells as they are more highly acetylated as compared to normal human cells. This observation could explain the selectivity of some cancer drugs towards cancer cells. If the cancer cells are highly acetylated to begin with treatment with a drug that induces acetylation will cause the cancer cells to become hyperacetylated which is associated with cell growth arrest, differentiation, and/or apoptosis. It has been shown in an anaplastic carcinoma cell line that treatment with the drug doxorubicin leads to apoptosis through the hyperacetylation of histone H3 (135). Arsenic trioxide is a clinically active agent that has been shown to

inhibit growth, reduce intracellular Bcl-2 levels, and induce apoptosis of several myeloid leukemias, including acute promyelocytic leukemia and multiple myeloma (136). It has since been shown in human leukemic cells that clinically relevant concentrations of arsenic trioxide induce the hyperacetylation of histones H3 and H4 (136). This hyperacetylation of histones may be responsible for altering the transcription of genes leading to the observed growth inhibition and apoptosis seen with arsenic trioxide treatment. This suggests that the hyperacetylation of histone H3 seen with fludarabine treatment of CLL cells plays a role in its induction of apoptosis, possibly through acetylating genes such as death receptor 5 and leading to their increased expression.

6.4 Conclusion

In conclusion, we have shown that the binding of p53 and NFκB in the first intronic region of the DR5 gene, as well as histone acetylation are involved in the regulation of the DR5 gene in HEK293 cells. Using CLL as our model system, we have shown that NFκB, p53, and histone acetylation may be involved in the regulation of the DR5 gene. We have also shown that CLL cells are more highly acetylated than normal cells, offering an explanation for the upregulation of DR5 in transformed versus non-transformed cells. As well, the induced acetylation following fludarabine treatment could lead to the hyperacetylation of CLL cells and thereby inducing apoptosis, possibly through the increased expression of genes such as DR5.

REFERENCES

1. Dbaibo GS, Hannun YA. Signal transduction and the regulation of apoptosis: roles of ceramide. Apoptosis 1998;3(5):317-34.
2. Hengartner MO. The biochemistry of apoptosis. Nature 2000;407(6805):770-6.
3. Hacker G. The morphology of apoptosis. Cell Tissue Res 2000;301(1):5-17.
4. Schulze-Osthoff K, Ferrari D, Los M, Wesselborg S, Peter ME. Apoptosis signaling by death receptors. Eur J Biochem 1998;254(3):439-59.
5. Strasser A, O'Connor L, Dixit VM. Apoptosis signaling. Annu Rev Biochem 2000;69:217-45.
6. Thornberry NA, Lazebnik Y. Caspases: enemies within. Science 1998;281(5381):1312-6.
7. Johnson DE. Noncaspase proteases in apoptosis. Leukemia 2000;14(9):1695-703.
8. Rossi D, Gaidano G. Messengers of cell death: apoptotic signaling in health and disease. Haematologica 2003;88(2):212-8.
9. Jaroszewski L, Rychlewski L, Reed JC, Godzik A. ATP-activated oligomerization as a mechanism for apoptosis regulation: fold and mechanism prediction for CED-4. Proteins 2000;39(3):197-203.
10. Takimoto R, El-Deiry WS. Wild-type p53 transactivates the KILLER/DR5 gene through an intronic sequence-specific DNA-binding site. Oncogene 2000;19(14):1735-43.
11. Johnston JB, Kabore AF, Strutinsky J, Hu X, Paul JT, Kropp DM, et al. Role of the TRAIL/APO2-L death receptors in chlorambucil- and fludarabine-induced apoptosis in chronic lymphocytic leukemia. Oncogene 2003;22(51):8356-69.
12. Gibson SB, Oyer R, Spalding AC, Anderson SM, Johnson GL. Increased expression of death receptors 4 and 5 synergizes the apoptosis response to combined treatment with etoposide and TRAIL. Mol Cell Biol 2000;20(1):205-12.
13. Shetty S, Gladden JB, Henson ES, Hu X, Villanueva J, Haney N, et al. Tumor necrosis factor-related apoptosis inducing ligand (TRAIL) up-regulates death receptor 5 (DR5) mediated by NFkappaB activation in epithelial derived cell lines. Apoptosis 2002;7(5):413-20.
14. Yoshida T, Maeda A, Tani N, Sakai T. Promoter structure and transcription initiation sites of the human death receptor 5/TRAIL-R2 gene. FEBS Lett 2001;507(3):381-5.
15. Cory S, Adams JM. The Bcl2 family: regulators of the cellular life-or-death switch. Nat Rev Cancer 2002;2(9):647-56.
16. Solary E, Droin N, Bettaieb A, Corcos L, Dimanche-Boitrel MT, Garrido C. Positive and negative regulation of apoptotic pathways by cytotoxic agents in hematological malignancies. Leukemia 2000;14(10):1833-49.
17. Schuler M, Green DR. Mechanisms of p53-dependent apoptosis. Biochem Soc Trans 2001;29(Pt 6):684-8.
18. Emerson BM. Specificity of gene regulation. Cell 2002;109(3):267-70.
19. Kadam S, McAlpine GS, Phelan ML, Kingston RE, Jones KA, Emerson BM. Functional selectivity of recombinant mammalian SWI/SNF subunits. Genes Dev 2000;14(19):2441-51.

20. Kal AJ, Mahmoudi T, Zak NB, Verrijzer CP. The Drosophila brahma complex is an essential coactivator for the trithorax group protein zeste. Genes Dev 2000;14(9):1058-71.
21. Baldwin AS, Jr. The NF-kappa B and I kappa B proteins: new discoveries and insights. Annu Rev Immunol 1996;14:649-83.
22. Ghosh S, May MJ, Kopp EB. NF-kappa B and Rel proteins: evolutionarily conserved mediators of immune responses. Annu Rev Immunol 1998;16:225-60.
23. Mahlknecht U, Ottmann OG, Hoelzer D. When the band begins to play: histone acetylation caught in the crossfire of gene control. Mol Carcinog 2000;27(4):268-71.
24. Ashburner BP, Westerheide SD, Baldwin AS, Jr. The p65 (RelA) subunit of NF-kappaB interacts with the histone deacetylase (HDAC) corepressors HDAC1 and HDAC2 to negatively regulate gene expression. Mol Cell Biol 2001;21(20):7065-77.
25. Grimm S, Bauer MK, Baeuerle PA, Schulze-Osthoff K. Bcl-2 down-regulates the activity of transcription factor NF-kappaB induced upon apoptosis. J Cell Biol 1996;134(1):13-23.
26. Hockenbery DM, Oltvai ZN, Yin XM, Milliman CL, Korsmeyer SJ. Bcl-2 functions in an antioxidant pathway to prevent apoptosis. Cell 1993;75(2):241-51.
27. Osborn L, Kunkel S, Nabel GJ. Tumor necrosis factor alpha and interleukin 1 stimulate the human immunodeficiency virus enhancer by activation of the nuclear factor kappa B. Proc Natl Acad Sci U S A 1989;86(7):2336-40.
28. Schreck R, Rieber P, Baeuerle PA. Reactive oxygen intermediates as apparently widely used messengers in the activation of the NF-kappa B transcription factor and HIV-1. Embo J 1991;10(8):2247-58.
29. Schutze S, Potthoff K, Machleidt T, Berkovic D, Wiegmann K, Kronke M. TNF activates NF-kappa B by phosphatidylcholine-specific phospholipase C-induced "acidic" sphingomyelin breakdown. Cell 1992;71(5):765-76.
30. Karin M. How NF-kappaB is activated: the role of the IkappaB kinase (IKK) complex. Oncogene 1999;18(49):6867-74.
31. Ghosh S, Karin M. Missing pieces in the NF-kappaB puzzle. Cell 2002;109 Suppl:S81-96.
32. Henson ES, Gibson EM, Villanueva J, Bristow NA, Haney N, Gibson SB. Increased expression of Mcl-1 is responsible for the blockage of TRAIL-induced apoptosis mediated by EGF/ErbB1 signaling pathway. J Cell Biochem 2003;89(6):1177-92.
33. Kreuz S, Siegmund D, Scheurich P, Wajant H. NF-kappaB inducers upregulate cFLIP, a cycloheximide-sensitive inhibitor of death receptor signaling. Mol Cell Biol 2001;21(12):3964-73.
34. Wang CY, Mayo MW, Korneluk RG, Goeddel DV, Baldwin AS, Jr. NF-kappaB antiapoptosis: induction of TRAF1 and TRAF2 and c-IAP1 and c-IAP2 to suppress caspase-8 activation. Science 1998;281(5383):1680-3.
35. Mahlknecht U, Hoelzer D. Histone acetylation modifiers in the pathogenesis of malignant disease. Mol Med 2000;6(8):623-44.

36. Shetty S, Graham BA, Brown JG, Hu X, Vegh-Yarema N, Harding G, et al. Transcription factor NF-kappaB differentially regulates death receptor 5 expression involving histone deacetylase 1. Mol Cell Biol 2005;25(13):5404-16.
37. Ryan KM, Ernst MK, Rice NR, Vousden KH. Role of NF-kappaB in p53-mediated programmed cell death. Nature 2000;404(6780):892-7.
38. Vogelstein B, Lane D, Levine AJ. Surfing the p53 network. Nature 2000;408(6810):307-10.
39. Chumakov PM. Function of the p53 gene: choice between life and death. Biochemistry (Mosc) 2000;65(1):28-40.
40. Espinosa JM, Emerson BM. Transcriptional regulation by p53 through intrinsic DNA/chromatin binding and site-directed cofactor recruitment. Mol Cell 2001;8(1):57-69.
41. Arrowsmith CH. Structure and function in the p53 family. Cell Death Differ 1999;6(12):1169-73.
42. Hupp TR, Meek DW, Midgley CA, Lane DP. Regulation of the specific DNA binding function of p53. Cell 1992;71(5):875-86.
43. Gu W, Roeder RG. Activation of p53 sequence-specific DNA binding by acetylation of the p53 C-terminal domain. Cell 1997;90(4):595-606.
44. Kirch HC, Flaswinkel S, Rumpf H, Brockmann D, Esche H. Expression of human p53 requires synergistic activation of transcription from the p53 promoter by AP-1, NF-kappaB and Myc/Max. Oncogene 1999;18(17):2728-38.
45. Spencer VA, Davie JR. Role of covalent modifications of histones in regulating gene expression. Gene 1999;240(1):1-12.
46. Spencer VA, Davie JR. Signal transduction pathways and chromatin structure in cancer cells. J Cell Biochem Suppl 2000;Suppl 35:27-35.
47. Hake SB, Xiao A, Allis CD. Linking the epigenetic 'language' of covalent histone modifications to cancer. Br J Cancer 2004;90(4):761-9.
48. Davie JR, Spencer VA. Control of histone modifications. J Cell Biochem 1999;Suppl 32-33:141-8.
49. Sun JM, Spencer VA, Chen HY, Li L, Davie JR. Measurement of histone acetyltransferase and histone deacetylase activities and kinetics of histone acetylation. Methods 2003;31(1):12-23.
50. Singh TR, Shankar S, Srivastava RK. HDAC inhibitors enhance the apoptosis-inducing potential of TRAIL in breast carcinoma. Oncogene 2005;24(29):4609-23.
51. Alcendor RR, Kirshenbaum LA, Imai S, Vatner SF, Sadoshima J. Silent information regulator 2alpha, a longevity factor and class III histone deacetylase, is an essential endogenous apoptosis inhibitor in cardiac myocytes. Circ Res 2004;95(10):971-80.
52. Kouzarides T. Acetylation: a regulatory modification to rival phosphorylation? Embo J 2000;19(6):1176-9.
53. Imhof A, Yang XJ, Ogryzko VV, Nakatani Y, Wolffe AP, Ge H. Acetylation of general transcription factors by histone acetyltransferases. Curr Biol 1997;7(9):689-92.

54. Kiernan R, Bres V, Ng RW, Coudart MP, El Messaoudi S, Sardet C, et al. Post-activation turn-off of NF-kappa B-dependent transcription is regulated by acetylation of p65. J Biol Chem 2003;278(4):2758-66.
55. Wen J, Ramadevi N, Nguyen D, Perkins C, Worthington E, Bhalla K. Antileukemic drugs increase death receptor 5 levels and enhance Apo-2L-induced apoptosis of human acute leukemia cells. Blood 2000;96(12):3900-6.
56. Chen LF, Greene WC. Regulation of distinct biological activities of the NF-kappaB transcription factor complex by acetylation. J Mol Med 2003;81(9):549-57.
57. Liu L, Scolnick DM, Trievel RC, Zhang HB, Marmorstein R, Halazonetis TD, et al. p53 sites acetylated in vitro by PCAF and p300 are acetylated in vivo in response to DNA damage. Mol Cell Biol 1999;19(2):1202-9.
58. Luo J, Li M, Tang Y, Laszkowska M, Roeder RG, Gu W. Acetylation of p53 augments its site-specific DNA binding both in vitro and in vivo. Proc Natl Acad Sci U S A 2004;101(8):2259-64.
59. Liu L, Scolnick DM, Trievel RC, Zhang HB, Marmorstein R, Halazonetis TD, et al. p53 sites acetylated in vitro by PCAF and p300 are acetylated in vivo in response to DNA damage. Mol Cell Biol 1999; 19:1202-09.
60. Sakaguchi K, Herrera JE, Saito S, Miki T, Bustin M, Vassilev A, et al. DNA damage activates p53 through a phosphorylation-acetylation cascade. Genes Dev 1998;12(18):2831-41.
61. Luo J, Su F, Chen D, Shiloh A, Gu W. Deacetylation of p53 modulates its effect on cell growth and apoptosis. Nature 2000;408(6810):377-81.
62. Nowak SJ, Corces VG. Phosphorylation of histone H3: a balancing act between chromosome condensation and transcriptional activation. Trends Genet 2004;20(4):214-20.
63. Jelinkova L, Kubelka M. Neither Aurora B activity nor histone H3 phosphorylation is essential for chromosome condensation during meiotic maturation of porcine oocytes. Biol Reprod 2006;74(5):905-12.
64. Dunn KL, Espino PS, Drobic B, He S, Davie JR. The Ras-MAPK signal transduction pathway, cancer and chromatin remodeling. Biochem Cell Biol 2005;83(1):1-14.
65. Cheng X, Collins RE, Zhang X. Structural and sequence motifs of protein (histone) methylation enzymes. Annu Rev Biophys Biomol Struct 2005;34:267-94.
66. Shi Y, Lan F, Matson C, Mulligan P, Whetstine JR, Cole PA, et al. Histone demethylation mediated by the nuclear amine oxidase homolog LSD1. Cell 2004;119(7):941-53.
67. Kubicek S, Jenuwein T. A crack in histone lysine methylation. Cell 2004;119(7):903-6.
68. Martin C, Zhang Y. The diverse functions of histone lysine methylation. Nat Rev Mol Cell Biol 2005;6(11):838-49.
69. Shiio Y, Eisenman RN. Histone sumoylation is associated with transcriptional repression. Proc Natl Acad Sci U S A 2003;100(23):13225-30.

70. Shin JA, Choi ES, Kim HS, Ho JC, Watts FZ, Park SD, et al. SUMO modification is involved in the maintenance of heterochromatin stability in fission yeast. Mol Cell 2005;19(6):817-28.
71. Jaylata Devi B, Sharan RN. Progressive reduction in poly-ADP-ribosylation of histone proteins during Dalton's lymphoma induced ascites tumorigenesis in mice. Cancer Lett 2005;26:26.
72. Griffith TS, Chin WA, Jackson GC, Lynch DH, Kubin MZ. Intracellular regulation of TRAIL-induced apoptosis in human melanoma cells. J Immunol 1998;161(6):2833-40.
73. Wiley SR, Schooley K, Smolak PJ, Din WS, Huang CP, Nicholl JK, et al. Identification and characterization of a new member of the TNF family that induces apoptosis. Immunity 1995;3(6):673-82.
74. Walczak H, Miller RE, Ariail K, Gliniak B, Griffith TS, Kubin M, et al. Tumoricidal activity of tumor necrosis factor-related apoptosis-inducing ligand in vivo. Nat Med 1999;5(2):157-63.
75. Koornstra JJ, Kleibeuker JH, van Geelen CM, Rijcken FE, Hollema H, de Vries EG, et al. Expression of TRAIL (TNF-related apoptosis-inducing ligand) and its receptors in normal colonic mucosa, adenomas, and carcinomas. J Pathol 2003;200(3):327-35.
76. Pan G, O'Rourke K, Chinnaiyan AM, Gentz R, Ebner R, Ni J, et al. The receptor for the cytotoxic ligand TRAIL. Science 1997;276(5309):111-3.
77. Screaton GR, Mongkolsapaya J, Xu XN, Cowper AE, McMichael AJ, Bell JI. TRICK2, a new alternatively spliced receptor that transduces the cytotoxic signal from TRAIL. Curr Biol 1997;7(9):693-6.
78. Sheridan JP, Marsters SA, Pitti RM, Gurney A, Skubatch M, Baldwin D, et al. Control of TRAIL-induced apoptosis by a family of signaling and decoy receptors. Science 1997;277(5327):818-21.
79. Wu GS, Burns TF, McDonald ER, 3rd, Jiang W, Meng R, Krantz ID, et al. KILLER/DR5 is a DNA damage-inducible p53-regulated death receptor gene. Nat Genet 1997;17(2):141-3.
80. Walczak H, Degli-Esposti MA, Johnson RS, Smolak PJ, Waugh JY, Boiani N, et al. TRAIL-R2: a novel apoptosis-mediating receptor for TRAIL. Embo J 1997;16(17):5386-97.
81. Nakata S, Yoshida T, Horinaka M, Shiraishi T, Wakada M, Sakai T. Histone deacetylase inhibitors upregulate death receptor 5/TRAIL-R2 and sensitize apoptosis induced by TRAIL/APO2-L in human malignant tumor cells. Oncogene 2004;23(37):6261-71.
82. Marini P, Denzinger S, Schiller D, Kauder S, Welz S, Humphreys R, et al. Combined treatment of colorectal tumours with agonistic TRAIL receptor antibodies HGS-ETR1 and HGS-ETR2 and radiotherapy: enhanced effects in vitro and dose-dependent growth delay in vivo. Oncogene 2006;24:24.
83. Menoret E, Gomez-Bougie P, Geffroy-Luseau A, Daniels S, Moreau P, Le Gouill S, et al. Mcl-1L cleavage is involved in TRAIL-R1 and TRAIL-R2 mediated apoptosis induced by HGS-ETR1 and HGS-ETR2 human mAb in myeloma cells. Blood 2006;25:25.

84. Zeng Y, Wu XX, Fiscella M, Shimada O, Humphreys R, Albert V, et al. Monoclonal antibody to tumor necrosis factor-related apoptosis-inducing ligand receptor 2 (TRAIL-R2) induces apoptosis in primary renal cell carcinoma cells in vitro and inhibits tumor growth in vivo. Int J Oncol 2006;28(2):421-30.
85. Georgakis GV, Li Y, Humphreys R, Andreeff M, O'Brien S, Younes M, et al. Activity of selective fully human agonistic antibodies to the TRAIL death receptors TRAIL-R1 and TRAIL-R2 in primary and cultured lymphoma cells: induction of apoptosis and enhancement of doxorubicin- and bortezomib-induced cell death. Br J Haematol 2005;130(4):501-10.
86. Kabore AF, Sun J, Hu X, McCrea K, Johnston JB, Gibson SB. The TRAIL apoptotic pathway mediates proteasome inhibitor induced apoptosis in primary chronic lymphocytic leukemia cells. Apoptosis 2006;11:11.
87. Keane MM, Ettenberg SA, Nau MM, Russell EK, Lipkowitz S. Chemotherapy augments TRAIL-induced apoptosis in breast cell lines. Cancer Res 1999;59(3):734-41.
88. Timmermann S, Lehrmann H, Polesskaya A, Harel-Bellan A. Histone acetylation and disease. Cell Mol Life Sci 2001;58(5-6):728-36.
89. Urnov FD, Rebar EJ, Reik A, Pandolfi PP. Designed transcription factors as structural, functional and therapeutic probes of chromatin in vivo. Fourth in review series on chromatin dynamics. EMBO Rep 2002;3(7):610-5.
90. Johnstone RW, Licht JD. Histone deacetylase inhibitors in cancer therapy: is transcription the primary target? Cancer Cell 2003;4(1):13-8.
91. Marks PA, Rifkind RA, Richon VM, Breslow R. Inhibitors of histone deacetylase are potentially effective anticancer agents. Clin Cancer Res 2001;7(4):759-60.
92. Kramer OH, Gottlicher M, Heinzel T. Histone deacetylase as a therapeutic target. Trends Endocrinol Metab 2001;12(7):294-300.
93. Marks P, Rifkind RA, Richon VM, Breslow R, Miller T, Kelly WK. Histone deacetylases and cancer: causes and therapies. Nat Rev Cancer 2001;1(3):194-202.
94. Marks PA, Richon VM, Breslow R, Rifkind RA. Histone deacetylase inhibitors as new cancer drugs. Curr Opin Oncol 2001;13(6):477-83.
95. Insinga A, Monestiroli S, Ronzoni S, Gelmetti V, Marchesi F, Viale A, et al. Inhibitors of histone deacetylases induce tumor-selective apoptosis through activation of the death receptor pathway. Nat Med 2005;11(1):71-6.
96. Dighiero G, Travade P, Chevret S, Fenaux P, Chastang C, Binet JL. B-cell chronic lymphocytic leukemia: present status and future directions. French Cooperative Group on CLL. Blood 1991;78(8):1901-14.
97. McLaughlin F, Finn P, La Thangue NB. The cell cycle, chromatin and cancer: mechanism-based therapeutics come of age. Drug Discov Today 2003;8(17):793-802.
98. Henderson C, Brancolini C. Apoptotic pathways activated by histone deacetylase inhibitors: implications for the drug-resistant phenotype. Drug Resist Updat 2003;6(5):247-56.
99. Zhang XD, Gillespie SK, Borrow JM, Hersey P. The histone deacetylase inhibitor suberic bishydroxamate: a potential sensitizer of melanoma to TNF-related

apoptosis-inducing ligand (TRAIL) induced apoptosis. Biochem Pharmacol 2003;66(8):1537-45.
100. Herishanu Y, Polliack A. Chronic lymphocytic leukemia: a review of some new aspects of the biology, factors influencing prognosis and therapeutic options. Transfus Apher Sci 2005;32(1):85-97.
101. Bannerji R, Byrd JC. Update on the biology of chronic lymphocytic leukemia. Curr Opin Oncol 2000;12(1):22-9.
102. Abbott BL. Advances in the diagnosis and treatment of chronic lymphocytic leukemia. Hematol Oncol 2005;23(1):34-40.
103. Byrd JC, Stilgenbauer S, Flinn IW. Chronic lymphocytic leukemia. Hematology (Am Soc Hematol Educ Program) 2004:163-83.
104. Kipps TJ. Chronic lymphocytic leukemia. Curr Opin Hematol 2000;7(4):223-34.
105. Juliusson G, Oscier DG, Fitchett M, Ross FM, Stockdill G, Mackie MJ, et al. Prognostic subgroups in B-cell chronic lymphocytic leukemia defined by specific chromosomal abnormalities. N Engl J Med 1990;323(11):720-4.
106. Begleiter A, Mowat M, Israels LG, Johnston JB. Chlorambucil in chronic lymphocytic leukemia: mechanism of action. Leuk Lymphoma 1996;23(3-4):187-201.
107. Begleiter A, Verburg L, Ashique A, Lee K, Israels LG, Mowat MR, et al. Comparison of antitumor activities of 2-chlorodeoxyadenosine and 9-beta-arabinosyl-2-fluoroadenine in chronic lymphocytic leukemia and marrow cells in vitro. Leukemia 1995;9(11):1875-81.
108. Genini D, Adachi S, Chao Q, Rose DW, Carrera CJ, Cottam HB, et al. Deoxyadenosine analogs induce programmed cell death in chronic lymphocytic leukemia cells by damaging the DNA and by directly affecting the mitochondria. Blood 2000;96(10):3537-43.
109. Genini D, Budihardjo I, Plunkett W, Wang X, Carrera CJ, Cottam HB, et al. Nucleotide requirements for the in vitro activation of the apoptosis protein-activating factor-1-mediated caspase pathway. J Biol Chem 2000;275(1):29-34.
110. MacFarlane M, Inoue S, Kohlhaas SL, Majid A, Harper N, Kennedy DB, et al. Chronic lymphocytic leukemic cells exhibit apoptotic signaling via TRAIL-R1. Cell Death Differ 2005;12(7):773-82.
111. Kang YC, Kim KM, Lee KS, Namkoong S, Lee SJ, Han JA, et al. Serum bioactive lysophospholipids prevent TRAIL-induced apoptosis via PI3K/Akt-dependent cFLIP expression and Bad phosphorylation. Cell Death Differ 2004;11(12):1287-98.
112. Hu YL, Albanese C, Pestell RG, Jaffe RB. Dual mechanisms for lysophosphatidic acid stimulation of human ovarian carcinoma cells. J Natl Cancer Inst 2003;95(10):733-40.
113. Hu X, Haney N, Kropp D, Kabore AF, Johnston JB, Gibson SB. Lysophosphatidic acid (LPA) protects primary chronic lymphocytic leukemia cells from apoptosis through LPA receptor activation of the anti-apoptotic protein AKT/PKB. J Biol Chem 2005;280(10):9498-508.
114. Chou CH, Wei LH, Kuo ML, Huang YJ, Lai KP, Chen CA, et al. Up-regulation of interleukin-6 in human ovarian cancer cell via a Gi/PI3K-Akt/NF-kappaB

pathway by lysophosphatidic acid, an ovarian cancer-activating factor. Carcinogenesis 2005;26(1):45-52.
115. Raj GV, Sekula JA, Guo R, Madden JF, Daaka Y. Lysophosphatidic acid promotes survival of androgen-insensitive prostate cancer PC3 cells via activation of NF-kappaB. Prostate 2004;61(2):105-13.
116. He S, Sun JM, Li L, Davie JR. Differential intranuclear organization of transcription factors Sp1 and Sp3. Mol Biol Cell 2005;16(9):4073-83.
117. Srivastava RK. TRAIL/Apo-2L: mechanisms and clinical applications in cancer. Neoplasia 2001;3(6):535-46.
118. Ichikawa K, Liu W, Zhao L, Wang Z, Liu D, Ohtsuka T, et al. Tumoricidal activity of a novel anti-human DR5 monoclonal antibody without hepatocyte cytotoxicity. Nat Med 2001;7(8):954-60.
119. Webster GA, Perkins ND. Transcriptional cross talk between NF-kappaB and p53. Mol Cell Biol 1999;19(5):3485-95.
120. Tergaonkar V, Pando M, Vafa O, Wahl G, Verma I. p53 stabilization is decreased upon NFkappaB activation: a role for NFkappaB in acquisition of resistance to chemotherapy. Cancer Cell 2002;1(5):493-503.
121. Wadgaonkar R, Phelps KM, Haque Z, Williams AJ, Silverman ES, Collins T. CREB-binding protein is a nuclear integrator of nuclear factor-kappaB and p53 signaling. J Biol Chem 1999;274(4):1879-82.
122. Higuchi H, Grambihler A, Canbay A, Bronk SF, Gores GJ. Bile acids up-regulate death receptor 5/TRAIL-receptor 2 expression via a c-Jun N-terminal kinase-dependent pathway involving Sp1. J Biol Chem 2004;279(1):51-60.
123. Meng RD, McDonald ER, 3rd, Sheikh MS, Fornace AJ, Jr., El-Deiry WS. The TRAIL decoy receptor TRUNDD (DcR2, TRAIL-R4) is induced by adenovirus-p53 overexpression and can delay TRAIL-, p53-, and KILLER/DR5-dependent colon cancer apoptosis. Mol Ther 2000;1(2):130-44.
124. Baldwin AS. Control of oncogenesis and cancer therapy resistance by the transcription factor NF-kappaB. J Clin Invest 2001;107(3):241-6.
125. Chen X, Kandasamy K, Srivastava RK. Differential roles of RelA (p65) and c-Rel subunits of nuclear factor kappa B in tumor necrosis factor-related apoptosis-inducing ligand signaling. Cancer Res 2003;63(5):1059-66.
126. Ravi R, Bedi GC, Engstrom LW, Zeng Q, Mookerjee B, Gelinas C, et al. Regulation of death receptor expression and TRAIL/Apo2L-induced apoptosis by NF-kappaB. Nat Cell Biol 2001;3(4):409-16.
127. Zhong H, May MJ, Jimi E, Ghosh S. The phosphorylation status of nuclear NF-kappa B determines its association with CBP/p300 or HDAC-1. Mol Cell 2002;9(3):625-36.
128. Campbell KJ, Rocha S, Perkins ND. Active repression of antiapoptotic gene expression by RelA(p65) NF-kappa B. Mol Cell 2004;13(6):853-65.
129. Aron JL, Parthun MR, Marcucci G, Kitada S, Mone AP, Davis ME, et al. Depsipeptide (FR901228) induces histone acetylation and inhibition of histone deacetylase in chronic lymphocytic leukemia cells concurrent with activation of caspase 8-mediated apoptosis and down-regulation of c-FLIP protein. Blood 2003;102(2):652-8.

130. Nebbioso A, Clarke N, Voltz E, Germain E, Ambrosino C, Bontempo P, et al. Tumor-selective action of HDAC inhibitors involves TRAIL induction in acute myeloid leukemia cells. Nat Med 2005;11(1):77-84.
131. Rosato RR, Almenara JA, Dai Y, Grant S. Simultaneous activation of the intrinsic and extrinsic pathways by histone deacetylase (HDAC) inhibitors and tumor necrosis factor-related apoptosis-inducing ligand (TRAIL) synergistically induces mitochondrial damage and apoptosis in human leukemia cells. Mol Cancer Ther 2003;2(12):1273-84.
132. Chen L, Fischle W, Verdin E, Greene WC. Duration of nuclear NF-kappaB action regulated by reversible acetylation. Science 2001;293(5535):1653-7.
133. Lucas DM, Davis ME, Parthun MR, Mone AP, Kitada S, Cunningham KD, et al. The histone deacetylase inhibitor MS-275 induces caspase-dependent apoptosis in B-cell chronic lymphocytic leukemia cells. Leukemia 2004;18(7):1207-14.
134. Inoue S, MacFarlane M, Harper N, Wheat LM, Dyer MJ, Cohen GM. Histone deacetylase inhibitors potentiate TNF-related apoptosis-inducing ligand (TRAIL)-induced apoptosis in lymphoid malignancies. Cell Death Differ 2004;11 Suppl 2:S193-206.
135. Rho JH, Kang DY, Park KJ, Choi HJ, Lee HS, Yee SB, et al. Doxorubicin induces apoptosis with profile of large-scale DNA fragmentation and without DNA ladder in anaplastic thyroid carcinoma cells via histone hyperacetylation. Int J Oncol 2005;27(2):465-71.
136. Perkins C, Kim CN, Fang G, Bhalla KN. Arsenic induces apoptosis of multidrug-resistant human myeloid leukemia cells that express Bcr-Abl or overexpress MDR, MRP, Bcl-2, or Bcl-x(L). Blood 2000;95(3):1014-22.
137. Packham G and Stevenson FK. Bodyguards and assassins: Bcl-2 family proteins and apoptosis control in chronic lymphocytic leukaemia. Immunology 2005;114(4):441-9.